Tomas Bata University in Zlín
Centre of Polymer Systems

Doctoral Thesis

Preparation of reconstituted tissues

Příprava rekonstituovaných tkání

Author: Ing. Kristýna Valášková

Degree programme: P0711D130023 Biomaterials and Biocomposites

Supervisor: doc. Ing. Zdenka Víchová, Ph.D.

Consultant: prof. Ing. Petr Humpolíček, Ph.D.

Zlín, September 2025

ACKNOWLEDGEMENT

I would like to express my deepest thanks to my doctoral thesis supervisor, doc. Ing. Zdenka Víchová Ph.D., from the Centre for Polymer Systems at Tomas Bata University in Zlín, for her professional guidance, constructive criticism, time sacrifice, and kind attitude. Furthermore, I would like to thank prof. Ing. Petr Humpolíček Ph.D., for his valuable advice during my academic journey.

Finally, I would like to express my sincere gratitude to all my colleagues at the Centre of Polymer Systems. Their support, collaboration, and shared experiences have significantly contributed to creating a supportive workplace that has greatly enriched my work.

Not least, I would like to thank my family for their unceasing support during my PhD studies.

ABSTRACT

Living tissues are highly dynamic systems in which continuously changing structural, mechanical, biochemical, and biological cues are intrinsically combined within three-dimensional structures. Cells and tissue scaffolds (extracellular matrix) play a critical and synergistic role, not only in the formation of tissue architecture but also in the maintenance of its physiological function. Therefore, both the role of cells and scaffolds are required to play integral roles in the construction of reconstituted tissues. This is a dynamic and multidisciplinary area of research. Models are finally applicable to tissue engineering and regenerative medicine, disease modeling, and *in vitro* experiments. Within the thesis, the main attention is paid to *in vitro* reconstituted three-dimensional (3D) models of skin. Models should allow the reconstitution of a skin architecture, and micro-environment, to enable the investigation of cell-matrix and cell-cell interactions between different cell types, and finally even mimic the function and physiology of their *in vivo* tissue counterparts. In the case of the 3D models of the skin tissue, it is an *in vitro* co-culture system of human neonatal keratinocytes grown at the air-liquid interface on collagen gel together with human dermal fibroblasts. The dermal component of the skin models comprises human dermal fibroblasts embedded in a rat-tail collagen type I hydrogel. Collagen represents the initial "scaffold" but without the 3D architecture. A multilayered epidermis forms at the apical part of the models upon inoculation with human epidermal keratinocytes and subsequent culture at the air-liquid interface. The work aims to clarify the preparation of the collagen layer and the subsequent provision of an appropriate fibroblast-keratinocyte co-culture resulting in the functional skin equivalent *in vitro*.

Regardless of this, the skin tissue cells, respectively, dermal fibroblasts, can be used as cell-assembled extracellular matrix (CAM) bio-scaffolds. Instead of using synthetic or natural materials as scaffolds, this approach harnesses the inherent ability of cells to produce their own ECM. The 3D architecture of CAM sheet can be formed and controlled by external factors such as mechanical stimulation. In our research, human dermal fibroblasts were cultured *in vitro* with ascorbic acid to promote cell-made scaffold assembly and deposition, resulting in intact ECM that preserves tissue composition and architecture, with enhanced cell-instructive properties like anisotropy. Beyond passive scaffolds, CAM dynamically regulates cellular behaviours via mechanotransduction, emphasising the value of advanced *in vitro* 3D models. While CAM replicates biochemical and some structural ECM features, it lacks full hierarchical complexity and mechanical properties of native tissue. These cell-instructive properties influence CAM quality and functionality, shaped by cell-ECM interactions and modifiable through biophysical and biochemical cues for tissue engineering applications. To

study this, a co-culture platform of human dermal fibroblasts and H9c2 cardiomyoblasts was established at varying ratios. This approach aligns with findings from decellularised CAM scaffolds, which preserve key ECM components critical for cell adhesion and growth. CAM scaffolds similarly support H9c2 proliferation, providing a fully cellular, immunogenically safe, biologically native substrate that enhances cell signalling and enables physiologically relevant tissue models.

Keywords: *tissue engineering, three-dimensional skin model, organotypic culture, biomaterials, cell-assembled extracellular matrix, co-culture*

ABSTRAKT

Živé tkáně jsou vysoce dynamické systémy, v nichž neustále probíhá a mění se řada strukturálních, mechanických, biochemických a biologických podnětů v rámci trojrozměrné struktury. Buňky a tkáňové scaffoldy (extracelulární matrix) hrají rozhodující a synergickou roli nejen při tvorbě architektury tkáně, ale také při udržování její fyziologické funkce. Proto musí být při přípravě rekonstituovaných tkání splněna úloha jak buněk, tak i scaffoldů. Jedná se o dynamickou, multidisciplinární oblast výzkumu, kde jsou modely v závěru použitelné pro tkáňové inženýrství a regenerativní medicínu, modelování nemocí a případné experimenty *in vitro*. V rámci práce je hlavní pozornost věnována rekonstituovaným trojrozměrným (3D) modelům kůže. Modely by tedy měly umožnit rekonctituci architektury kožní tkáně a jejího mikroprostředí, umožnit zkoumání interakce buňka-matrix a mezi různými typy kožních buněk, a koneckonců i funkci a fyziologii kožní tkáně *in vivo*. V případě trojrozměrných modelů kůže se jedná o *in vitro* ko-kultivační systém lidských neonatálních keratinocytů pěstovaných na rozhraní vzduch-kapalina na kolagenovém gelu společně s lidskými dermálními fibroblasty. Dermální složka kožních modelů tedy zahrnuje lidské dermální fibroblasty zapuštěné v hydrogelu kolagenu typu I odvozeného z ocasu potkana. Kolagen představuje výchozí "nosič", ale bez 3D architektury. Následná kultivace na rozhraní vzduch-kapalina se lidské epidermální keratinocyty diferencují do vícevrstevné epidermis. Cílem práce je objasnit přípravu kolagenové vrstvy a následné zajištění správné ko-kultivace fibroblasty-keratinocyty s výsledkem vytvořeného plně funkčního kožního ekvivalentu in vitro.

Bez ohledu na to mohou být buňky kožní tkáně, respektive dermální fibroblasty, použity jako scaffoldy extracelulární matrix samosestavené z fibroblastových buněk (CAM). Tato metodika využívá vlastní schopnost buněk produkovat vlastní extracelulární matrix (ECM), místo použití syntetických nebo přírodních materiálů jako scaffold. CAM scaffold může být vytvořen a řízen i vnějšími faktory, jako je mechanická stimulace. V této práci byly kultivovány lidské kožní fibroblasty za podmínek *in vitro* s kyselinou askorbovou, podporující tvorbu ECM. Výsledkem je neporušená ECM, která zachovává složení a strukturu původní tkáně a zároveň vykazuje vylepšené vlastnosti pro řízení buněčného chování, například anizotropii. CAM sheet nejsou jen pouze pasivními strukturami, ale dynamicky regulují buněčné procesy prostřednictvím mechanotransdukce, což podtrhuje význam pokročilých 3D *in vitro* modelů. Přestože CAM dokáže věrně napodobit biochemické a některé strukturální rysy ECM, postrádá plnou hierarchickou složitost a mechanické vlastnosti přirozené tkáně. Tyto instruktivní vlastnosti buněk poté ovlivňují kvalitu a funkčnost CAM scaffoldů a jsou utvářeny interakcemi mezi buňkami a ECM, které lze modulovat

pomocí biochemických a biofyzikálních signálů pro potřeby tkáňového inženýrství. Pro studium těchto interakcí jsme vytvořili ko-kultivační platformu, kde byly lidské dermální fibroblasty kultivovány společně s H9c2 kardiomyoblasty v různých poměrech. Tento přístup koresponduje s výsledky studií na decelularizovaných CAM, které zachovávají klíčové složky extracelulární matrix zásadní pro buněčnou adhezi a růst. CAM scaffoldy obdobně podporují proliferaci buněčné linie H9c2, poskytují plně buněčný, imunologicky bezpečný a biologicky přirozený substrát, který zlepšuje buněčné signály a umožňuje tvorbu fyziologicky relevantních tkáňových modelů.

Klíčová slova: *tkáňové inženýrství, trojrozměrný model kůže, organotypická kultura, biomateriály, extracelulární matrix sestavená z buněk, kokultivace*

TABLE OF CONTENT

ACKNOWLEDGEMENT 3
ABSTRACT 4
ABSTRAKT 6
TABLE OF CONTENT 8
1. INTRODUCTION 11
2. FUNDAMENTALS OF SKIN TISSUE ENGINEERING 14
2.1 Anatomy and Physiology of the Skin 14
2.1.1 Embryonic Origins of Skin 15
2.1.2 Epidermis 17
2.1.3 Dermis 20
2.2 The Role of Fibroblasts and Keratinocytes in Cellular Dynamics of the Skin Tissue 21
2.2.1 Fibroblast of the Skin 21
2.2.2 Role of Fibroblasts within the 3D Matrices 23
2.2.3 Keratinocytes' Role in Skin Function 24
2.2.4 Keratinocytes in 3D Skin Model 26
3. THREE-DIMENSIONAL SKIN MODELS 27
3.1 Overview of 3D Skin Models 28
3.1.1 Skin Organoids 29
3.1.2 3D Skin-on-a-chip 30
3.1.3 3D *in vitro* Skin Models 30
Reconstructed Human Epidermis Model (RHEs) 31
Human Skin Equivalents (HSEs) 32
3.2 Polymicrobial Skin Models 34
3.2.1 Microorganisms play a crucial role in maintaining human skin health 34
3.2.2 Polymicrobial Interactions 35
3.2.3 Importance in Studying Host-Microbe Interactions 37
3.2.4 Challenges in Modeling Polymicrobial Skin 38
4. CELL-ASSEMBLED EXTRACELLULAR MATRIX (CAM) PRODUCTION 40

4.1 Extracellular Matrix Composition and Function 40
4.2 Techniques for Cell-Assembled ECM 42
4.3 Co-cultivation Systems for Enhanced ECM Production 43
4.4 Applications in Tissue Engineering 45
5. AIM OF DOCTORAL THESIS 47
6. EXPERIMENTAL PART 49
6.1 Cell line maintenance 49
6.1.1 Human Dermal Fibroblast 49
6.1.2 Spontaneously Transformed Human Keratinocyte 49
6.1.3 Embryonic Rat Cardiomyocytes 49
6.2 Bacterial cell culture methods 51
6.2.1 Bacterial strains 51
6.2.2 Bacteria culture conditions 51
6.2.3 Preparation of bacteria supernatants 51
6.3 Construction of 3D Normal Skin Tissue Models 52
6.3.1 Preparation of the Acellular Collagen Hydrogel 53
6.3.2 Fabrication of the Cellular Part of 3D Skin Equivalents 54
6.4 Histological analysis 56
6.5 *In vitro* Skin Irritation Test Using 3D Normal Skin Model 57
6.6 The influence of the microbiome on skin cell lines 59
6.6.1 Trypan Blue staining viability test 59
6.6.2 HaCaT proliferation assay 59
6.6.3 HaCaT co-culture with bacteria cells 61
6.7 *In vitro* mixed infection 3D skin model 62
6.7.1 3D Skin Model 62
6.7.2 Bacteria colonization of the 3D Skin Model 62
6.7.3 *In vitro* infection 3D Skin model cytotoxicity 62
6.7.4 Determination of 3D skin model bacteria colonization 63
6.8 CAM sheet production 64
6.8.1 Human dermal fibroblast culture and CAM production 64
6.8.2 CAM devitalization/decellularization 65
6.8.3 Assessing H9c2 cell line proliferation using CAM sheets 65

6.8.4 Histological analysis of CAM sheets....66
6.8.5 Preparation of CAM co-culture platform....66
6.9 Investigating the CAM sheet components....67
6.9.1 RNA isolation and qRT-PCR reaction....67
6.9.2 SDS-PAGE electrophoresis....71
Preparation for SDS–PAGE electrophoresis....71
CAM sheet sample preparation and SDS-PAGE electrophoresis....72
6.9.3 Semi-dry Western Blotting....72
6.9.4 Immunodetection....73
6.10 *In vitro* cultivation chamber....74
7. SUMMARY OF RESULTS....75
7.1 Establishment of an *in vitro* 3D Skin Culture Model....76
7.2 Bacterial behavior on HaCaT monolayers as a foundation for 3D skin model experiments....83
7.2.1 HaCaT viability and proliferation in the presence of microbiome....84
7.2.2 The influence of bacteria adhesion on HaCaT cell line....87
7.3 Fabrication of CAM sheets as cell-made scaffolds....89
7.3.1 CAM sheets generation....89
7.3.2 Impact of HDF-H9c2 co-culture on CAM scaffold generation and biochemical and molecular evaluation of CAM....90
7.4 Characterization and biological evaluation of advanced polymeric materials....94
8. CONTRIBUTION TO SCIENCE....96
REFERENCES....98
LIST OF FIGURES....120
LIST OF TABLES....122
LIST OF ABBREVIATIONS AND SYMBOLS....123
CURRICULUM VITAE....124
LIST OF PUBLICATIONS....127

1. INTRODUCTION

Tissue engineering and regenerative medicine (TERM) represent an interdisciplinary field that seamlessly marries principles from biology, engineering, and medicine to innovate therapeutic strategies capable of restoring, repairing, or even replacing damaged tissues (Auxenfans *et al.* 2009). In this realm, TERM applications commonly encompass 3D scaffolds for providing a suitable microenvironment for the incorporation of cells and supporting factors to regenerate damaged tissues/organs. These scaffolds, in the 3D scale, can serve as architectural frameworks providing suitable microenvironments with mechanical support, and physical, or biochemical stimuli for optimal cell growth and function. It facilitates the organization and growth of cells, ultimately leading to the formation of functional tissues. Critically, the seeded cells adhere to the scaffold and are cultured under controlled conditions, allowing them to proliferate and organize into tissue-specific structures (Loh and Choong 2013; Choudhury and Das 2020). Skin substitutes are nowadays commercially available. There are many types of skin derivatives, including acellular forms, containing scaffolds - the matrix based on natural or synthetic materials with the required physical and chemical structure allowing easy access to host cells. Furthermore, cellular products with or without matrix include cell sheets, tissue constructs or replacements, and tissue equivalents (Zhong, Zhang, and Lim 2010; Lanza, Langer, and Vacanti 2007).

The development of *in vitro* reconstituted skin models to mimic living tissue is important for investigating therapeutic approaches. It can also mitigate animal testing and bridge the inter-species translational gap. Reconstituted tissue models from cells and extracellular matrix (ECM) simulates natural tissues. It provides simplified biological systems to study cell-matrix interactions in tissue development and wound healing (Watakatsuki *et al.* 2000).

Skin is an essential complex organ of the human body. Skin structure consists of two components. It is the multistratified epidermis consisting of the basal, spinous, granular, and cornified strata, and the second one is the dermis. It is the upper-most part of the skin which can be very interesting for the study of barrier properties (Gangatikar *et al.* 2007). The first developed skin co-cultures used two-dimensional cultivation as a feeder layer for seeding the cells, concretely - the combination of keratinocytes and fibroblasts. The problematic part of this skin tissue cultivation is the limitation of the stratification and partial differentiation of the keratinocytes and overall, the complex cellular response due to the lack of 3D tissue architecture. Accordingly, developments over the last decade have allowed construction of the tissue-engineered models that can simulate native skin. This model is known as skin equivalent (SE) (Fell 2016; Garlick 2006; Laurent and

Denesvre 2021). The SE model consists of 2 parts: the first is an acellular collagen layer in combination with a dermal component of fibroblasts embedded in a collagen matrix, and the second is an epidermal component of differentiated keratinocytes. In this type of SE, the acellular collagen layer with the dermal component is cultured to form a platform for keratinocytes. Keratinocytes are seeded onto cell culture inserts and cultured submerged in a culture medium to allow the keratinocytes to proliferate. The construct is then subjected to the air-liquid interface, thus encouraging the differentiation of keratinocytes (Niehues *et al.* 2008).

The knowledge of the SE has an important impact on facilitating the experimental system's progression to study skin biology and its potential diseases. Historically, various skin cell types have been studied using two-dimensional (2D) cultivation, but still individually as a monolayer system. The cultivation did not capture the complexity of the *in vivo* microenvironment and possible cell-cell interactions. Besides, it was found that there were significant differences in cell migration, proliferating, extracellular matrix synthesis, cellular signaling, and responses to various stimuli in the case of the cultivation of the same skin tissue cells under 2D or 3D culture conditions. Therefore, it is important to embrace the complex 3D environment for spreading and migration of the skin cells to create the appropriate SE (Eberlin *et al.* 2020; Stark *et al.* 2004; Choudhury and Das 2020).

In this thesis, we employed the representatives of the traditional scaffold-free Transwell chamber system approach. The experiment was designed to evaluate possible interactions between the collagen layer and cells for the development of a highly adaptable skin organotypic culture model. In addition, a possible method for gaining knowledge about the dynamic skin equivalent interactions in the combination of the resident microbes is to develop a polymicrobial skin model. An identical skin equivalent is assembled, enriched with a component of skin microbiota and possible pathogens. The scaffold-free 3D skin model was then used for cell cytotoxicity and biochemical analysis, skin irritation testing with high-throughput cell function, and testing the safety of cosmetic applications and pharmaceutical studies of pathogens or probiotics.

Moreover, SE and other skin tissue engineering-related products have breakthrough potential and are currently the focus of extensive worldwide research. A breakthrough technology can be a cell-assembled extracellular matrix (CAM) produced *in vitro* by normal adult skin fibroblasts (Potart *et al.* 2023). Dermal fibroblast cells for CAM sheet production are readily available in the skin, making them easily accessible for isolation and culture. In addition, the dermal fibroblast cells are well-known for their role in producing ECM components in the body. Overall, the use of dermal fibroblast cells for CAM production is

a strategic choice that is consistent with mimicking the native tissue environment. These cells deposit ECM components in a manner that closely mimics the structure and composition of healthy tissue. The versatility of the CAM material allows it to be applied across a broad range of regenerative medicine applications, without being restricted to a specific tissue or organ system (Kawecki *et al.* 2024; Borchiellini *et. al.* 2023).

In a recent experiment, we obtained a biological ECM-enriched scaffold made of CAM material, which favorably preserves the composition and architecture of the original tissue in a controlled manner. Moreover, we enriched this experiment by performing a co-culture of human dermal fibroblasts with cardiomyoblasts in defined ratios, thereby creating a novel type of CAM sheet. This long-term culture system resulted in tissue-like structures with enhanced cell-instructive properties. The CAM sheet material was finally analyzed using biochemical and molecular analysis confirming the structural and functional properties of the CAM scaffold.

2. FUNDAMENTALS OF SKIN TISSUE ENGINEERING

2.1 Anatomy and Physiology of the Skin

The skin is the largest vital and the most visible organ of the human body. The main function of the skin is to act as a barrier, protecting the internal environment from the essentially hostile, external environment. As a total barrier, it can be also permeable to many substances including chemicals, drugs, perfumes, or dyes with which we may be in frequent contact. Apart from protection, the skin plays a critical role in the control of body functions, such as thermoregulation and assistance in the control of blood pressure. It contains numerous sensory receptors and has endocrine functions or synthesis of vitamin D possibility (Casey 2002).

The integumentary system of skin is accounting for about 15 % of the total adult body weight and is formed by the skin and its derivative structures, as seen in Figure 1. (Kolarsick P., Kolarsick A. and Goodwin 2011)

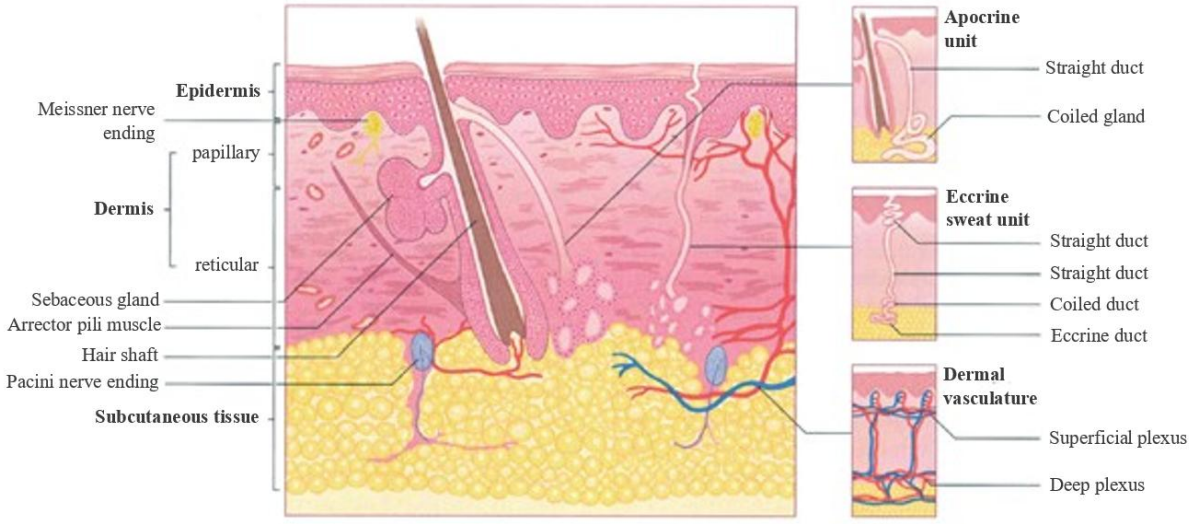

Figure 1: Structure of the skin (Kolarsick P., Kolarsick A. and Goodwin 2011)

Human skin is a complex organ made up of 3 layers (epidermis, dermis, and hypodermis), cell layers, and cell types whose primary function is to act as a barrier preventing dehydration and keep most chemicals, toxins, bacteria, and viruses out of the body. Skin mainly consists of dermal and epidermal tissues (Eberlin *et al.* 2020).

2.1.1 Embryonic Origins of Skin

Supposing the creation of the functioning organ, or even an entire organism, a precise temporal and topical schedule of the interaction of all the signaling molecules involved in development must be maintained. In the case of embryonic skin development, it begins to form already at the interface of the 1st and 2nd months from the two germinal layers of the embryo - ectoderm and mesoderm. The epidermis and the nervous system develop from the ectoderm. The mesoderm and then the mesenchyme are the source of the development of the dermis and subcutis. (Koster and Roop 2007).

After the gastrulation process, the embryo surface is established as a single layer of neuroectoderm. It ultimately specifies the nervous system and skin epithelium. The fate of the neural and epidermal ectodermal cell creation is based on the effects of Wnt, fibroblast growth factor (FGF), and bone morphogenetic protein (BMP) signalling following gastrulation. The fate of the neural and epidermal ectodermal cell creation is based on the effects of Wnt/β-catenin („Wingless-related integration site“), FGF, and BMP signaling following gastrulation. Wnt signaling can block the ability of the ectoderm to respond to FGF. FGFs are a family of polypeptide growth factors required for neural induction (Hu *et al.* 2018; Böttcher and Niehrs 2005). In the case of FGF absence, the cells express BMP, and the cells are committed to differentiate into the epidermis, resulting in a single layer of multipotent epithelial cells. This layer is covered by a transient protective layer of tightly connected squamous endodermis-like cells. Such a layer, named a periderm, is shed after the epidermis stratification and differentiation. Opposite, in the absence of Wnt signaling, the embryonic ectoderm can accept activating cues by FGF, which then attenuate the BMP effect through inhibitory cues (Stern 2005; Fuchs 2007). The signaling steps are visible in Figure 2.

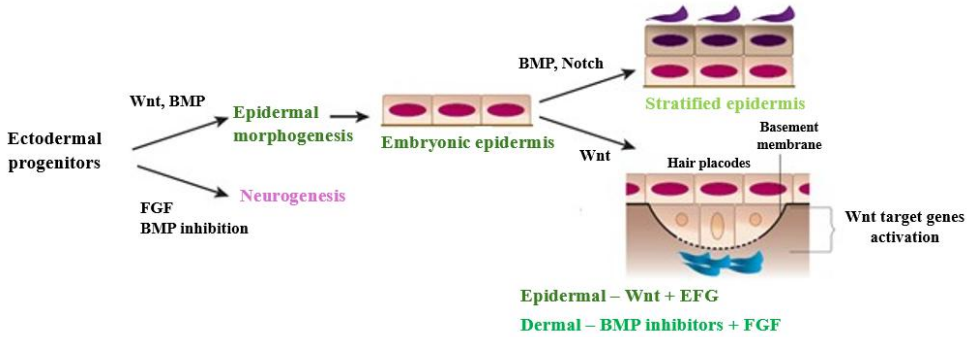

Figure 2: Signalling steps in the specification of embryonic skin (Fuchs 2007)

The mutual interaction of epidermal and dermal structures is also significant. As with other organs, it is distinguished between the periods of organogenesis,

histogenesis, and maturation in the development of the skin (Liu *et al.* 2013). Individual layers are formed during organogenesis, and the basement membrane and adnexa also begin to develop. Simultaneously, precursors of melanocytes and Langerhans cells migrate into the skin, and the first blood vessels also appear in the future area between the dermis and subcutaneous tissue. Nevertheless, the boundary between the skin and the underlying muscles is invisible (Liu *et al.* 2013; Hoath *et al.* 2014). In the subsequent period of histogenesis, there is a stratification of the epidermis, a division of mesenchymal structures into a layer of dermis and hypodermis. Glands, hair follicles, and nails are also formed. Vegetative innervation, follicles, and sweat glands continue to develop. Specialized nerve endings responsible for tactile sensation are also created. Melanin is produced by melanocytes. Finally, the dermis is distinctly cellular and contains a few thin fibers and abundant water. Fat cells differentiate in the subcutaneous tissue. The last period is the maturation of the skin. The final stages occur after the transition to an external environment with lower temperature, humidity, and the presence of pathogens (Pispa and Thesleff 2003; Mikkola 2007; Ness *et al.* 2013).

At this end of embryonic development, the maturity of the interfollicular epidermis (IFE) is reached. The multipotent epithelial cells in the surface ectoderm create the embryonic epidermal basal layer of the stratifying epidermis. It rises into all structures of the future epidermis (Lawron and Kaur 2015). The whole process is followed by the development of the basement membrane, which separates the epidermis from the dermis and provides epidermal basal cells with growth factors. The proteins p63 and Notch are expressed in the basal layer, which is important for the initiation of epithelial stratification. Above the basal layer lies the outer squamous layer, the so-called periderm, as seen in Figure 3 (Hu *et al.* 2018). The cells of the basal layer proliferate, they form an ‘intermediate layer’ of cells under the periderm. This intermediate layer is transient and exists only in embryonic skin. Next, the layer is divided into spinous cells. Keratinocytes express basic structural proteins - keratins K - intermediate filaments of epithelia at this period. The expression has happened in the intermediate layer and spinous cells express keratin K1 induced by Notch signalling. Notch signalling leads the spinous cells to differentiate and migrate toward the surface of the skin to form

the granular layer and cornified layer. Notch signaling is important for initiating terminal differentiation of embryonic skin (Kim *et al.* 2006; Hu *et al.* 2018).

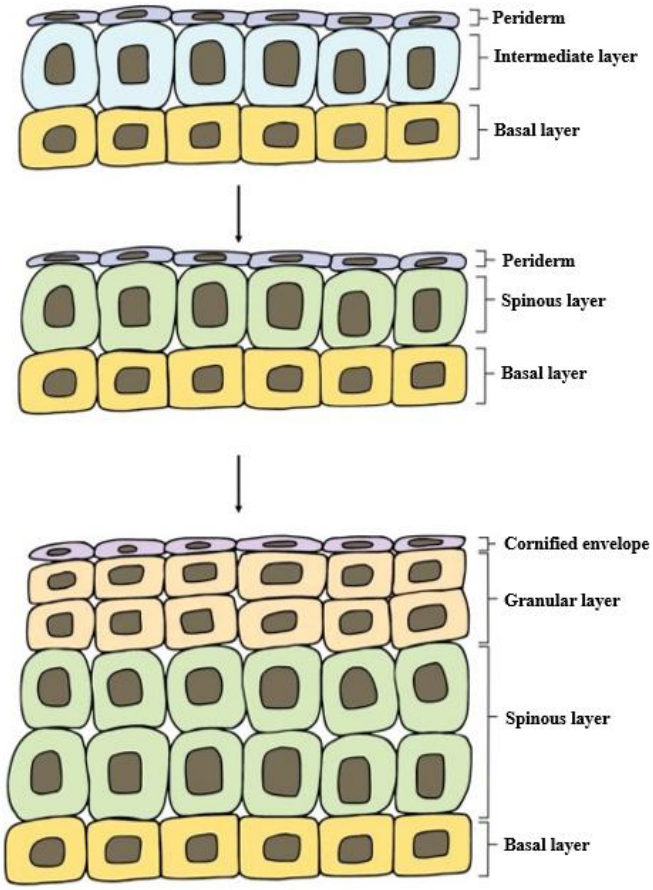

Figure 3: Embryonic skin maturing (adapted from Hu et al. 2018),

2.1.2 Epidermis

The epidermis is defined as the outermost layer of the skin and consists of a basal layer, which is at the bottom of the epidermis, and a suprabasal layer (the upper part of the epidermis). The epidermis is commonly divided into four layers according to the morphology and position of the keratinocytes. Based on the differentiation of the keratinocytes, they can be referred to as the basal cell layer (*stratum germinativum*), the squamous cell layer (*stratum spinosum*), the granular cell layer (*stratum granulosum*), and the cornified or horny cell layer (*stratum corneum*) (James *et al.* 2006).

This part of the skin morphology performs several functions. The cell layers of the epidermis are derived from germinative cells in the basal layer. This part contains the skin´s stem cell-generating the daughter cells. The daughter cells emerge from the basal layer and mature. Eventually, these cells develop protein bridges to each other, creating cell-cell communication. This connection gives the

layer a typical spiny contour - *stratum spinosum* (Kenneth and Roberts 2019). Additionally, depending on differentiation and stratification status, a suprabasal layer is also further divided into three different sublayers, which contain cells that play important roles in the skin. These include pigment-producing melanocytes, immune Langerhans cells, and touch-receptor Merkel cells (Díaz-García *et al.* 2021).

The spinous cell layer is located between the *stratum granulosum* and the *stratum basale* of the epidermis. It consists of a single layer of columnar or cuboidal cells with a large nucleus that is constantly dividing by mitosis to replenish the upper layers of the epidermis. Each cell is connected to the others through desmosome and hemidesmosome connections (Yadav *et al.* 2019). This layer is involved in providing strength and support to the epidermis. Cells in the *stratum spinosum* also begin to produce keratin, a tough fibrous protein that contributes to the structural integrity of the skin. This protein is produced by keratinocytes (Lai-Cheong and McGrath 2017). The keratinocytes differ from the "clear" dendritic cells by possessing intercellular bridges and ample amounts of stainable cytoplasm. Located in the basal layer of the epidermis, these types of keratinocytes can retain a stem cell-like property and thus support continuous cell division. Figure 4 shows the initiation of a differentiation program, as keratinocytes gradually exit the cell cycle and enter a terminally differentiated state. The differentiation process occurs during cell migration from the basal layer to the surface of the skin (Choi and Lee 2015; Roger *et al.* 2019).

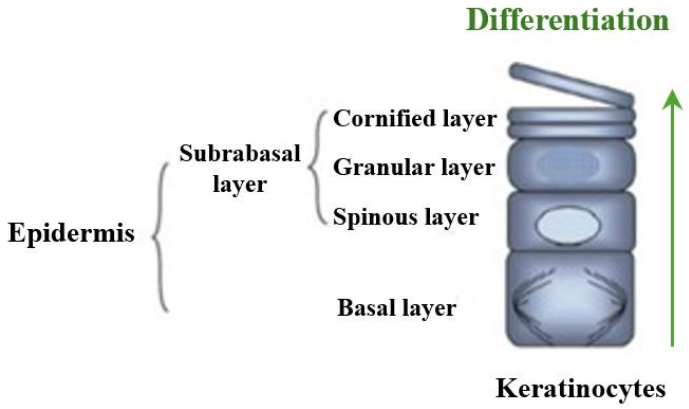

Figure 4: Schematic diagram of normal keratinocytes in different layers of the epidermal tissue. An arrow indicates the direction and levels of epithelial differentiation (Choi and Lee 2015)

As the keratinocyte cells move from the *stratum basale* to the *stratum spinosum*, their shape becomes more rounded and they can synthesize differentiation-specific keratins and other early differentiation markers (e.g. involucrin) (Lai-Cheong and McGrath, 2017).

The following structure is the granulosum layer. The cells in this layer are characterized by containing granules filled with keratohyalin, a protein that helps to bind keratin filaments together and form keratin fibers. These cells are undergoing apoptosis, and the cytoplasm is starting to fill with keratin. (Yadav *et al.* 2019;). Keratohyalin secretes the keratin proteins tonofilaments and filaggrin which together form pre-keratin structures called tonofibrils. These structures play an important role in keratinization (Bragulla and Falabella 2001). Keratohyalin granules contain predominantly profillagrin and loricrin. They are two important structural components in the formation of the cornified envelope in subsequent layers. It serves as a storage or transport compartment for a multitude of lipids, enzymes, and proteases. Secretion is equally important for the formation of a functional barrier in the next layer - the stratum corneum. Thus, the stratum granulosum is important for the waterproofing and barrier function of the skin (Kenneth and Roberts 2019).

The outermost layer of the epidermis, *stratum corneum*, is made up of several layers of flattened, dead cells called corneocytes. These cells are filled with keratin. They lose their cellular organelles, and the contents of the cell are consolidated into a mixture of filaments and amorphous cell envelopes. The process of maturation leading to cell death is known as terminal differentiation (Montagna 1974; Yadav *et al.* 2019). Keratinocytes shed their intracellular contents and transform into tightly packed, flattened cells. This keratinocyte morphology can be facilitated by the collapse and aggregation of intermediate filaments with supporting proteolytically cleaved filaggrin. Keratinocytes are constantly being shed from the skin surface by a process called desquamation. This process is facilitated by the degradation of corneodesmosomal components (desmoglein and corneodesmosin) by serine proteases (Laly *et al.* 2021)
The *stratum corneum* acts as a barrier to protect the body from external threats such as pathogens, UV radiation, and water loss. The key aspect of the epidermal permeability barrier function is provided by lipid lamellae. It is formed by cholesterol, ceramides, and free fatty acids that surround the protein components of the cornified envelope. In addition, the incorporation of antimicrobial peptides, such as beta-defensins and cathelicidins, provides a microbial barrier. Each layer of the epidermis plays a vital role in maintaining the integrity and function of the skin, ensuring that it remains resilient and able to fulfill its protective functions (Roger *et al.* 2019).

The epidermis is a continually renewing layer. It also arises derivative structures, such as the pilosebaceous apparatuses, nails, and sweat glands from

here. The basal cells of the epidermis undergo cycles of proliferation that can provide renewal of the outer epidermis. It is a dynamic structure in which cells are constantly in unsynchronized motion, as differing individual cell populations not only pass each other but also move towards the skin surface (melanocytes, Langerhans cells) (Kolarsick P., Kolarsick A. and Goodwin 2011).

2.1.3 Dermis

The dermis is a critical component of the body, providing the nutritive, immune, and other support systems for the epidermis, through a thin papillary layer adjacent to the epidermis. The dermis comprises the bulk of the skin and provides pliability, elasticity, and tensile strength. It protects the body from mechanical injury and binds water. It also plays a role in regulating temperature, pressure, and pain. The dermis interacts with the epidermis to maintain the properties of both tissues. There is a dermal-epidermal junction, where the epidermis and dermis work together during development in morphogenesis and with the epidermal appendages in repairing and remodeling the skin as wounds heal.

The dermis is composed of collagen fibers (70 %), which provide a scaffold for support and cushioning. There is also elastic connective tissue which provides elasticity in a semi-gel matrix of mucopolysaccharides. In general, the dermis has a sparse cell population. The main cells present are the fibroblasts, which produce the connective tissue components of collagen, laminin, fibronectin, and vitronectin. The next cell type is mast cells, which are involved in the immune and inflammatory responses, and melanocytes, which are involved in the production of the pigment melanin (Walters and Roberts 2002; Kolarsick P., Kolarsick A., and Goodwin 2011).

2.2 The Role of Fibroblasts and Keratinocytes in Cellular Dynamics of the Skin Tissue

2.2.1 Fibroblast of the Skin

Fibroblasts can be defined as mesenchymal cells that create and maintain an anatomically diverse array of ECM-rich connective tissues. However, fibroblasts exhibit a high degree of heterogeneity. They are found in different tissues at different stages of development. Moreover, fibroblasts serve essential organ functions, like resistance to injuries, especially in the skin, or stretching/elastic recoiling of the organs. It provides positional information for neighboring cells using microarchitectural, biomechanical, and biochemical cues in the ECM, including the regulated secretion of soluble mediators such as cytokines, growth factors, and metabolites (Driskell and Watt 2014; Plikus *et al.* 2021).

In the case of skin tissue, fibroblasts are spindle-shaped cells found primarily in the dermis, the second layer of the skin. Their main function is the synthesis and deposition of collagen, the primary structural protein in connective tissue. Through their robust production of collagen, fibroblasts contribute significantly to the tensile strength and resilience of the skin, giving it the ability to withstand mechanical stress and maintain its structural integrity. In addition to the aforementioned function of synthesizing and secreting extracellular matrix molecules, growth factors, cytokines, and chemokines contribute to immune regulation and wound healing by influencing the migration and proliferation of keratinocytes. (Wong *et al.* 2007; Watt and Fujiwara 2011).

In addition to collagen, fibroblasts secrete various other components of the ECM, including elastin, fibronectin, and proteoglycans. Fibroblasts can create a foundation that supports the epithelial keratinocytes of the outward-facing stratified epidermis and its numerous appendages, primarily hair follicles and sweat glands. Fibroblast´s ECM creation as a connective tissue serves to deposit fiber-and sheet-forming collagens, proteoglycans, elastin, fibronectin, microfibrillar proteins, and laminins, which together form the microsome. It also actively re-modulate microstructure of the ECM through covalent cross-linking, protein glycosylation, and controlled proteolysis via the balanced secretion of modifying enzymes such as lysyl oxidase, matrix metalloproteinases (MMPs) and MMP inhibitors. There are three anatomically distinct layers formed by fibroblasts and other cells of the mesenchymal lineage. These are the papillary and reticular dermis and the dermal white adipose tissue (dWAT), as shown in Figure 5 (Sorell and Caplan 2009; Plikus *et al.* 2021). The epidermis and upper papillary dermis are separated by a sheet of collagen – and laminin-rich basement membrane, which is produced by the interplay between epidermal keratinocytes and papillary fibroblasts. Fibroblasts within the often very thick reticular dermis

produce the densely packed ECM that gives the skin its mechanical strength. All three dermal layers also contain immune cells, epidermal appendages, sensory neurons, blood and lymphatic vessels. The whole architecture forms a complex network of cell communities that collectively support the skin's protective functions (Driskell and Watt 2014).

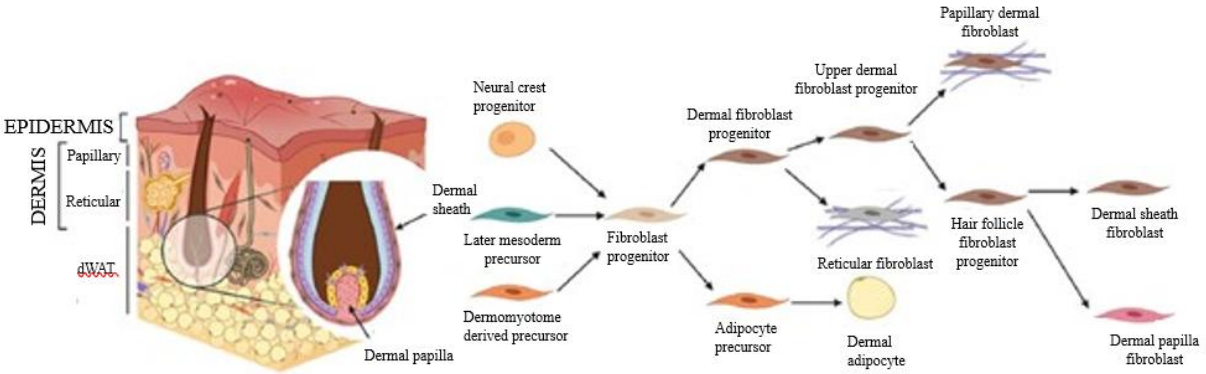

Figure 5: Skin-specific fibroblast organization and lineage relationships (Plikus et. al. 2021)

The synthesis and deposition of new collagen and ECM components play a key role in the wound-healing process. Mobilized to the site of injury, fibroblasts proliferate and migrate into the wound bed. This activity not only promotes tissue repair and regeneration but also contributes to the formation of scar tissue, which serves as a temporary scaffold for tissue remodelling and reconstruction (Wong *et al.* 2007). Beyond their role in tissue repair, fibroblasts are actively involved in the regulation of inflammation and immune responses within the skin. By secreting cytokines, chemokines and other signaling molecules, fibroblasts modulate the activity of immune cells – macrophages, neutrophils and lymphocytes. In doing so, they influence the immune milieu within the skin and contribute to the maintenance of immune homeostasis and resolution of inflammatory processes, ensuring the maintenance of skin health or function (Bello *et al*. 2001).

All these aspects orchestrate a myriad of processes essential for the maintenance of skin structure, function, and homeostasis. Fibroblast biology and its interactions within the skin microenvironment hold great promise for the development of novel therapeutic strategies for various skin diseases and conditions (Lim 2021).

2.2.2 Role of Fibroblasts within the 3D Matrices

As already mentioned, fibroblasts are the primary cell type responsible for unique properties, especially collagen synthesis and the buildup of connective tissue. Furthermore, the cells themselves are responsible for normal tissue homeostatic processes, including tissue repair in response to injury, fibrosis, or cancer progression. Moreover, fibroblast-ECM remodeling is a pivotal design element in tissue engineering (Rhee 2009). Skin fibroblasts contribute significantly to the formation, organization, and function of skin-like structures within 3D matrices. 3D culture systems are typically used to mimic the natural ECM features found in vivo. They are manufactured to provide a tissue-like environment for cells cultured under in vitro conditions. Very often, fibroblasts are cultured in a 3D collagen matrix environment and have unique morphologies ranging from dendritic to bipolar depending on the stiffness and tension of the matrix. Due to this construction, fibroblasts associate with collagen fibrils, which develop reciprocal mechanical interactions with the collagen matrix. This leads to interactions between the cells and the collagen matrix and formulates the mechanical entanglement between the fibroblast and the surrounding matrix. Finally, the junction induces local and global remodeling of the fibroblast-collagen matrix to achieve tensile homeostasis (Grinnell 2003; Joe *et al.* 2022).

Fibroblasts in 3D skin models are primarily responsible for synthesizing and organizing the ECM components that constitute the dermal layer. They deposit these ECM molecules in a spatially organized manner. It resembles the native dermis. The linkage of the fibroblast with the collagen matrix can synthesize new collagen as a part of ECM and regulate its deposition, cross-linking, and turnover processes. This dynamic remodeling by fibroblasts helps to maintain the mechanical properties and architecture of the engineered skin tissue, which is essential for its functionality. Furthermore, fibroblasts interact with the ECM and neighboring cells within 3D skin models through cell-matrix adhesions, cell-cell contacts, and paracrine signaling pathways. These interactions regulate fibroblast behavior, ECM remodeling, and cell differentiation, contributing to tissue organization and function. Fibroblasts also secrete growth factors, cytokines, and extracellular vesicles that modulate cellular responses and tissue morphogenesis in the engineered skin tissue. Overall, combination fibroblast-collagen used as the first platform in 3D skin matrices are indispensable for the structural organization, mechanical properties, and functionality of 3D skin models. Their role in all these aspects makes them essential for mimicking the complexity and functionality of *in vitro* skin tissue (Grinnell 2008; Rhee 2009; Joe *et al.* 2022).

2.2.3 Keratinocytes' Role in Skin Function

Keratinocytes are the predominant cell type in the epidermis constituting the outermost layer of the skin. They are responsible for forming the epidermal barrier, which serves as the first line of defense against environmental insults, pathogens, and UV radiation (Komine *et al.*2021).

Epidermal keratinocytes form a stratified epithelium. Gradual differentiation occurs through the layers – from basal, spinous and granular to the cornified layer. Keratinocytes have different characteristics depending on their function and state of differentiation. As keratinocytes mature, they undergo a process called keratinisation, during which they produce and accumulate the protein keratin. This process results in the formation of multiple layers of dead, flattened cells filled with keratin, known as the stratum corneum. The stratum corneum acts as a waterproof barrier, preventing excessive water loss from the body and protecting underlying tissues (Gutowska-Owsiak et al.2020). It maintains skin hydration by regulating the production and distribution of lipids within the epidermis. Lipids produced by keratinocytes, such as ceramides, cholesterol and fatty acids, contribute to the formation of the skin's natural moisturising factor (NMF), which helps to retain water and maintain skin hydration. (Komine *et al.* 2021).

The primary and most important role of keratinocytes is to act as a physical barrier to the skin in addition to their role in responding to external stimuli. The formation of a functional skin barrier depends on keratinocyte differentiation and cornification. Cornification is a process that leads to programmed keratinocyte death, resulting in the formation of a cellular remnant known as a corneocyte (Eckert and Rocke 1989). The corneocytes, together with the inter-cornified cell lipids, form protective cell barriers and mechanical hardness for the inner body against harsh external environmental stimuli. Proteins, together with the corneocytes, help to strengthen the barrier by being incorporated into the insoluble cornified envelope (CE), also known as the cornified cell envelope (CCE). In addition, lipids support the elastic properties of the stratum corneum (Akiyama 2017; Gutowska-Owsiak *et al.*2020). Among the multiple processes in the epidermis, keratinocyte differentiation in vitro is reflected by multiple

morphological changes, which coincide at the organellar and molecular levels (Figure 6).

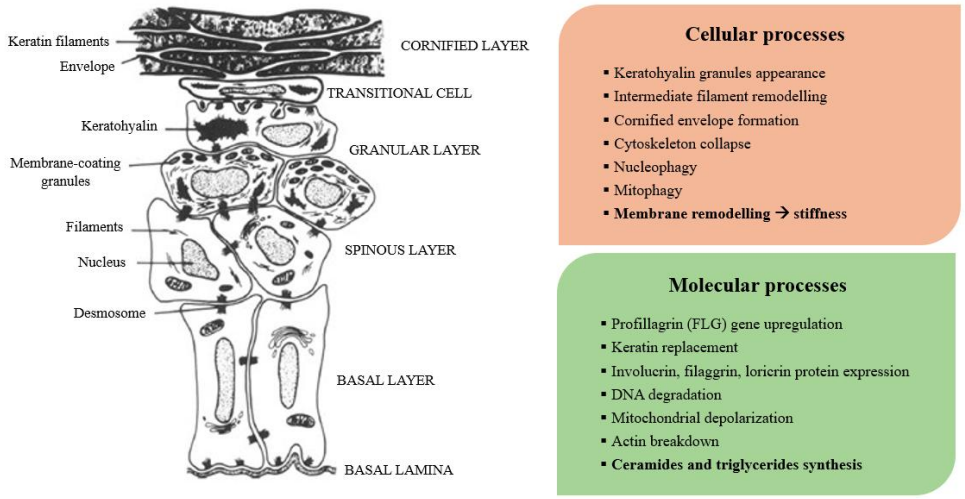

Figure 6: Keratinocytes differentiation process
(adapted from Eckert and Rocke 1989; Gutowska-Owsiak et al.2020)

These characteristics are reflected in multiple morphological changes (the cell shape and adherence) and distinct organellar transformations. For instance, the cornified cells upon catalysis by transglutaminase 1, form a cornified cell envelope. It is a strong structure composed of filaggrin that aggregates keratin filaments, with various protein components (involucrin, loricrin, SPR, and desmosomal proteins). This is a strong structure composed of filaggrin, which aggregates keratin filaments, with various protein components (involucrin, loricrin, SPR, and desmosomal proteins). There is also the appearance and maturation of keratohyalin granules, nuclear condensation and extrusion, cytoskeletal collapse, and alterations in mitochondria (Ipponjima *et al.* 2020). At the molecular level, shifts in cytokeratin expression have been observed, with keratins 5 and 14 gradually being replaced by keratins 1 and 10. At the same time, other proteins such as involucrin and transglutaminase are upregulated. The late envelope proteins (involucrin, filaggrin, loricrin) are also defined (Kirfiel and Herzog 2004; Poumay and Faway 2023).

2.2.4 Keratinocytes in 3D Skin Model

In 3D skin models, as well as in native skin, keratinocytes play essential roles in simulating the epidermal layer and thus contribute to the structural integrity, barrier function, and differentiation of the engineered skin tissue (Tahri *et al.* 2023).

Keratinocytes are mainly used to construct the skin surface and replace the missing epidermis. Simultaneously, fibroblasts are in the lower layer of 3D skin matrices to stimulate the dermis and create a comprehensive 3D model. Moreover, they secrete glycosaminoglycans, proteoglycans, and collagen to restore damaged tissue structure. This process can keratinocytes promote the healing process and help epidermal formation at the same time (Cai et al. 2023). The *in vitro* 3D culture of keratinocytes is commonly used as an essential research tool widely used for assaying dermal toxicity, pharmacological testing, and tissue repair to initiate the healing process and re-epithelization. In this process, keratinocytes relocate from the basement membrane to the stratum corneum during the keratinization. Keratin is then synthesized and facilitated to completely close the wound and promote epidermal regeneration during periods of inflammation (Randall *et al.* 2008). The collagen-based model supports the growth of keratinocytes and also fibroblasts and in connection with that cell behavior, organization, and requirements in the wound healing layer. This process, called re-epithelialization, is necessary for a successful wound closure. Morphologically, it is about the disassembling of the links between the basement membrane and the keratinocytes and the retraction of intracellular filaments to allow the propagation and formation of peripheral cytoplasmic actin filaments (Tahri *et al.* 2023). Keratinocytes become activated and migrate to the wound, where they start proliferating to fill the defect. They produce MMPs for loosening the adhesion of the keratinocyte to the dermal matrix thereby allowing re-epithelization. During wound healing, interactions between keratinocytes, fibroblasts, and immune cells are critical for a successful healing process, even so for creating successful 3D skin matrices (El Ghalbzouri *et al.* 2004).

3. THREE-DIMENSIONAL SKIN MODELS

Understanding the structure and composition of the skin is crucial in various fields including dermatology, cosmetics, and medical research. This includes cytotoxicity studies, drug targeting, testing testing of new therapeutics and treatment strategies (Bell *et al.* 1983, Reijnders *et al.* 2005). These areas of research require appropriate test systems. However, animal models are not ideal for these applications. Except for the ethical issue, the economical relevance is also important. Although some inexpensive species, such as rodents, are used, their skin composition is too different from human skin to be comparable. On the other hand, animals with more human-like skin – pigs – are too difficult to use on a regular basis, and there are also ethical reasons why animal models are becoming less attractive for skin research. (Mukherjee *et al.* 2022).

While traditional 2D cultivation provides valuable insights, a 3D model of native skin provides a more complete understanding of its intricate layers and components. This 2D culture environment lacks the natural 3D architecture of skin tissue. Cell-cell and cell-ECM interactions in 2D cultures are limited compared to 3D cultures, where cells typically form monolayers and may not fully recapitulate the complex cellular interactions found in native skin tissue. It is simpler and easier to manipulate, but may not accurately represent the physiological responses and behaviour of cells *in vivo*. A 3D model more closely represents the complexity of the skin's structure, and the structure typically represents the epidermis, dermis and subcutaneous tissue, with each layer contributing different characteristics to the overall function and appearance of the skin (Carlson *et al.* 2008; Saji *et al.* 2019).

In the case of the skin equivalent, it is composed of fibroblasts, collagen, and keratinocytes, and, like the native skin, the epithelium is stratified and differentiated. In addition to serving as an experimental model for studying skin development and other circumstances where the basement membrane disruption may have occurred, another potential benefit of this model is the ability to demonstrate epithelial dermal invasion and provide information on how epithelial organization is affected by the presence of alterations or experimental manipulations (Vaughan *et al.* 2009).

3.1 Overview of 3D Skin Models

Understanding healthy and diseased skin conditions is a significant advancement in many areas of basic and applied skin research from risk assessment of chemicals (including cosmetics) to offering versatile platforms for studying skin biology, disease mechanisms, and therapeutic interventions. Animal models are currently used extensively only in the preclinical phase of drug development for risk assessment and identification of the mode of action of drugs. The weakness of these tests is that they are poor predictors of human response due to differences in skin physiology and immunity. Moreover, the pharmaceutical and cosmetic industries are calling for the reduction, refinement, and replacement of animal testing, in particular the 7th Amendment to the EU Cosmetics Directive 76/768/EEC (European Commission (European Commission [online]; Idress *et al.* 2021; Jang *et al.* 2023). As a replacement can serve as human *ex vivo* skin explants and can be used for risk assessment and drug testing. A major drawback is the many experimental variables involved in testing skin biopsies and obtaining sufficient samples for experimental testing. This problem has led to the development of many in vitro skin culture models. These include spheroids as classic 3D models for skin research, 3D *in vitro* skin models or the development of 3D skin-on-chips and potential 3D skin bioprinting (Figure 7). (Mathes *et al.* 2014; van den Broek *et al.* 2017; Klicks *et al.* 2017)

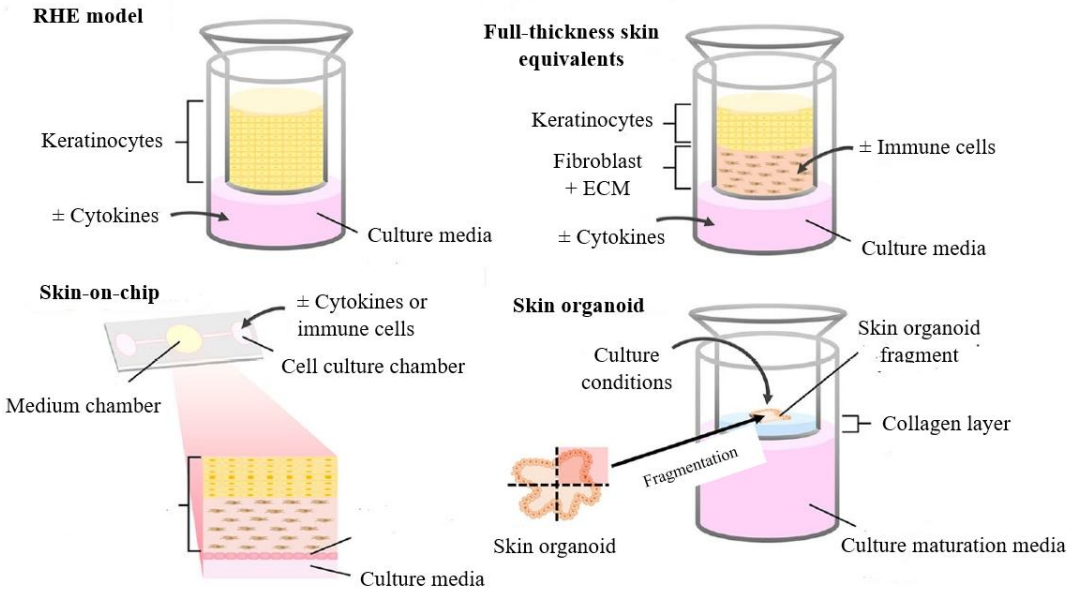

Figure 7: An overview of 3D skin models (Jang et al. 2023)

3.1.1 Skin Organoids

An organoid is characterized as a self-assembled organ-like tissue that resembles the functionality of an organ. It is composed of a variety of cell types. Organoids are typically derived from pluripotent stem cells (PSCs), or adult stem cells isolated from skin tissue. These cells are capable of self-organizing into structures that mimic the cellular composition and architecture of the skin, including the epidermis, dermis, and associated appendages such as sweat glands or hair follicles. It mimics fetal skin under treatment with growth factors such as FGF factor along with inhibitors for bone morphogenic protein and transforming growth factor-beta. Skin organoids can also respond to external stimuli such as UV radiation, pathogens, and pharmacological agents (Heo *et al.* 2022; Yan *et al.* 2023).

Skin organoids are cultured in specialized media containing growth factors and signaling molecules that promote cell proliferation, differentiation, and tissue morphogenesis. Skin organoids are mostly made by the hanging drop method or using non-adherent U-bottom-shaped plates. These culture conditions are carefully optimized to mimic the microenvironment of developing skin tissue *in vivo*. As a result of this culture optimization, organoids exhibit a high degree of structural complexity, with distinct layers of epidermal keratinocytes, dermal fibroblasts, and other specialized cell types arranged in a spatially organized manner. This architecture closely resembles that of native skin tissue, allowing for the study of cell-cell interactions, tissue morphogenesis, and barrier function. At this moment, there is a skin organoid created of HaCaT cells or fibroblasts co-cultured with melanoma cells in the format used to obtain tumor models. Nevertheless, skin cell organoids have limitations in achieving full differentiation and full layer stratification as for standard hydrogel or 3D printing models. A promising result has been reported with spherical skin microtissues called 3D InSight™ Skin Microtissue (InSphero, Schlieren, Switzerland). 3D InSight is composed of different keratinocyte layers and a dermal fibroblast core, which produces extracellular matrix proteins without the need for exogenous collagen (Klicks *et al.* 2017; Ho *et al.* 2018; Hong *et al.* 2023).

These miniature 3D structures faithfully recapitulate the complexity and functionality of native skin tissue making them invaluable for a wide range of applications in dermatology and regenerative medicine. By harnessing the regenerative potential of skin stem cells, organoid-based approaches may offer novel strategies for repairing damaged or diseased skin tissue, allowing researchers to study disease mechanisms, screen potential therapeutics and develop drug treatments (Hong *et al.* 2023).

3.1.2 3D Skin-on-a-chip

Skin-on-chip technology represents a microfluidic device made of silicone or polymer materials composed of several compartments or microchannels that mimic different layers of the skin. Skin-on-chip devices typically consist of microfluidic platforms. A cell culture chamber is constructed and lined with skin cells, including keratinocytes, fibroblasts, melanocytes, and immune cells, to mimic the cellular composition of native skin tissue. These cells are cultured on porous membranes/scaffolds to facilitate nutrient exchange and cell-cell interactions (Ponmozhi *et al.* 2021). The basic structure is the epidermal layer is separated from the dermal layer by placing a microporous membrane between those two compartments. This prevents keratinocytes and fibroblasts from mixing but allows nutrients to diffuse across the membrane. The chip allows for precise control over the flow of nutrients, media, and other substances to the cultured skin cells. These microfluidic systems enable dynamic culture conditions, including the perfusion of media and the application of mechanical forces, such as shear stress, to mimic physiological conditions (Risueño *et al.* 2021; Jang *et al.* 2023).

One of the critical aspects of skin-on-chip models is the recreation of the epidermal barrier function. The skin-on-chip system enables mechanical stimulation of skin cells. It means, that keratinocytes are cultured under controlled unidirectional media flow, which results in improved cell alignment with increased barrier integrity. These specialized culture conditions are employed to promote the formation of an intact stratum corneum, which acts as a barrier against the diffusion of molecules and pathogens (van den Broek *et al.* 2017). The potential of skin-on-chip can be used as a highly relevant platform for assessing the efficacy, safety, and toxicity of pharmaceutical compounds and cosmetic ingredients. These models allow researchers to evaluate drug permeability, metabolism, and adverse effects on the skin in a more physiologically relevant context than traditional cell culture or animal models (Lee *et al.* 2021).

3.1.3 3D *in vitro* Skin Models

As we mentioned above, the great challenge in the field of skin tissue engineering has been to create physiologically relevant *in vitro* skin models comprising all skin layers – epidermis, dermis, and subcutis. 3D *in vitro* skin models represent an important advancement in skin research, offering a more sophisticated platform compared to traditional 2D cell cultures, which have limitations such as the inability to develop a stratified epidermis and the absence of 3D multicellular interactions. Although the skin can be viewed as a 2D surface composed primarily of keratinocytes, 3D skin reconstitution is essential to accurately reflect the physiology of multi-layered human skin tissue (Choudhury *et al.* 2020; Jang *et al.* 2023). Therefore, these models aim to replicate the complex

architecture and cellular interactions of native human skin, providing valuable tools for studying skin biology, disease mechanisms, and drug responses. Two advanced in vitro skin models have been developed – reconstructed human epidermis (RHEs) and full-thickness human skin equivalents (HSEs). 3D tissue-engineered skin involves the construction of scaffolds that can reproduce the structure of an ECM into which to support dermal fibroblasts seeded, or scaffolds free where increased secretion of fibroblasts by the presence of ascorbic acid and giving rise to a well-organized dermal layer. Epidermal keratinocytes are then seeded onto the construct. A RHEs model consists only of keratinocytes, whereas the HSEs model possesses dermal and epidermal layers (Zhang and Michniak-Kohn 2012; Hoffmann *et. al.* 2023).

Reconstructed Human Epidermis Model (RHEs)

The RHE model is an advanced *in vitro* system designed to mimic the structure and function of the human epidermis, the outermost layer of the skin. Unlike the full-thickness skin model, the RHE consists of primary human keratinocytes isolated from skin biopsies or commercially available cell lines. The keratinocytes are seeded onto a 3D scaffold or matrix support made of synthetic/bio-materials such as collagen, fibrin, or agarose. This scaffold provides a framework for cell attachment and supports the keratinocytes' growth and differentiation. It only simulates the human epidermis (the epidermal substitutes) (Pedrosa *et al.* 2017). The RHE model exhibits a normal development into a stratified epithelium consisting of multiple layers of keratinocytes. These layers typically include the basal layer, spinous layer, granular layer, and cornified layer (*stratum corneum*), which closely resemble the layers of the native epidermis. The key feature of RHE models is their ability to form a functional barrier similar to the stratum corneum of native skin. RHE expresses differentiation markers characteristic of native epidermis, such as keratins (e.g., keratin 10 and 14), filaggrin, involucrin, and loricrin. The expression of these markers indicates the formation of terminally differentiated keratinocytes in the upper layers of the epidermis. Depending on the specific model, RHEs might also incorporate additional cell types like melanocytes (pigment-producing cells) and Langerhans cells (immune cells) (Suhonen *et al.* 2003; Pappinen *et al.* 2008). Several commercially available skin models of RHE are SkinEthicTM or SkinEthic RHE 2.0 (EpiSkin, France), EpiDerm™ (MatTek Corporation, USA) or ZenSkin RHE-24 (ZenBio, USA). These RHE models serve as valuable human-relevant platforms for replacing and testing the efficacy and safety of topical medications (applied to the skin) compared to animal models. RHEs can be used for drug testing and to assess the safety and potential irritation of cosmetic products (Netzlaff *et al.* 2005).

Human Skin Equivalents (HSEs)

Full-thickness HSEs are *in vitro* models that closely mimic the structure and function of native human skin. In contrast to simpler epidermal models RHE, HSEs contain layers simulating the dermis and epidermis, facilitating the complex interactions between these crucial skin components. HSEs are typically constructed using a combination of keratinocytes, which are responsible for forming the epidermis, fibroblasts that create the dermal layer's supportive structure, and finally ECM as a network of proteins and molecules providing the structural foundation for the skin layers. ECM can be either natural (e.g. collagen) or synthetic (Rossi *et al.* 2015; Niehues *et al.* 2018).

First HSEs model, cultured human epidermal cells were seeded on a decellularized de-epidermized dermis (DED). The DED was suitable to induce epidermal cell differentiation and substituted the basal lamina. However, the key point was to develop a composite skin reconstruction using the dermis and epidermis with cell cultivation on hydrogel systems. Employing hydrogels for creating the HSE model is the most dominant technique. Hydrogel systems serve as a scaffold for dermal fibroblasts, which are then co-cultured with keratinocytes on their surface. Collagen is the typical hydrogel material thanks to its inclusion in native ECM and dermal fibroblast cells are usually distributed within the collagen gel to mimic the dermal layer. Adding a suspension of keratinocytes on top generates the epidermis layer. The HSE is raised to the air-liquid interface, enabling the top layer of cells to be exposed to air. This triggers essential differentiation processes. (Bell *et al.* 1981; El Ghalbzouri *et al.* 2009) Except that collagen serves as a mechanical scaffold, it enables cell-cell/cell-matrix interaction and also improves the function of the cells with high biocompatibility. One disadvantage of this model is its relatively short lifespan due to collagen's low mechanical resistance. Collagen-based matrices usually deform during the culture process. According to this collagen-cell combination model, several commercially available 3D skin models are put on the market, such as EpiDermFT™ (MatTek, USA), Episkin (L´Oreal; SkinEthic, France), or Labskin (Innovenn, Ireland) (Schmidt *et al.* 2020; Idrees *et al.* 2021).

The second approach combines the cell with chemical compounds and growth factors to develop viable biological substitutes. It is designing an HSE exclusively from cultured fibroblasts and keratinocytes without using any hydrogel/synthetic system. The well-organized dermal layer can be created by self-assembling fibroblasts´ extracellular matrix. Fibroblast ECM contains collagen as a major protein, thus it can be feasible with the addition of ascorbic acid for fibroblast metabolism support in long-term cultivation. This dynamic interaction leads to the formation of structured sheets, which can be reached by the addition of ascorbic acid for fibroblast metabolism support in long-term cultivation. This

dynamic interaction leads to the formation of a structured platform for keratinocytes that form a stratified epithelium when raised to an air-liquid (ALI) interface (Auxenfans *et al.* 2009; Hayden and Harbell 2021).

The HSE model allows a suitable cellular environment for cell metabolism and function as they do in the native tissue. This microenvironment mimics critical aspects of the *in vivo* setting through the biological and chemical milieu to which the cells are exposed. The HSE model can be a backbone approach of any tissue-engineered skin substitute (Savoji *et al.* 2018). There are main similarities between HSE and native tissue, however, some differences in SC function have remained, especially the higher permeability of the models than that of native human skin. Despite this fact, HSE´s reproducible quality and the possibility of standardization are the advantages for the potential for studying the irritation, toxicity, and corrosivity of applied substances (Pappinen *et al.* 2012; Savoji *et al.* 2018).

3.2 Polymicrobial Skin Models

3.2.1 Microorganisms play a crucial role in maintaining human skin health

Microorganisms play a crucial role in maintaining human skin health. The skin is home to a diverse community of microorganisms, including bacteria, fungi, and viruses, collectively known as the skin microbiota (Figure 8). The microbial composition is strikingly different on different parts of the skin and is determined by their physical, chemical, and biological characteristics. The skin surface lacks nutrients beyond basic proteins and lipids. To survive in this hostile environment, the microbes must adapt and utilize available resources in the stratum corneum, such as sphingolipids, amino acids, peptides, and nitric oxide. Also, the sweat, containing NaCl, H_2O, HCO_3^+, glucose, amino acids, free fatty acids, urea, ammonia, lactate, vitamins, peptides, sterols, mucopolysaccharides, and sebum with free fatty acids, sterols, squalene, wax esters are important for the microbiome conditions (Grice and Segre 2011; Byrd *et al.* 2018; Patra *et al.* 2020).

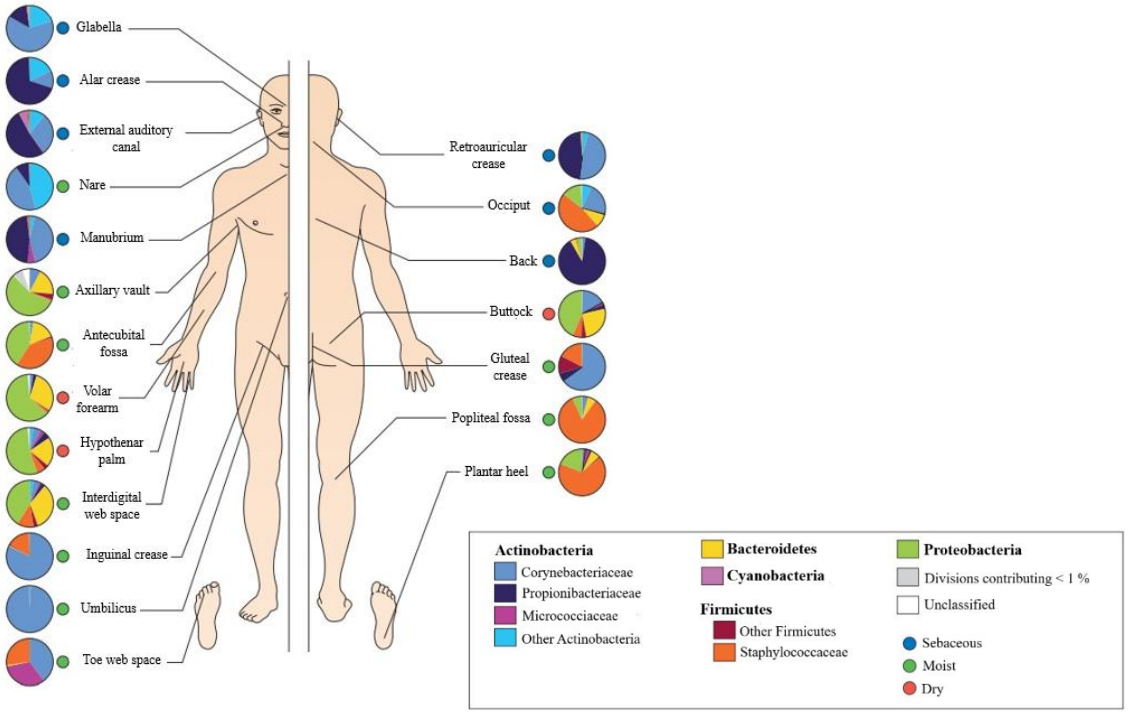

Figure 8: Bacteria distribution on the skin sites (Grice and Segre 2011)

The skin microbiome comprises two main groups of microbes. First, the resident microbiome is a fixed group that can replenish itself following any perturbations. On the other hand, the transient microbiome does not permanently reside on the skin, it occurs for a few hours or days on the skin depending on the environment. Both types of microbiomes are non-pathogenic in the case of

healthy skin. Common phyla residing on the skin include *Actinobacteria*, *Firmicutes*, *Proteobacteria*, and *Bacteroides*. These are mostly gram-positive bacteria belonging to the genera *Corynebacteria*, *Propionibacteria*, and *Staphylococci*. Each microenvironment on the skin is located on other parts of the body, for example surrounding the sebaceous follicles, there is an anaerobic, lipid-rich environment, that harbors the *Propionibacterium*. The axillary area mainly consists of gram-positive bacteria of the genera *Staphylococcus*, *Micrococcus*, *Corynebacterium* as well as *Propionibacterium*. Next, the *Staphylococcus*, *Propionibacterium*, *Micrococcus*, *Corynebacterium*, *Enhydrobacter*, and *Streptococcus* species mostly grow in the drier regions of the body. Moreover, gram-negative bacteria, including *Enterobacteriaceae*, nonfermenting or anaerobes, are usually underestimated skin commensal organisms but are also part of the transient fraction of the skin microbiota (Sfriso *et al.* 2020; Boxberger *et al.* 2021; Habeebuddin *et al.* 2022). Another type of skin microbiota composition is Eukaryota, such as fungi and *Desmodex*. Fungi, including *Malassezia*, *Cryptococcus*, *Rhodotorula*, or *Candida* species, are identified as human skin commensal organisms. Yeast, called *Malassezia*, is especially present on the scalp, with *Demodex folliculorum* a mite species. *Malassezia* can also colonize the central sites of the body and arms. More diverse fungi are situated on the foot sites (Grice and Segre 2011; Byrd *et al.* 2018). Very little information is available on the viral fraction found on the skin. However, bacteriophages predominate and their activity is related to the modulation of bacterial populations. Bacteriophages may therefore be involved in the homeostasis of the skin microbiota. The sequencing analysis shows that *Cutibacterium* and *Staphylococcus* phages are the most abundant skin phages (Hannigan *et al.* 2015).

The study of the human microbiome is diverse at an interpersonal or intrapersonal level. Moreover, the structure of the skin microbiome depends on the environment, gender, race, or age. The long-term stability of the skin microbiome also reflects the specific lifestyle of the host. Thus, skin health reflects the balanced skin microbiome, and any alterations lead to the overgrowth of pathogenic strains linked to various skin diseases (Hwang *et al.* 2021).

3.2.2 Polymicrobial Interactions

Polymicrobial interactions within the skin microbiome represent a spectrum of relationships among various microorganisms (bacteria, fungi, viruses, and other microbes) existing together in the same microenvironment. These microorganisms are in constant competition for space and enabling dynamic control. This process is essential for skin health, as it keeps harmful microorganisms under control and supports skin homeostasis. Central to these interactions are processes such as quorum sensing, metabolic exchanges, and the

production of antimicrobial compounds including bacteriocins, proteases, phenol-soluble modulins (PSMs), and short-chain fatty acids. These processes can deter opportunistic pathogens, lower their virulence, and disrupt biofilm formation, thereby reinforcing resistance to colonization on the skin (Claesen and Fischbach 2015; Anju *et al.* 2022).

The interactions among microbial species range from mutualism and commensalism to antagonism and competition. As an example of a positive interaction, the commensal bacterium *Staphylococcus epidermidis* produces antimicrobial peptides and proteases (e.g., Esp) that inhibit *Staphylococcus aureus*, and its short-chain fatty acids have the potential to inhibit *Cutibacterium acnes* in anaerobic conditions. Quorum sensing also holds positive significance, where skin microbes possess the capability to secrete molecules that interfere with pathogen-specific signalling pathways, e.g., the Agr system in *Staphylococcus aureus*, affecting virulence gene regulation and hindering colonisation. Certain microbes derive advantages from metabolites produced by others, such as skin fermentation products, which foster mutual survival and ecological stability. These microbial interactions are finely tuned and responsive to environmental signals and inter-species communications. Bacteria are capable of sensing and adjusting to changes in microbial populations or metabolic conditions, modifying gene expression to preserve community structure. On the other hand, negative interactions is coagulase-negative *Staphylococcus* species produce bacteriocins like epidermin, Pep5, Epilancin K7, and capidermicin, which hinder gram-positive pathogens, including MRSA (Chen *et al.* 2022; Caballero *et al.* 2023; Joshi *et al.* 2023; Glatthardt *et al.* 2024)

Moreover, polymicrobial interactions extend beyond bacterial-bacterial relationships. Yeast, such as *Malassezia*, and bacteriophages are significant in the complex interactions of the skin microenvironment, influencing microbial competition and host immune response. Disruptions of these interactions, broadly termed dysbiosis, have been observed in skin diseases like atopic dermatitis and psoriasis. It is also under investigation whether dysbiosis is a cause or consequence of disease, but its link to impaired colonisation resistance highlights the importance of a healthy microbiome. Within a wide range, polymicrobial interactions in the skin are intricate and essential for health-maintaining processes such as colonisation resistance, immune modulation, and pathogen suppression. The application of a skin microbial network, along with the molecular mediators and dynamics involved, can lead to the establishment of novel therapeutic strategies in the field of tissue engineering, particularly concerning *in vitro* skin tissues (Flowers and Grice 2020; Wu and Yao 2023; Bényei *et al.* 2024)

3.2.3 Importance in Studying Host-Microbe Interactions

The skin microbiome is dynamic throughout life, nevertheless, it is acquired at birth. Skin colonisation continues during breastfeeding and an equilibrium is finally achieved during adulthood. Skin is a unique ecosystem that primarily hosts a commensal microbiome. Concerning that the skin provides nutrients and abiotic factors, such as temperature and humidity allowing the growth of skin microorganisms, it is possible the settle not only commensal bacteria but also pathogens. However, commensal microorganisms can prevent pathogens' colonization, directly or indirectly benefiting the host (Boxberger *et al.* 2021).

The maintenance of skin homeostasis with the barrier function plays a key protective role against potential pathogens and environmental issues. The skin microbiota forms a protective barrier against pathogenic organisms by occupying space and competing for nutrients. This competition helps prevent the colonization of harmful bacteria, fungi, and viruses that could cause infections. Secondly, commensal microorganisms produce metabolites that contribute to the integrity and function of the skin barrier (Chen *et al.* 2018). Generally, the secretion of protease enzymes by skin microbes strengthens the level of the desquamation process and stratum corneum renewal. The skin microbiome produces short-chain fatty acids that help with the sebum maintain the acidic pH of the skin, which is essential for barrier function. Moreover, another microbiome role is the biofilm production, bacteriocins, and quorum sensing. It ensures protection against potential pathogenic microorganisms by competition and antimicrobial peptide (AMP) production by commensal bacteria or Malassezia fungi, which produce a range of indoles that inhibit many other yeasts/molds (Grice *et al.* 2008). Specifically, *Staphylococcus epidermidis* is one of the dominant skin-associated bacteria, which produces several antimicrobial compounds and proteases for the limitation of the formation of biofilms by pathogens. This bacterium also activates the production of the Toll-like receptors for the keratinocyte response to pathogens and simultaneously can inhibit other receptors for speeding the process of wound healing during skin inflammation. Another example could be coagulase-negative *Staphylococcus* species. They produce bacteriocins with antibacterial properties. Bacteriocins limit the survival of pathogenic bacteria on the skin surface. A thick sebum barrier can be secured by modification of the lipid composition on the skin´s surface, which can be modified by the *Corynebacterium* species (Scharschmidt *et al.* 2013; Newstead *et al.* 2020; Habeebuddin *et al.* 2022).

The interaction between commensal microorganisms and the immune system is vital for maintaining immune tolerance and preventing excessive inflammation or immune-related skin disorders. A wide range of molecular and cellular processes within the skin and beyond is influenced by the skin microbiome. Skin

immunity can be remodeled by inducing the IL-17A$^+$ CD8$^+$ T cells that migrate to the epidermis, enhancing immunity and limiting pathogen invasion. The whole process is activated by *Staphylococcus epidermidis*. The next approach can be the abundant presence of coagulase-negative *staphylococci*, which produce beneficial products that augment host immunity. This activity aims for specifically targeted antimicrobial, anti-inflammatory, or anti-neoplastic function while also promoting broad innate and adaptive immune responses. Wound healing can be also promoted by skin immunity. Certain beneficial bacteria on the skin can stimulate the immune response by secreting antimicrobial substances and aiding in tissue regeneration. Probiotic treatments containing these bacteria have been explored for their potential to enhance wound healing (Linehan *et al.* 2018; Zheng *et al.* 2020; Boxberger *et al.* 2021).

3.2.4 Challenges in Modeling Polymicrobial Skin

Increasing the complexity of 3D *in vitro* reconstructed human skin models raises several issues in pursuing more representative models with their reliability and predictability. Construction of the full-thickness skin model contains relatively straightforwardly layered living fibroblasts and keratinocytes. Thus, the research attempts to incorporate all the relevant skin cell types, such as melanocytes or Langerhans cells, and the interaction between them. Nevertheless, all interaction is not only between cell types, but the skin surface can play a significant role in supporting skin health (Bojar 2015). The skin microbiota plays a crucial role in developing 3D skin models due to its considerable influence on various skin processes and barrier functions. First and foremost, the skin microbiota is involved in maintaining the physical barrier of the skin. They influence the differentiation of keratinocytes, the formation of the stratum corneum and the regulation of intercellular contacts. They are also involved in the regulation of skin pathogenesis and an adequate immune response. It is therefore expected that 3D models of the skin, including the microbiota, could be able to simulate the complex system of the skin, the progression of disease and the effects of different treatments. Based on these key aspects of incorporating skin microbiota to colonise the apical side of the 3D skin model, it is expected the improvement of the realism of 3D skin models *in vivo* conditions (Galvan *et al.* 2024; Kim 2023).

A representative model of the skin ecosystem could be the colonization of 3D *in vitro* reconstructed human skin models with microorganisms. It is designed to mimic the complex microbial communities present on human skin. The first research was based on the 2D culturing of human skin cells - keratinocytes or sebocytes, with bacteria or their metabolites. Polymicrobial biofilms, which are used for experiments, are a combination of microorganisms to represent the

complex microbial community found on human skin. It is a mixture of commensal strains, such as *Staphylococcus epidermidis* and *Micrococcus luteus*, and pathogens, especially *Staphylococcus aureus* and *Pseudomonas aeruginosa*. This interaction between skin cells and bacteria ensured the understanding of the pathways involved in pathogen infections or commensal benefits for the skin. In more detail, the keratinocytes were usually incubated with sterile filtered bacteria medium, such as *S. aureus* medium. Several studies showed that keratinocyte cultivation in these conditions increased the production of proteolytic enzymes, followed by the degradation of skin barrier proteins, such as desmoglein or filaggrin. This pathogen strain also induced cell cytotoxicity and increased the production of pro-inflammatory cytokines in skin cells. To compare, commensal *S. epidermidis* increased the keratinocyte production of antimicrobial peptides. Unfortunately, these monolayer systems do not reflect the skin surface and the bacteria strain has a faster growth rate of bacteria than human cells, thus 2D models cannot be maintained for more than 24 h (Poppov *et al.* 2014; Rademacher *et al.* 2018; Jordana-Lluch *et al.* 2020).

The development of 3D skin models, such as RHE or HSE, colonized with bacteria could reproduce the skin barrier to study long-term interactions between the skin and its microbiota. Each selected microorganism is cultured under conditions that mimic the skin environment, including temperature, pH, and nutrient availability. These conditions are optimized to promote the formation of biofilms. An assembling polymicrobial skin model is considered when the bacteria are introduced onto a substrate that mimics the surface of a 3D skin model. Then they are adhered to the surface and begin to proliferate, eventually forming a polymicrobial biofilm. This biofilm structure allows for interactions between different microorganisms and facilitates their colonization of the keratinocyte layer. Once the biofilm-keratinocyte model is established, interactions between the microorganisms and host cells can be studied, for example, the examining microbial growth dynamics, gene expression profiles, host immune responses, and the impact of antimicrobial agents on biofilm formation and viability (Rademacher *et al.* 2018; Emmert *et al.* 2020; Lizardo *et al.* 2022). Modeling of polymicrobial skin models using the biofilm-keratinocyte is analyzed to gain insights into the complex interactions between microorganisms and host cells, as well as the effects of antimicrobial interventions and understanding of skin microbiota dynamics, host-pathogen interactions, and the development of new strategies for managing skin infections and promoting skin health (van Belkum *et al.* 2023).

4. CELL-ASSEMBLED EXTRACELLULAR MATRIX (CAM) PRODUCTION

4.1 Extracellular Matrix Composition and Function

The ECM defined as a complex 3D network of macromolecules that provides structural support and biochemical cues to cells within tissues and organs. Initially viewed as a passive, inert scaffold providing mechanical support, the ECM is now recognized as a dynamic, 3D structures critical for cell survival, physiology, development of tissue etc. Thus, it patronizes the architectural structure/strength, and regulates biological processes, offering physical protection and signaling cues (Rozario *et al.* 2010). The ECM influences cell behavior, including proliferation, orientation, gene expression, migration, and differentiation. For instance, the ECM determines the biochemical and mechanical properties of organs, including tensile strength, compressive strength, and elasticity. It also plays a role in maintaining extracellular homeostasis and water retention, acting as a buffer. While primarily composed of water, polysaccharides, and proteins, the ECM's composition and topology of the ECM varies from tissue to tissue due to dynamic interactions between fibroblasts, epithelial cells, adipocytes, and proteins during tissue development. It also binds growth factors that interact with cell surface receptors, regulating gene transcription and initiating signaling pathways (Muncie *et al.* 2018; Karamanos *et al.* 2021).

The ECM is comprised of multiple components that interconnect to form a sophisticated network of molecules within a 3D framework (Figure 9). These ECM constituents exhibit diverse characteristics in terms of size, morphology, and arrangement. The unique composition of ECM in various tissues and organs is a result of differential gene expression related to ECM synthesis. Processes such as post-transcriptional splicing and post-translational modifications also play a key role in this expression. This intricate interplay of ECM elements contributes to the structural integrity and functional diversity observed in different biological systems (Dzobo *et. al.* 2023). In general, the ECM is composed of two primary domains: the basement membrane, a condensed layer adjacent to various cell types such as epithelial, mesothelial, meningothelial, synovial, muscle, Schwann cells, adipocytes, and then the interstitial matrix. While both domains share a collagen scaffold as their basic structure, the composition and 3D architecture of the collagens differ significantly between them (Bosman and Stamenkovic 2003). There are various proteins (glycoproteins, proteoglycans) and polysaccharides, that are organized in a highly dynamic and intricate manner. Glycosaminoglycans (GAGs) and proteoglycans (PGs) form a hydrated gel-like substance that resists compressive forces and allows rapid diffusion. Adhesive glycoproteins, including laminin, tenascin, and proteoglycans typically adhere to

collagen scaffold and interact with cells within or in proximity to the matrix. These interactions are mediated by matrix receptors, with integrins representing the most significant class of receptors involved. Other ECM proteins are fibrous proteins that provide strength and elasticity to the matrix. These insoluble components are synthesized by fibroblasts and other cells residing within connective tissue. (Frantz *et al.* 2010; Theocharis et al. 2016).

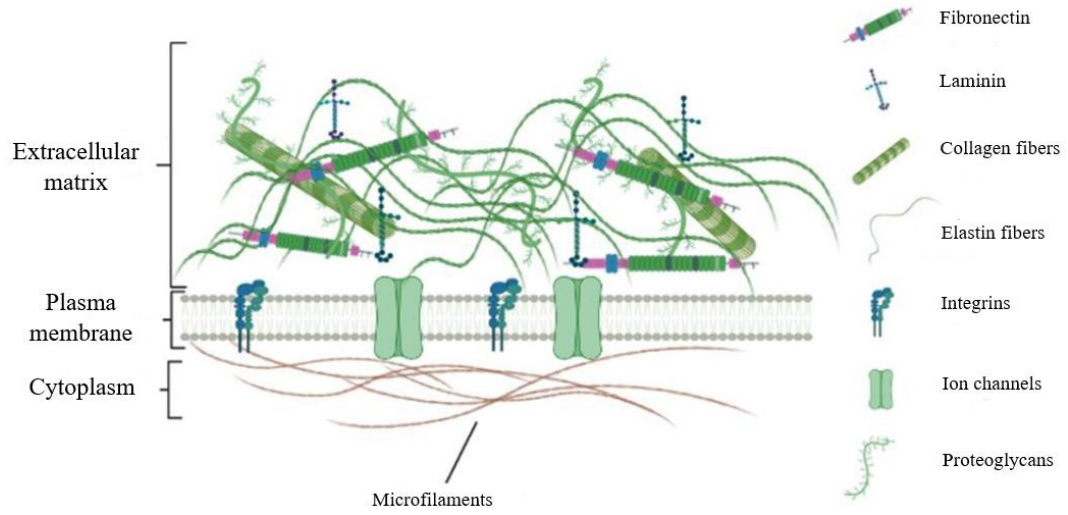

Figure 9: Extracellular matrix composition (Dzobo et al. 2023)

In addition to structural proteins, a group of ECM molecules known as matricellular proteins (e.g., thrombospondin-1 and -2, tenascin-C, or osteopontin) play a pivotal role in modulating cell-matrix interactions and cellular functions. Although they do not directly contribute to the structural framework of the ECM, matricellular proteins exert a significant influence on cellular behavior (Järveläinen *et al.* 2009).

The ECM also undergoes constant turnover and remodeling in response to various signals. This process is particularly enhanced during inflammatory responses or wound repair. Key enzymes involved in ECM remodeling include MMPs and urokinase-type plasminogen activators (uPAs). MMPs and uPAs are responsible for degrading components of the basement membrane, as well as proteins and proteoglycans within the connective tissue, liberating latent growth factors from their storage sites within the ECM (Leight *et al.* 2017; Marangio *et al.* 2022).

4.2 Techniques for Cell-Assembled ECM

In tissue engineering, an optimal scaffold should possess structural, physicochemical, and mechanical properties that are conducive to remodeling the implant into functional tissue by the host body. In addition, the biochemical properties of the scaffold are important to consider due to their significant role in cell-to-matrix interactions. Various biomaterials have been developed to fulfill these criteria and can be broadly categorized into two subtypes: naturally occurring and synthetic materials (Kawecki *et al.* 2020). Traditionally, tissue engineering has relied heavily on synthetic biomaterials to shape and provide mechanical properties to engineered tissues. These can include biodegradable synthetics (e.g., polylactic acid, polyglycolic acid, and polycaprolactone) or biologics (e.g., chitosan, alginate, and collagen). Synthetic scaffolds offer advantages in cost-effectiveness and precise control over composition, geometry, and structure. For instance, synthetic materials can be manufactured precisely and consistently, resulting in minimal variability. Furthermore, their properties, including mechanical strength and degradation profile, are easily modifiable, multiple polymers can be seamlessly integrated within a single material can be easily modified, and multiple polymers can be seamlessly integrated into a single material. However, they are often hindered by drawbacks such as unpredictable degradation rates, chronic inflammation, and limited biological activity. In contrast, naturally occurring materials are typically derived from whole ECMs or purified individual ECM components, such as collagen, laminin, fibronectin, and silk. They provide inherent physiological cell-to-matrix interactions that facilitate tissue regeneration. Thus, synthetic scaffolds could be replaced with ECMs synthesized by cells cultured *in vitro*. These efforts culminated in the development of relevant tissue-engineered implants resulting in scaffolds with suitable mechanical properties (Hussey *et al.* 2018; Mangan *et al.* 2020).

Cell-derived ECM (CAM) partially mirrors the intricate biological machinery of native tissue. Derived from human cell cultures by gentle decellularisation, bioactivity is preserved while immunogenic components are removed. *In vitro* derivation permits the selection of appropriate ECM-producing cell types, genetic modification, and exposure to specific stimuli, facilitating the creation of ECM with desired properties. Consequently, CAM gained significant interest in TERM due to its potential to create more biomimetic and functional tissue constructs. Cell-derived ECM can be generated by culturing cells scaffold-free in 2D and 3D cultures, where the cells can self-assemble into 3D spheroids through hanging drop culture, non-adherent plates, or micro-molded wells. Alternatively, cells can also be seeded within hydrogels or scaffolds, forming hybrid ECM-based materials. Simultaneously, 3D bioprinting technology allows the precise deposition of cells, wherein cell-assembled ECM, cells are co-printed with ECM

components to generate tissues with controlled architecture and composition (Lee *et al.* 2007; Nicolas *et al.* 2020; Assunção *et al.* 2020).

The CAM can assist in the construction of 3D tissue without the use of other materials. This innovative approach exploits on the inherent ability of mesenchymal cells, such as fibroblasts, smooth muscle cells, adipose-derived stem cells, and bone marrow-derived stem cells, to assemble a completely biological and internally secreted ECM in vitro. Generally, cells are the traditional ECM builders and create tissue modules with precision and stoichiometric competence. This ability can lead to the development of cell-assembled prototype scaffolds, held together by cell-cell and cell-ECM junctions used for skin, blood vessels, and corneas. These tissues demonstrate reparative/ regenerative efficacy, including in clinical settings. Moreover, the ability of cells to self-assemble can be enhanced by biophysical cues (surface topography, substrate elasticity), biochemical signals (ascorbic acid supplementation), and biological signals (growth factor supplementation, co-culture systems). The CAM exhibits remarkable mechanical strength and has emerged as a promising form of potential biomaterial scaffold (Kumar *et al.* 2015; Mangan *et al.* 2018; Oliveira *et al.* 2021).

4.3 Co-cultivation Systems for Enhanced ECM Production

Cell co-culture refers to the cultivation of two or more different types of cells—either from the same or different specimens—within a shared culture system. It is a foundational tool in biological research, widely used to investigate natural and synthetic interactions between cell populations. Since the 1980s, cell co-culture technology has attracted increasing attention for its broad applications, including inducing stem cell differentiation, enhancing metabolite production, improving cell viability and function, and constructing tissue-like environments *in vitro* (Nakazawa *et al.* 1998; Goers *et al.* 2014). Compared with monoculture techniques, co-cultures provide a more physiologically relevant model by better mimicking the *in vivo* cellular microenvironment. This allows to observe not only natural cell-to-cell interactions but also interactions between cells and their surrounding environment (Figure 10). Moreover, co-cultures are offering in vivo-like models that can outperform animal models for drug testing, enabling high-throughput assays and precise monitoring of cell communication (Goers *et al.* 2014; Vis *et al.* 2020).

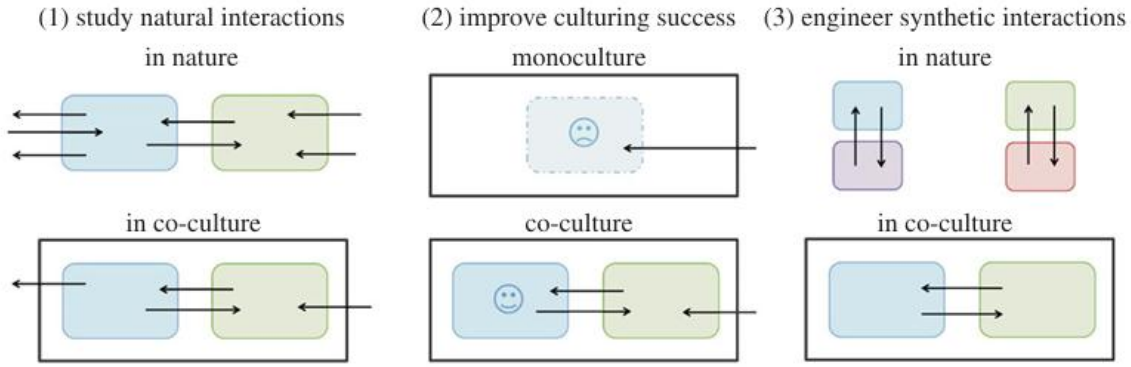

Figure 10: Overview of co-culture systems (Goers et al. 2014) (1) Natural interactions between cell lines. (2) Improving cultivation success for certain cell lines. (3) Establishing synthetic interactions between cell lines.

Cell co-culture systems are generally categorised based on the degree of contact between the cultured cell types. These include direct contact co-culture, indirect contact co-culture and finally 3D cell co-culture. In the direct contact co-culture method, different cell types are grown together in direct physical contact, enabling juxtacrine communication through surface receptors and gap junctions. This method is easy to perform, requires minimal equipment, and closely mimics native tissue by maintaining both cytokine exchange and direct cell-to-cell interactions. In contrast, indirect contact co-culture involves a physical separation between cell types, such as using a semi-permeable membrane (a transwell insert). Although the cells do not physically touch, they can still communicate through their secretome, which comprises soluble factors, extracellular vesicles (EVs), and other signalling molecules. Finally, 3D cell co-culture involves the organisation of cells in a 3D structure, creating more realistic and complex tissue models. These systems better reflect the spatial organization and function of real tissues and are widely used in tissue engineering and regenerative medicine (Vis *et al.* 2020; Liu *et al.* 2022; Aydin *et al.* 2022).

The direct contact co-culture method is, in our experiments, particularly well-suited for applications involving the co-cultivation of human dermal fibroblasts (HDFs) and H9c2 cardiomyoblasts, as it enables direct cell–cell interactions that are critical for cardiac tissue engineering. This co-culture setup allows HDFs to provide not only paracrine support but also rich extracellular matrix (ECM) components that enhance cell adhesion, viability, organisation, and functional maturation—key factors in the successful formation of scaffold-free cardiac cell sheets. The ECM itself is a complex and dynamic network composed of collagens, adhesion molecules, proteoglycans, growth factors, and cytokines. Its unique architecture plays a vital role in regulating cell behavior, including proliferation, differentiation, polarity, and migration. Compared to traditional ECM coatings such as fibronectin, gelatin, or collagen, increasing evidence supports the superior

biological relevance of ECM derived from in vitro cultured cells. In this context, fibroblast-derived matrix, as a type of cell-derived matrix, is being explored as a promising ECM platform for cardiac tissue engineering. It provides a highly biomimetic microenvironment that supports cell adhesion, growth, and cardiomyogenic differentiation. The H9c2 cardiomyoblast cell line, derived from embryonic rat heart tissue and well characterized for its ability to differentiate into skeletal and cardiac myocytes, is commonly used as a model system to assess these effects. In this case, direct co-culture of HDFs and H9c2 cells not only facilitates direct intercellular communication but also generates a functional, cell-derived ECM platform that enhances cardiac tissue formation. This approach holds strong promise for regenerative medicine applications and offers valuable insights into both cell–cell and cell–ECM interactions in engineered cardiac environments (Suhaeri *et al.* 2015; Rother *et al.* 2015; Iwamiya *et al.* 2016; Suhaeri *et al.* 2017).

4.4 Applications in Tissue Engineering

The ECM is a sophisticated and distinctive complex framework comprising structural proteins and glycosaminoglycans crucial for the precise transmission of intrinsic physical and chemical cues. These signals profoundly influence cellular behaviors, tissue regeneration, revascularization, and homeostatic regulation. Thus, the application of a cell-assembled extracellular matrix involves harnessing the innate ability of cells to construct and organize their surrounding ECM. This approach emphasizes utilizing the synergistic interactions between cells and their secreted ECM components to fabricate biomimetic tissue constructs. By cultivating cells in a controlled environment conducive to ECM production, CAM facilitates the creation of tissue-like structures that closely resemble native tissues in terms of architecture and function. The promising capacity of cell-assembled extracellular matrix biomaterials is not limited to tissue engineering, but also has broader biomedical applications (Yao *et al.* 2019; Assunção *et al.* 2020). More specifically, the utilization of CAM can be either in its pure form or integrated into biomaterials. 3D scaffolds composed of cell-assembled ECM are developed through various methods, such as decellularizing stacked cell sheets/pellets or depositing ECM within materials - tubes/foams. For specific applications with mechanical properties, CAM may be combined with synthetic materials to form hybrid scaffolds. Typically, CAM is applied as a coating by decellularizing cells on the surface of biomaterials. A newly used approach involves using only the CAM sheets (Hussey *et al.* 2018; Kawecki *et al.* 2022). As mentioned, the cell line of the connective tissues (fibroblasts) can synthesize ECM components, in particular collagen. Furthermore, the combination of cell culture with ascorbic acid and its derivatives can stimulate collagen production. In general, the CAM is

then investigated and utilized for skeletal and cardiovascular repair (cartilage, biological tissue-engineered vascular grafts, cardiac patches for cell delivery), as well as other applications such as in skin (skin patches for drug delivery) or peripheral nerve repair (Mangan *et al.* 2018; Torres *et al.* 2021; Kawecki *et al.* 2022).

5. AIM OF DOCTORAL THESIS

Skin, with its outermost layer called the *stratum corneum*, acts as the primary barrier against externally applied compounds. This barrier function is in the centre of attention once the safety/risk assessment of materials/compounds is considered. I*n vitro prepared* monolayer or two-dimensional keratinocyte cultures lack this crucial barrier function. Thus, the development of advanced in vitro skin-reconstituted tissues focuses on creating of complex model mimicking *in vivo* skin tissue functions. The remarkable adaptability of these 3D skin equivalents extends their utility across diverse fields within scientific exploration. Whether surveying the intricacies of skin diseases or innovations in cosmetic investigations, 3D skin tissue models stand as indispensable instruments across scientific disciplines. They provide intricate insights into human skin physiology, shaping advancements in understanding and application. Recently, the additional part of skin, microbiome, has come into the centre of our attention. For this purpose, the doctoral thesis is aimed:

- To achieve a thorough understanding of the methodology for in vitro formation of reconstituting full-thickness skin tissue model, and to master the practical skills required for their preparation.
- To establish the protocols for the preparation of the reconstituted full-thickness skin tissue model in the laboratory.
- To **integrate** advanced reconstituted full-thickness skin tissue model models with the **microbiome to further enhance their scientific value**, particularly in the context of wound healing research.

Additionally, the ability of skin tissue cells, particularly dermal fibroblasts, to produce an extracellular matrix by self-assembling (CAM) can create an attractive biomaterial. This CAM scaffold resembles native tissue ECM in composition and architecture, offering enhanced cell-instructive properties for tissue regeneration. These “cell-made scaffolds” exhibit excellent biocompatibility, biodegradability, and tissue-specific cues, making them ideal for tissue repair and regeneration applications. Thanks to the findings, the doctoral thesis is also aimed:

- To master culturing techniques enabling the self-assembly of three-dimensional multilayered fibroblast structures, thereby generating extracellular matrix (ECM) with native-like architecture and composition.
- To investigate the modifiability of structural architecture in cell-made scaffolds through external stimuli (e.g., mechanical, biochemical), and evaluate their functional utility as bioactive scaffolds post de-/re-cellularization.

Last, but not least – the skills in advanced cell/biology and microbiology laboratory techniques allow me to support the studies of other colleagues, where my expertise help to provide a specific type of experiments..

6. EXPERIMENTAL PART

6.1 Cell line maintenance

6.1.1 Human Dermal Fibroblast

Human Dermal Fibroblasts HDF (Cat. N.: 106-05n, Cell Sigma-Aldrich) were routinely cultivated in T75 flasks (TPP, Trasadingen, Switzerland) in Basal Medium Eagle (BME, Sigma Aldrich, USA) with 10% fetal bovine serum (FBS, BioSera, France) and 1% Penicillin/Streptomycin (GE Healthcare HyClone, United Kingdom). BME medium was changed every other day and passaged when 80-85% confluent.

6.1.2 Spontaneously Transformed Human Keratinocyte

Spontaneously Transformed Human Keratinocyte HaCaT (Cat. N.: PCS-200-011, ATCC, USA) cultivated in T75 flasks in Dulbecco's Modified Essential Medium DMEM (Biosera, France) with 10% FBS and 1% Penicillin/Streptomycin (GE Healthcare HyClone, United Kingdom). This medium was pre-supplemented with stabilized 1 mM Sodium Pyruvate (Life Technologies Limited, UK). Cells were maintained between 80–85% confluence.

6.1.3 Embryonic Rat Cardiomyocytes

Embryonic Rat Cardiomyocytes H9c2 (CRL-1446, ATTC, USA) were grown routinely in T75 flasks (TPP, Trasadingen, Switzerland) in Dulbecco's Modified Essential Medium DMEM (Biosera, France) with 10% FBS and 1% Penicillin/Streptomycin (GE Healthcare HyClone, United Kingdom). This medium was pre-supplemented with stabilized 2 μM L-glutamine (Biosera, France).

All cells were maintained at 37 °C in a 95% humidified atmosphere and 5% CO_2. The cell culture medium was changed every second day. For routine passaging, cells were washed twice with PBS, trypsinized with 0.25% v/v trypsin/EDTA (Biosera, France), and split at a 1:2–1:4 ratio following standard cell culture methods. Cells were maintained between 80–90% confluence.

For cryopreservation storage, cells were trypsinized and harvested for the final concentration of 5×10^6 cells.ml^{-1}. The cells were then centrifuged at 1.200 RPM for 5 min and re-suspended at the freezing medium containing the appropriate medium for the cells without antibiotics with the 10% DMSO as a cryoprotectant. Cryovials were mixed thoroughly and then placed in an ultra-low freezer at - 80 °C.

In the case of cell line thawing, cryovials were thawed in a 37 °C water bath and mixed with fresh culture media in the conical tube. The cell suspension was centrifuged for 5 min at 1.200 RPM at room temperature. The supernatant was removed and 2 ml of the complete growth medium was added into the centrifuge tube. Finally, the cell suspension was transferred into the culture flask containing the complete growth medium (T75 culture flask – 15 ml).

6.2 Bacterial cell culture methods

6.2.1 Bacterial strains

Staphylococcus epidermidis CCM 4418, *Micrococcus luteus* CCM 732 and *Staphylococcus aureus* CCM 4516, *Pseudomonas aeruginosa* CCM 1961 were obtained from the Czech Collection of Microorganisms (CCM).

Prior to commencing the experimental procedures, it was essential to revive the bacteria from gelatinous discs, which required culturing them on tryptone soy agar (TSA; MP290, HiMedia Laboratories, Mumbai, India) in Petri dishes at 37 °C in aerobic conditions. Following the formation of colonies, the bacteria were moved to tryptone soy broth (TSB; M077-500G, HiMedia Laboratories, Mumbai, India), where they were cultivated for 24 hours for additional recovery.

6.2.2 Bacteria culture conditions

All media for bacterial cultures were prepared according to the manufacturer's instructions. Briefly, to prepare the bacteria culture medium, the proper amount of medium powder was dissolved in distilled water for a final volume of 400 ml and sterilized by autoclaving at 121 °C for 15 minutes.

6.2.3 Preparation of bacteria supernatants

Bacterial cultures were adjusted to 0.5 McFarland standard as inoculum. The inoculum was then diluted 1:10 in fresh TSB and incubated at 37 °C for 24 hours. For subsequent experiments, samples of bacterial supernatant were collected following 24 hours of incubation to ensure complete growth. After collection, bacterial cultures were centrifuged at 3000 RPM for 10 minutes to isolate the cultures and washed twice in sterile DPBS. Bacterial cell wall digestion was initiated using lysozyme (20 μg/ml) at 37 °C for 1 hour, followed by sonication on ice (10 cycles of 30 s with 30 s cooling intervals) to ensure complete lysis. The supernatants were cleared of cell debris by high-speed centrifugation and sterilized by filtration through a 0.22 μm membrane filter.

To verify the absence of live bacteria, culture samples (30 μl) were placed onto Petri agar plates containing PCA agar and incubated for 24 hours at 37 °C and 95% relative humidity to confirm there were no viable bacteria present. Bacterial supernatants were stored at -20 °C for later experiments. Throughout all experiments, the concentration of cultures in the culture medium was maintained at 10 %.

6.3 Construction of 3D Normal Skin Tissue Models

3D human skin models enable the investigation of cell-matrix and cell-cell interactions between different cell types. These cultures consist of two components. The first is a dermal equivalent consisting of a mixture of collagen matrix and fibroblasts. Collagen provides scaffolding, nutrient delivery, and potential for cell-to-cell interaction. The second is an epidermis that develops from keratinocytes plated on the dermal equivalent. e coculture system is thus grown at the air-liquid interface on collagen matrices. Initially, dermal equivalents, containing human passaged fibroblasts seeded in a collagen matrix, are grown on porous filters placed in the Transwell system. After a few days, primary human keratinocytes are seeded onto this base. This leads to the differentiation of the keratinocytes, which are visible as artificial skin after a couple of days. Finally, the overall procedure can be completed in 3 weeks (Figure 11). (Gangatikar *et al.* 2007; Fell 2016)

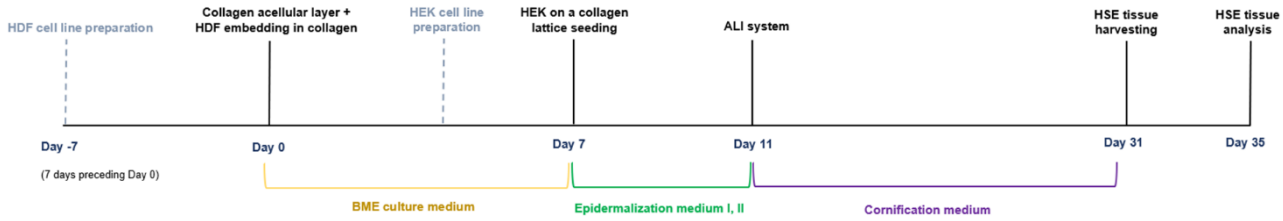

Figure 11: 3D skin model condition

6.3.1 Preparation of the Acellular Collagen Hydrogel

For the acellular collagen layer, rat tail collagen I (Corning® Collagen I, High Concentration, 100 mg; Corning, USA) was mixed with the neutralization buffer (NB). The collagen basal layer for a 3D skin model is usually prepared by neutralizing the acidic collagen solution. The NB buffer was prepared for this purpose before gelation to ensure a final pH of 7.4 for the hydrogel. The contents of the NB buffer are shown in Table 1.

Table 1: Preparation of the NB buffer

Ingredient	**Volume [ml]**
10× PBS	10
HEPES	2
7.5% sodium bicarbonate	6
1M NaOH	0.575
dH_2O	56.4
Final volume	75

To prepare 1 ml of neutralized acellular collagen layer at a final concentration of 1 $mg \cdot ml^{-1}$, 750 µl NB buffer was first added to a test tube placed on ice, followed by 250 µl of collagen stock solution was added to the tube. The next step was to homogenize the mixture by slow and repeated pipetting, taking care to avoid air bubbles during pipetting. The NB-collagen mixture (1 ml) was added to a 12well plate in quadruplicate – 250 µl collagen mixture per 1 insert. The plate was incubated at 37 °C for 45 minutes to generate a clear hydrogel. This acellular collagen layer was generally used within 2 hours after preparation. The thickness of the collagen hydrogel was 1 mm in the 12well plates.

6.3.2 Fabrication of the Cellular Part of 3D Skin Equivalents

HDF was cultured and passaged the day before incorporation at a split ratio of 9:10. The pre-mix solution was then prepared according to Table 2 below. This solution was mixed on ice, filtered, and sterilized with a 0.22 mm filter before use (without cell component and collagen). The HDF cell line suspension was resuspended to a final concentration of 3×10^5 cells·ml^{-1} and then was supplemented to the neutralized collagen solution. The HDF-collagen mixture was pipetted into inserts (Millicell® 12-well hanging cell culture insert; Sigma Aldrich, USA) with 750 µl in each insert on top of the gelled acellular collagen matrix. The inserts were then transferred to an incubator for 60 min to allow complete polymerization of the collagen-fibroblast gels.

Table 2: Construction of cellularized collagen matrix

Component		**Cellular collagen matrix [µl]**
Premix solution	10x DMEM	255
	L-glutamine	23
	FBS	286
	$NaHCO_3$	79
Collagen		2 123
Fibroblast suspension		230
Final volume		3 000

When the cellularized collagen was completely gelled, the DMEM/F12 was pipetted as a feeding medium by adding 1.6 ml of to the well around the insert and 0.4 ml of directly onto the insert. This HDF cell layer was then incubated for 5-7 days to allow complete gel contraction.

For epidermal development, the HEK cell line was trypsinized with trypsin/EDTA for 5 min at 37 °C to obtain a single-cell suspension and then resuspended in a volume of epidermalization I (EP I) medium in a total volume of 5×10^5 cells per 50 µl for one insert. Before HEK seeding, the fibroblast culture medium was removed so that HEK suspension was seeded onto a moist collagen gel. The cell suspension was then carefully added to the center of cellularized collagen and for 15 min not moved to allow the HEK to attach. The following step was to incubate for 45 minutes at 37 °C without any additional medium to

allow complete attachment of the HEK suspension. Finally, EP I medium was added in the same volume as in the previous steps.

The different skin-equivalent culture media were used to generate a confluent cellular monolayer that will initiate tissue stratification – epithelialization. The contents of the skin equivalent culture media are listed in Table 3. The 3D skin model was cultured and changed every other day with appropriate skin equivalents culture media as follows: 2 ml of EP I medium was added for the first 4 days and then changed to EP II medium. From day 6 until the termination of the experiment, the cornification (C) medium was pipetted to the bottom of the well so that the insert just touched the C medium. Whole skin equivalents were cultured in the air-liquid interface (ALI).

Table 3: In vitro skin equivalent culture media

Ingredient	Final concentration	Epidermalization I medium [ml]	Epidermalization II medium [ml]	Cornification medium [ml]
DMEM medium		363	363	237
Ham´s F12		120	120	237
L-glutamine	4 mM	10	10	10
Adenine	40 µM	1	1	1
Hydrocortisone	1 µM	1	1	1
Triiodothyronine	20 nM	1	1	1
Transferrin	10 µg ml	1	1	1
Insulin	10 µg ml	1	1	1
Progesterone	2 nM	0.5	0.5	-
O-phosphorylethanolamine	0.1 mM	1	1	1
Calcium chloride	1.8 mM	-	1.8	1.8
FBS		0.5	0.5	10
Final volume		500	500	500

6.4 Histological analysis

For the histological analysis of the 3D skin model, the skin equivalents on the insert membrane were first washed in PBS and then cut out of the insert with a scalpel. They were then transferred to a disposable embedding mold (výrobce) and fixated in 4% paraformaldehyde (PFA) for 1 hour at room temperature. After fixation, the skin equivalent tissues were processed in ethanol in the following order: 30-90 % EtOH for 30 minutes each. After ethanol, the xylene was used as an agent for paraffin infiltration. Xylene is changed three times, each time for 30 minutes. Finally, the skin equivalents are submerged in paraffin - twice for 1 hour and then overnight. The PFA-fixed paraffin-embedded skin equivalents were trimmed using the microtome Panthome LS-2064A and 5 μm thin sample sections were prepared on the microscope slides. The microscope slide containing samples was dried and fixed overnight in an oven at 40 °C. The next day, the hematoxylin-eosin (H&E) staining was performed according to the standard protocol, as shown in Table 4.

Table 4: H&E staining

Process	Ingredient		Time [min]
Deparaffinization	Xylene		10
	Xylene		10
	Paper cotton drying		
Tissue rehydration	96% EtOH		10
	96% EtOH		10
		Tap water rinsing	
Hematoxylin Nuclear Stain	Mayer´s hematoxylin		5
		Warm tap water rinsing	
	Warm tap water		5
	Paper cotton drying		
Eosin counterstain	Eosin		3
		Tap water rinsing	
	Paper cotton drying		
Dehydratation	96% EtOH		10
	96% EtOH		10
	Paper cotton drying		
Clearing	Xylene		10
	Xylene		10
	Mount and cover-slipping		

6.5 *In vitro* Skin Irritation Test Using 3D Normal Skin Model

The *in vitro* 3D Skin Irritation Test is a method used to evaluate the potential irritancy of chemicals, cosmetics, pharmaceuticals, and other substances without the need for animal testing. During the 3-day test, the substance of interest is applied to the surface of the reconstructed epidermis. After application, the tissue is typically incubated for a period of time to allow any potential reactions to occur. Following the incubation period, the tissue is evaluated for signs of irritation. The severity of the irritation is assessed on the basis of predetermined criteria, often using a scoring system. The topical exposure of the test chemical to the 3D skin model is followed by a cell viability test and the metabolic activity of cells within tissue-like structures. The MTT (3-(4,5-dimethylthiazol-2-yl) -2,5-diphenyltetrazolium bromide) assay is a widely used colorimetric assay for measuring the viability, proliferation, and cytotoxicity of cells *in vitro*. It is based on the reduction of a yellow water-soluble tetrazolium salt to purple formazan crystals by mitochondrial enzymes in living cells. The amount of formazan produced is directly proportional to the number of viable cells in the culture (*In Vitro* EpiDerm™ Skin Irritation Test (EPI-200-SIT), MatTek [online]; Protocol Guide: MTT Assay for Cell Viability and Proliferation. [online]).

All reagents were prepared prior to the skin irritation test. Pre-warmed sterile DPBS was used as the negative control and 5% sodium dodecyl sulphate (SDS) as the positive control. The pre-warmed DMEM/F12 medium and ultrapure water (UPW) were used as test specimens. The MTT stock solution 5 $mg.ml^{-1}$ in DPBS was also prepared and can be stored frozen at -20 °C (2 months). The MTT stock solution must be filtered and diluted in the assay medium to a final concentration of 1 $mg.ml^{-1}$.

The *in vitro* 3D skin model irritation test involves several steps to assess the potential irritation caused by substances. The general outline of the procedure can be seen in Figure 12. A 3D skin tissue model was prepared for testing according to the manufacturer's instructions. In the case of the liquid form, 40 µL of the test substance was slowly dispensed in the center of the 3D skin model. Incubation for 1 hour at 37 °C in a 95% humidified atmosphere and 5% CO_2 allowed the substance to interact with the tissue and elicit any potential irritation response. After the incubation with the test substance exposure, the 3D skin model was rinsed with sterile PBS to remove any residual test material. The rinsed 3D skin model was post-incubated under the same conditions for the next 24 ± 2 hours in the same conditions. At the end of the 24 ± 2 hr incubation period, the 3D skin was examined for signs of irritation. The assessments included measuring cell viability using an MTT assay when 300 µL of MTT medium was pipetted in each insert stored in a 24well microtiter plate. The plate was placed in the incubator for 3 hours ± 5 min. After incubation, the MTT medium was aspirated from all wells,

and the inserts were immersed in 2 ml of DMSO in each insert. Formazan extraction was performed for at least 3 hours at laboratory temperature with shaking on a plate shaker. Finally, for each 3D skin model in the insert, the quadruplicate of 200µl aliquots of the blue formazan solution was pipetted into a 96-well microtiter plate. The DMSO solution was used as a blank. The optical density (OD) was read using an Infinite M200 PRO (Tecan, Switzerland) at 570 nm, without the use of a reference filter.

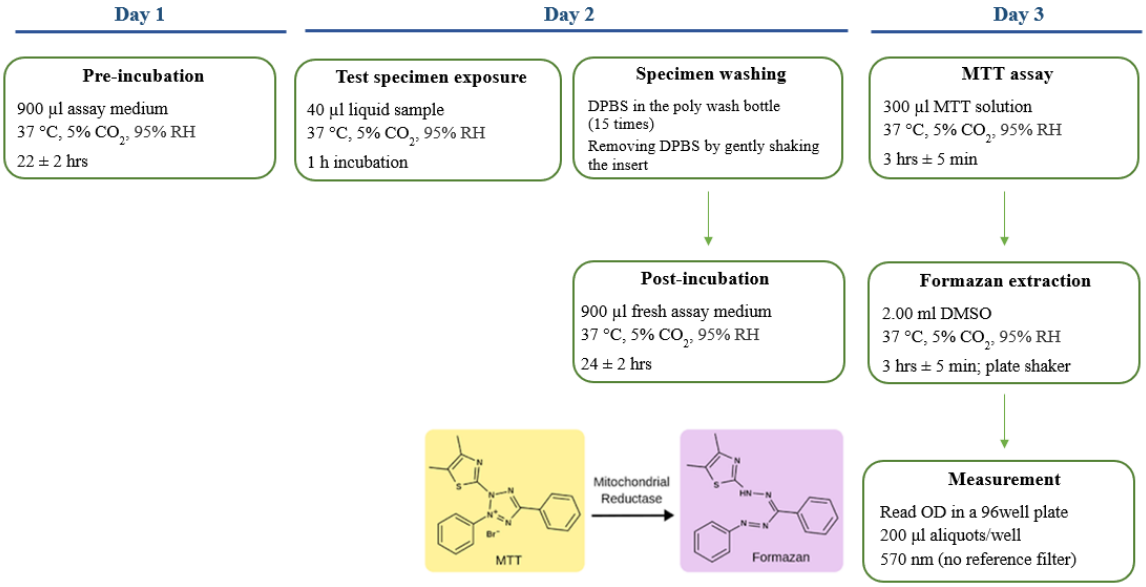

Figure 12: Diagram of in vitro 3D skin irritation test

6.6 The influence of the microbiome on skin cell lines

6.6.1 Trypan Blue staining viability test

The trypan blue exclusion test is among commonly used standard techniques to determine cell viability. It is a vital stain in the field of biology to selectively color necrotic (dead) cellswith microscopic examination (Strober 2015).
Trypan blue is an azo dye derived from toluidine and is unable to penetrate the membranes of living cells. This assay operates on the principle that viable cells possess intact membranes that block the entry of trypan blue, thereby preventing the dye from entering. Conversely, trypan blue can infiltrate the membranes of necrotic cells, which have compromised membrane integrity, permitting the dye to access the cytoplasm. Under a light microscope, only necrotic cells take up this blue dye, making them distinctly identifiable from viable cells (Avelar-Freitas *et al.* 2014; Abhishek *et al.* 2018).

The procedure for trypan blue viability testing involved preparing the cell suspension with 0.25% Trypsin-EDTA and then resuspending it in the cultivation medium. Subsequently, the cell suspension was combined with one part of 0.4% trypan blue solution (20 µl) and one part of the cell suspension (20 µl), leading to a 1:1 dilution. The resulting mixture was allowed to incubate for about 3 minutes at room temperature, after which the stained cell suspension (10 µl) was loaded into the Bürker chamber to count the stained (nonviable) and unstained (viable) cells using a light microscope.

6.6.2 HaCaT proliferation assay

A HaCaT proliferation assay is used to evaluate the growth rate of keratinocytes, which are the primary cells found in the epidermis. These assays are crucial in dermatological and pharmaceutical research, especially in studying wound healing and skin regeneration. The keratinocyte proliferation assay using the MTT colourimetric assay is a widely used method to assess cell growth by measuring metabolic activity. This assay is based on the ability of viable keratinocytes to reduce MTT into insoluble purple formazan crystals, which can be quantified spectrophotometrically (Mosmann 1983; Sylvester 2011).

In this study, the MTT assay was performed in 96-well plates to assess the proliferation of HaCaT keratinocytes after treatment with bacteria and their supernatants, respectively *Staphylococcus epidermidis*, *Micrococcus luteus* as commensals, and *Stapyhlococcus aureus*, *Pseudomonas aeruginosa* as pathogens for 24 and 48 hours. Bacterial supernatants were used at 10% v/v in the cultivation DMEM medium. HaCaT cells were seeded at a density of 1×10^5 cells per well and incubated overnight at 37°C in a 5% CO_2 environment. The HaCaT cells were then washed with DPBS, and experimental treatments including bacterial

suspensions and their supernatants were added to the wells. The DMEM cultivation medium was used as a control. After incubation time 0, 24 and 48 hours, an MTT assay was conducted to evaluate cell proliferation.
For the MTT assay, 5 $mg.ml^{-1}$ MTT stock solution in DPBS was prepared and filtered through a 0.22 μm filter. Then, 20 μL of MTT reagent (10% of the well volume) was added to each well. The cells were incubated for 3 hours ± 5 min at 37°C in a 5% CO_2 environment, allowing viable HaCaT to convert MTT into insoluble formazan crystals. Following incubation, the medium was discarded, and the formazan crystals at the bottom of the wells were dissolved in 80 μL of DMSO. The plate was then placed in the incubator for 15 minutes, and absorbance was measured at 570 nm using a spectrophotometer Infinite M200 PRO (Tecan, Switzerland), with the use of the reference at 630 nm.

Data analysis involved normalizing the absorbance values to untreated control cells, with relative proliferation calculated as a percentage. The absorbance of formazan produced by keratinocytes at time zero (at 70% confluency) was considered the normalized control, and any other time point was compared to this baseline. The percentage of the proliferation was measured using the Equation 1:

$$\text{Proliferation } \% = \frac{\text{The absorbance of formazan at any time point}}{\text{The absorbance of formazan at time zero}} \cdot 100 \qquad (1)$$

6.6.3 HaCaT co-culture with bacteria cells

To prepare the bacterial suspensions for co-culture with HaCaT cell line, overnight cultures of *Staphylococcus epidermidis* CCM 4418, *Micrococcus luteus* CCM 732, *Staphylococcus aureus* CCM 4516 and *Pseudomonas aeruginosa* CCM 1961 were centrifuged at 3.000 RPM for 5 minutes. The resulting pellets were washed twice with DPBS, and the optical density was adjusted to 0.5 McFarland in DPBS. The suspensions were then centrifuged again, after which the pellets were resuspended in 10 ml of DMEM medium without antibiotics.

The confluent HaCaT cell line at a density of 5×10^5 cells/ml was incubated for 30 minutes before the experiments in 1 ml of DMEM cultivation medium devoid of antibiotics within a 12well microtiter plate. For co-treatment, the HaCaT cells were exposed to 100 µL of the prepared bacterial cultures, achieving a multiplicity of infection (MOI) of approximately 1:20 for 2 hours. Additionally, the cells were treated with Staphylococcus epidermidis supernatant (SES). Following the incubation, the HaCaT cells were rinsed three times with DPBS to eliminate non-adherent bacterial cells. The cells were then detached using 0.25% trypsin-EDTA and gathered in 1 ml of cultivation medium. Subsequently, the cell suspension was serially diluted in PBS and spot-plated onto PCA agar plates to determine the count of adherent cells expressed as CFU/ml.

6.7 *In vitro* mixed infection 3D skin model

6.7.1 3D Skin Model

A 3D skin model (24 inserts) was constructed according to the protocol described in Section 6.3, Construction of 3D normal skin tissue models under laboratory conditions. It consisted of normal dermal fibroblasts (HDF cell line), derived from human neonatal foreskin or adult skin, and spontaneously transformed human keratinocytes (HaCaT cell line). This 3D skin model simulates the similar multi-layered structure of native human skin. It was incubated with 600 µl of pre-warmed DMEM medium per well at 37°C in a humidified atmosphere containing 5% CO_2 overnight prior to colonisation experiments.

6.7.2 Bacteria colonization of the 3D Skin Model

For the bacteria colonization of the 3D skin model, *Staphylococcus aureus* and *Staphylococcus epidermidis* were streaked onto Tryptone Soya Agar (TSA) plates and cultured overnight at 37°C. For each distinct strain, a single colony was carefully transferred to a Tryptone Soya Broth (TBS) and subsequently incubated overnight at 35°C. The bacterial cells were then centrifugated at 5000 ×g for 5 minutes, followed by two washing steps to effectively remove any residual medium. The resulting pellet was then resuspended in normal saline solution. The concentration of bacteria cells has been adjusted and diluted to obtain the initial inoculum concentration by measuring the optical density using McFarland densitometr (DEN-1B Grant-Bio; Grant Instruments, United Kingdom). The culture of each bacteria strain was adjusted to a 0.5 McFarland standard as the inoculum, which corresponds to a concentration of 6×10^6 CFU in the 30 µl of the applied suspension. Following inoculation, the 3D epidermal tissues were incubated at 37 °C in a humidified atmosphere supplemented with 5% CO_2 for a duration of 24 hours for bacterial adhesion.

6.7.3 *In vitro* infection 3D Skin model cytotoxicity

Following the bacteria colonization, the in vitro 3D skin model was then processed to quantitatively determine the lactate dehydrogenase (LDH) value, which serves as an indicator of cytotoxicity, and to assess the extent of colonisation of the 3D conjugate model by both *S. epidermidis* and *S. aureus* under conditions both in the absence and presence of the potential tested samples. This assay include the collecting of culture media at the time point (24 h) and the cytotoxicity was determined using the The Cytotoxicity Detection KitPLUS (LDH) (Merck, Germany). This assay involves a coupled reaction where LDH catalyzes the oxidation of lactate, leading to the reduction of NAD+ to NADH.

Subsequently, NADH reduces a tetrazolium salt (INT) to a red formazan product in the presence of diaphorase. The resulting color intensity, measured spectrophotometrically at approximately 490 nm, is directly proportional to the amount of LDH released and thus the extent of cell death. By comparing the absorbance readings of treated samples to those of untreated controls (Equation 3).

$$\text{Cytotoxicity } \% = \frac{(A_{490}\ \text{sample} - A_{490}\ \text{negative control})}{(A_{490}\ \text{positive control} - A_{490}\ \text{negative control})} \cdot 100 \quad (3)$$

The degree of cytotoxicity induced by the experimental conditions can be determined. This method provides a quantitative and reliable measure of cell damage based on the extracellular presence of LDH (Cytotoxicity Detection KitPLUS (LDH) [online]; Kohda et al. 2021).

6.7.4 Determination of 3D skin model bacteria colonization

In the context of this study, the primary purpose of employing the bacteria adhesion test is to investigate the intricate interactions occurring between the 3D skin model and microbial cells. Within broader biological contexts, these adhesion tests are instrumental in elucidating the mechanisms by which bacteria adhere to host tissues during processes such as potential infection establishment or wound healing (Kohda *et al.* 2021; Villata *et al.* 2024). The bacterial cells present in each insert carefully collected by thoroughly washing the surface of the 3D skin model with 1 mL of normal saline solution supplemented with 0.1% Triton X-100 (ThermoFisher Scientific, USA). Following the detachment of adhered bacteria from the surface, the released bacteria were serially diluted and cultured on selective agar plates, specifically designed for the isolation and differentiation of pathogenic staphylococci (NutriSelect® Plus 70193; Merck, Germany). For the precise assessment of bacterial adhesion in our experiments, the Colony Forming Unit (CFU) counting method was employed.

6.8 CAM sheet production

The extracellular matrix (ECM) plays a pivotal role in the formation of tissue architecture and orchestrating cellular phenotype. These properties can be mimicked by in vitro cell-assembled extracellular matrix (CAM) sheets, as an innovative form of biomaterial in tissue engineering and regenerative medicine. This cellular self-assembly approach has evolved from the inherent ability of cells to organise and deposit ECM components. It results in the ability of cells to actively participate in mimicking the native surrounding microenvironment and architecture of anisotropic tissues. (Assunção *et al.* 2020; Xing *et al.* 2020)

6.8.1 Human dermal fibroblast culture and CAM production

The aim of CAM sheet production is to obtain an intact ECM with preserved composition and architecture of the original tissue in a controlled manner, potentially leading to the creation of tissue-like structures with enhanced cell-instructive properties. For the production of CAM sheets, the HDF cell line was cultured in DMEM/F12 medium containing 20% FBS and 1% penicillin/streptomycin. Briefly, the HDF cell line was seeded at a density of 1×10^4 cells·cm^2 in T-25 flasks with the addition of 500 μM of sodium L-ascorbate (Sigma Aldrich, USA) to ensure the formation of ECM components, including collagen (Figure 13). To produce the CAM sheets, the HDF cell line was cultured for 6–12 weeks, and the culture medium was changed three times per week.

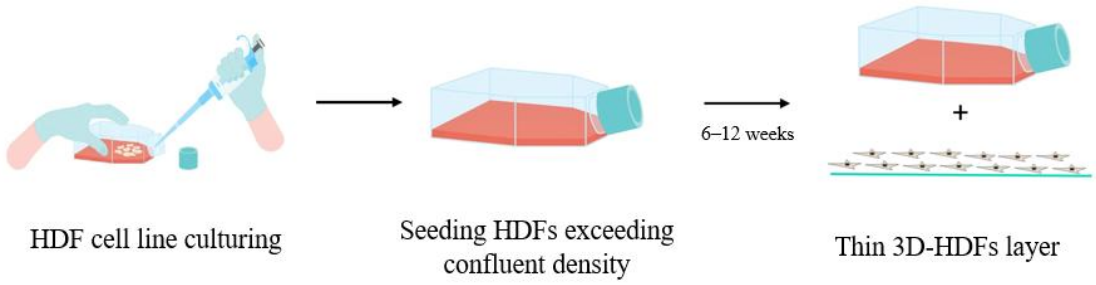

Figure 13: CAM sheet production overview – from HDF cell line to biomaterial scaffold

6.8.2 CAM devitalization/decellularization

After providing the CAM sheets, the devitalization and decellularization processes were carried out. After providing the CAM sheets, the devitalization and decellularization processes were carried out. To devitalize the tissue, CAM were quickly rinsed in distilled water and dried at room temperature in a laminar flow cabinet. Dried CAM was stored at −80 °C. The decellularization process was realized on the devitalized CAM sheets. Decellularization can be defined as a process that removes cellular components from tissues/organs, leaving behind the ECM scaffold. This scaffold retains the structural and biochemical cues that are essential for guiding cell behavior, making it an ideal template for tissue engineering and regenerative medicine applications. The decellularization process involves steps of PBS washing and chemical methods to remove cells while minimizing damage to the ECM structure and composition. Chemical methods of decellularization contain detergents, such as sodium dodecyl sulfate (SDS) or Triton X-100 which are used to solubilize cell membranes and nuclear material (Schmidt *et al.* 2017; Neishabouri *et al.* 2022). Devitalized CAM sheets were rehydrated in ultrapure water for 1 hour, rinsed with PBS, and then replaced with 5 ml of 0.66% SDS for 60 min. After the perfusion time, the SDS was removed, and the PBS was pipetted onto the CAM sheets. The perfusion time of the PBS was 10 min, and it was 5 times replaced for the whole process. Before further experiments, the CAM sheets were rehydrated in UPW and at 4 °C for 24 h.

6.8.3 Assessing H9c2 cell line proliferation using CAM sheets

CAM sheets can be used as a model scaffold for the deployment and proliferation of other cell lines, providing them with a support structure for growth and possibly orientation. The ECM complexity is not only typical for natural tissue but also essential for CAM and its possible biological functions. Thus, the cell-CAM scaffold interaction plays a prominent role in determining proliferation and testing biocompatibility. The acellular CAM sheets obtained by decellularisation were used to support the adhesion and growth of H9c2 myoblasts. First, the acellular CAM sheets were washed with sterile PBS and then placed into a 6well microtitrate plate. Subsequently, a prepared H9c2 cell line was then pipetted onto the surface of the CAM sheets at a concentration of $1\times 10^{5}\cdot ml^{-1}$. The seeded CAM sheets were placed in the incubator under appropriate conditions (at 37 °C in a humidified atmosphere with 5% CO_2). The H9c2 cell line was allowed to adhere and proliferate on the CAM sheet for the desired period of 3 and 7 days. After a period of time, fixation, permeabilization, and fluorescence staining of the cell culture were performed compared to control groups (H9c2 cells cultured on a 6-well microtitrate plate). The medium was aspirated from the wells and 2 ml of 4% PFA was pipetted in. After 15 minutes,

the PFA was removed, and the CAM sheets were washed with 1 ml PBS and removed again. An equal volume of 5% Triton X-100 was then added for 5 minutes and washed 3 times with PBS. Finally, ActinRed™ 555 dye and Hoechst 33258 in PBS were chosen as fluorophores and evaluated using an Olympus IX81 microscope.

6.8.4 Histological analysis of CAM sheets

Histology of CAM sheets was performed as described in Chapter 6.3. CAM sheets were fixed in 4% PFA overnight at room temperature, dehydrated in ethanol (30-90 % EtOH) for 30 minutes each, and embedded in paraffin. Five-µm-thick sample sections were cut on the microtome Panthome LS-2064A and finally stained hematoxylin and eosin.

6.8.5 Preparation of CAM co-culture platform

To establish the CAM co-culture platform, HDF cell line and H9c2 cardiomyoblasts were seeded into T-25 culture flasks. HDF and H9c2/AC16 were cultured together at varying density ratios of 1:1, 1:2, and 2:1, respectively. The co-culture process was done in complete DMEM/F12 medium with the addition of 500 µM of sodium L-ascorbate to ensure the formation of ECM components under standard conditions. To produce the CAM co-cultivation sheets, it was cultured for 6–12 weeks, with the culture medium being refreshed every 2–3 days.

6.9 Investigating the CAM sheet components

6.9.1 RNA isolation and qRT-PCR reaction

Total RNA was extracted from the CAM sheet samples utilizing the Total RNA Mini Kit (cat. n.: 031-100; A&A Biotechnology, Poland), adhering to the protocol outlined by the manufacturer. (Total RNA Mini Manual [online]) To assess the concentration and purity of the extracted RNA, absorbance measurements were taken at wavelengths of 260 nm and 280 nm, respectively, using a NanoDrop ND-1000 spectrophotometer (Thermo Fisher Scientific, Wilmington, DE).

For the synthesis of complementary DNA (cDNA), the NG dART RT Kit (E0801) was utilized, again following the manufacturer's instructions. NG dART RT kit is first-strand cDNA synthesis kit convenient for two step RT-PCR. Kit is based on modified reverse transcriptase with improved thermostability up to 65 °C. It enables amplification of DNA from any RNA with high specificity and sensitivity. NG dART RT mix contains dART reverse transcriptase and RNase Inhibitor. 5X NG cDNA buffer is optimised for RT buffer and dNTPs. cDNA synthesis is performed in the first step using either total RNA or poly(A)+-RNA primed with oligo(dT), random hexamers primers or reverse gene specific primer. The second step, in a separate tube is PCR in which cDNA is a template and specific primers are added to amplify double-stranded DNA of interest by the choice of polymerase (NG dART RT Kit [online]).

In the next step of quantitative real-time PCR (qRT-PCR), the RT PCR Mix SYBR® kit (2008-100; A&A Biotechnology, Poland) was chosen. It is a ready-to-use, master mix designed for real-time PCR applications utilizing SYBR® Green dye for DNA detection. Each reaction was carried out in a total volume of 20 µl, comprising 10 µl of 2× RT PCR Mix SYBR®, 5 µl of forward/reverse primer mix (10 µM) (Table 5), variable volume of template cDNA (corresponding to 10–100 ng), and nuclease-free water to adjust the final volume. Amplification was conducted on a real-time PCR thermal cycler under the following cycling conditions for analyzed genes. The analysed genes (see Tables 6.1 and 6.2) were selected based on their relevance to the formation of ECM, CAM scaffold, respectively. A melt curve analysis was performed at the end of the amplification protocol to confirm the specificity of the PCR products. All reactions were run in triplicate, and non-template controls were included in each run to monitor for potential contamination.

Table 5. Primer sequences used for real-time PCR analysis

Gene	Category	Sense	Antisense
MMP2	ECM remodeling enzyme	TGTGAAGTATGGGAACGCCG	GACAGAAGCCGTACTTGCCA
MMP7	ECM remodeling enzyme	TTACCGCATATTACAGTGGATCG	CATGATGTCAGCAGTTCCCCA
MMP9	ECM remodeling enzyme	GTGCGTCTTCCCCTTCACTTT	TCTTGTCGCTGTCAAAGTTCG
TIMP1	MMP inhibitor	GGGTTCCAAGCCTTAGGGGA	AATGAGAAACTCCTCGCTGC
TIMP2	MMP inhibitor	AAGAACATCAACGGGCACCA	CGAGAAACTCCTGCTTGGGG
IL-6	Cytokine/Inflammation	GTTCTGCCAAACCAGCCTTG	AGATCACCTAGTCCACCCCC
IL-8	Chemokine/Inflammation	GGTGCAGTTTTGCCAAGGAG	ACCAAGGCACAGTGGAACAA
COL11A1	ECM protein organization	AGCCTTTACCAATCTTGTCCTC	GCAGGTCTTTACAAGTTCGGG
p38 MAPK (MAPK14)	Signal transduction Stress response	GCGTCTGACAGGAACACC	GCATCTTCTCCAGCAAGTCG
MAP2K1	MAPK pathway kinase	CCACCTGGCACCCAAACATC	GACATCTGGAGCATGGGACTG
CSPG4	ECM-bound proteoglycan	CCAGTGACCATCCAGAGAGC	GCCTTGTGGCCCTGTAGTTGA
FOXD3	Transcription factor	GCCCAAGAACAGCCTAGTGA	GCAGTCGTTGAGTGAGAGGT
CD326 (EPCAM)	Epithelial marker Cell adhesion Used as negative control, helps confirm HDF purity (absence of epithelial cells).	AGGCAGAAATGAATGGCTCAA	CCAGCAGTGTTCACACACCA
GADPH	Metabolic housekeeping gene	TGCACCACCAACTGCTTAGC	GGCATGGACTGTGGTCATGAG
VEFG	ECM remodeling signaling Co-culture/ vascularization	GACAGACAGACACCGCCC	AGAACAGCCCAGAAGTTGGA

[*]*Sense and antisense primer sequences used for the amplification of target genes involved in cell-assembled extracellular matrix (CAM) remodeling, inflammation, signal transduction, cell adhesion, and housekeeping control during quantitative real-time PCR (qPCR) experiments.*

Table 6.1: Selected ECM-relevant genes for CAM scaffold analysis

Gene	Category	Relevance to HDFs	Function / ECM Role
COL11A1	Structural ECM (Collagen)	Collagen type XI, fibrillar collagen Minor ECM component, plays a role in matrix organization.	Forms heterotypic fibrils with COL1A1 and COL2A1.Important for cartilage ECM, involved in fibril formation and matrix stabilization.
CD326 *(EPCAM)*	Epithelial marker Cell adhesion	Not typically expressed in HDFs. EPCAM is a marker for epithelial cells, not fibroblasts. However, it can be used to confirm absence of epithelial contamination in fibroblast cultures.	Involved in cell-cell adhesion in epithelial tissues. Has no direct role in ECM production or fibroblast biology. Useful as a negative control in fibroblast experiments.
CSPG4	Cell surface proteoglycan / ECM-interacting protein	Low expression in adult HDFs but found in mesenchymal progenitors, pericytes, and sometimes in activated fibroblasts.	Binds to ECM components like collagen VI; involved in cell migration, proliferation, and wound repair. Marker for mesenchymal progenitor-like or activated states in fibroblasts.
FOXD3	Transcription factor / Neural crest marker	Rare in differentiated HDFs, more common in neural crest-derived cells, embryonic progenitors, and melanocyte precursors.	Regulates stemness and lineage commitment. Not typically active in mature fibroblasts, but may be relevant in studies involving reprogramming, dedifferentiation, or fibroblast plasticity.
IL6	Cytokine / Inflammation	Highly expressed by HDFs under stress, injury, or cytokine stimulation (e.g., TGFB1)	Promotes inflammation, fibroblast activation, and can indirectly stimulate ECM production via TGFB signaling
CXCL8 *(IL8)*	Chemokine / Inflammation	Secreted by HDFs in response to TNF-α, IL-1β, UV, or oxidative stress	Attracts immune cells (neutrophils), stimulates MMP production, and facilitates ECM degradation and tissue remodeling
MAP2K1	Signal transduction (MAPK pathway)	Expressed in HDFs ERK/MAPK signaling cascade regulating proliferation, migration, and ECM gene expression.	Activates ERK1/2 → promotes transcription of MMPs, collagens, fibronectin, and other ECM remodeling genes. Involved in mechanotransduction and matrix response.

Table 6.2: Selected ECM-relevant genes for CAM scaffold analysis

Gene	Category	Relevance to HDFs	Function / ECM Role
MAPK14 *(p38 MAPK)*	Signal transduction / Stress response	Expressed in HDFs and activated in response to cytokines, UV, oxidative stress, and mechanical tension**.**	Regulates inflammatory gene expression (e.g., IL6, IL8), MMPs, and ECM remodeling under stress or damage. Influences fibroblast senescence**,** proliferation, and matrix degradation**.**
MMP2	ECM remodeling enzyme	Involved in remodeling and wound healing	Matrix metalloproteinase – gelatinase
MMP7 *(matrilysin)*	ECM remodeling enzyme	Expressed at lower levels in HDFs compared to other MMPs (MMP1, MMP2). Can be induced under inflammatory or stress conditions (e.g., via IL1B, TNFα, or TGFB).	Degrades a broad spectrum of ECM proteins (e.g., proteoglycans, elastin, fibronectin, collagen IV). Involved in wound healing**,** fibrosis**,** and ECM turnover**.**
MMP9	ECM remodeling enzyme	Inflammatory and migratory fibroblast populations	Gelatinase – digests type IV and V collagen
TIMP1	MMP inhibitor	Regulates ECM degradation balance	Inhibits MMPs – regulates ECM degradation
TIMP2	MMP Inhibitor / ECM Remodeling Regulator	Expressed in HDFs, often in balance with MMPs. Regulates ECM homeostasis by inhibiting matrix degradation.	Binds to and inhibits MMPs (especially MMP2), preventing excessive ECM breakdown. Also involved in MMP2 activation complex formation with MT1-MMP (MMP14)**.**
VEGF	Growth factor / Angiogenesis	Expressed in HDFs**,** especially under hypoxia**,** mechanical strain, or TGFB1 stimulation**.** Upregulated during wound healing and in fibrotic environments**.**	Stimulates angiogenesis**,** promotes endothelial cell migration, and affects ECM indirectly by recruiting vascular support. Modulates ECM via MMP activation, and indirectly promotes remodeling and fibroblast activation.

6.9.2 SDS-PAGE electrophoresis

Preparation for SDS–PAGE electrophoresis

Prior to gel casting, it is essential to thoroughly clean the glass plates with a detergent solution, followed by rinsing them with both tap and distilled water. Additionally, treating them with 70% ethanol can be done to guarantee maximum cleanliness. Next, the electrophoresis chamber is constructed by placing the shorter glass plates atop the longer ones, with each plate fitted with spacers. The assembled plates are then inserted into a casting frame and secured with clamps. This frame is positioned into a casting stand. Finally, the resolving and stacking gels are prepared according to the specifications provided in Table 7. Importantly, the polymerization agents TEMED and APS should be added immediately before the gel casting.

Table 7: Composition of resolving/stacking gels for SDS-PAGE electrophoresis

Reagent	**Resolving gel [µl]**	**Stacking gel [µl]**
12% width gel between the glass	1.5 mm	
40% akrylamid	2 250	375
H_2O	2 205	3 187
1M TRIS (pH = 8.8)	3 370	-
1M TRIS (pH = 6.8)	-	375
10% SDS	90	30
10% APS	90	30
TEMED	9	3

The resolving gel solution is dispensed between the glass plates to a height of roughly 2 cm from the edge of the shorter plate. The surface of the gel is covered with 2–3 drops of distilled water to create a level interface and is allowed to polymerize for at least 30 minutes at room temperature. Subsequently, the stacking gel solution is pipetted to the upper edge of the shorter plate. A comb is carefully inserted into the stacking gel to create sample wells, taking care to avoid trapping any air bubbles. The gel is again allowed to polymerize for a minimum of 60 minutes at room temperature.

CAM sheet sample preparation and SDS-PAGE electrophoresis

The prepared gel plates are placed into the slots of the electrophoresis module, ensuring that the shorter plate is oriented inward to create a buffer chamber. The plates are fastened with clamps, and the entire assembly is positioned into the electrophoresis tank. The inner chamber is filled to the top with 1× TGS buffer. The CAM sheet samples were rehydrated and washed with PBS overnight before being lysed with ice-cold RIPA buffer containing protease and phosphatase inhibitors. Lysis of the CAM sheet was performed (1 h, 4 °C), followed by centrifugation for 10 minutes at 12,000x g, the removal of the supernatant, and dilution in 1x Loading Protein Buffer (E0269-01, EURx, Poland) along with a 5minute heating at 95 °C. A molecular weight marker (Perfect™ Tricolor Protein Ladder; E3210-01, EURx, Poland) is loaded next to the CAM samples to determine the molecular weights of the resolved protein bands. Each well receives between 5-30 ng of total protein. After loading the samples, the electrophoresis tank is sealed with the electrode lid and connected to a power source. An initial voltage of 100 V is applied for 15 minutes, after which the voltage is raised to 150 V. Electrophoresis proceeds until the dye front reaches the bottom of the resolving gel. The process is concluded by turning off the power, disconnecting the lid, and carefully removing the glass plates. The plates are rinsed with distilled water and gently separated. The stacking gel is discarded, while the resolving gel is prepared for subsequent western blot analysis.

6.9.3 Semi-dry Western Blotting

For subsequent semi-dry western blotting, the Trans-Blot Turbo™ RTA Transfer Kit (Bio–Rad, USA) was utilized. This kit includes a 5× transfer buffer and Trans-Blot Turbo Mini-size membranes and filter stacks. However, the PVDF membrane provided was replaced with a nitrocellulose membrane with 0.22 µm pore size (Bio–Rad, USA). A 1× transfer buffer was prepared by mixing 200 ml of 5× buffer, 600 ml of MilliQ water, and 200 ml of 96% ethanol. The filter stacks and nitrocellulose membrane were pre-soaked in this buffer. The transfer blot was assembled in the following order on the anode tray: pre-wetted filter stack, nitrocellulose membrane, SDS–PAGE gel, and a second filter stack. Any air bubbles between layers were carefully removed using a roller. The assembly was sealed with the cathode tray, and the standard transfer program (Trans-Blot Turbo™ Transfer System, Bio-Rad, USA) was run for 7 minutes. Transfer efficiency was verified by staining the membrane with Ponceau S for 5 minutes, followed by washing with distilled water. The membrane was then subjected to immunodetection.

6.9.4 Immunodetection

Following Ponceau S staining and destaining, the membranes were transferred into a blocking solution containing 5% bovine serum albumin (BSA) dissolved in TBS–T buffer (Tris-buffered saline with 0.1% Tween 20). Blocking was performed for 1 hour at room temperature using a rocking platform. The same blocking buffer was used for the dilution of both primary and secondary antibodies, with final antibody concentrations not exceeding 5 μg/ml. After blocking, the membranes were incubated with the diluted primary antibody overnight at 4 °C on a rolling platform. Following primary incubation, the membranes were washed three times for 5 minutes each in TBS–T. Next, the membranes were incubated with the secondary antibody, also diluted in 5% BSA in TBS–T, for 1 hour at room temperature, followed by another series of three 10-minute washes in TBS–T.

Detection was carried out using the Syngene G: Box Chemi XT 4 Chemiluminescence and Fluorescence Imaging System (Syngene, USA). Prior to imaging, the membranes were incubated for 5 minutes with WesternBright Quantum Kit (K-12042-D10, Advansta, USA), a chemiluminescent detection reagent.

6.10 *In vitro* cultivation chamber

To create the *in vitro* cultivation experiments under the addition of external mechanical stimulation, the additive-manufactured in vitro culture chamber was utilised. A schematic diagram of the culture chamber is shown in Figure 14, position A. The device dimensions, as shown by Figure 14 at point B, have been optimised for a 25 mm diameter growth space. The mechanical control system of the device is made up of a stepper motor, which provides linear motion via a linear actuator. The motion is precisely controlled by an Arduino-based microcontroller (Arduino Mega 2560) that dictates the trajectory of the actuator. Therefore, the device allows for variable and controllable distortion of the membrane within a preselected and selectable range.

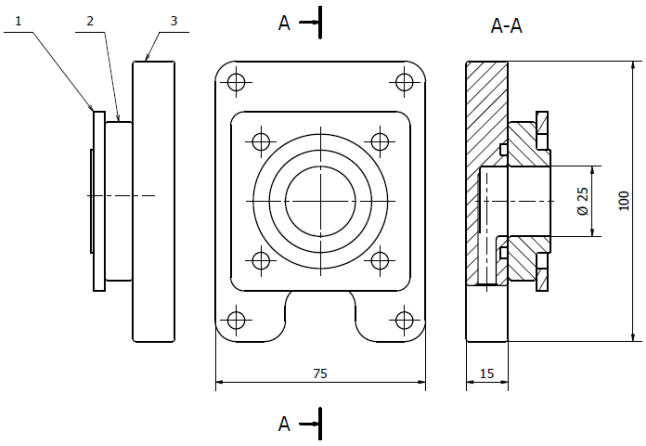

Figure 14: Technical drawing of mechanical stimulation device housing.
The illustration presents three views of the device component: a side view (left), a front view (center), and a section view (right) along the A–A axis. Mounting apertures and a central recess of 25 mm diameter are included in the design for customized use in cell culture applications. Dimensions are in millimeters.

In vitro cultivation experiments with external mechanical stimulation were performed under sterile conditions in a humidified atmosphere at 37 °C with 5% CO_2, using DMEM/F12 as the culture medium. The culture chamber materials were all sterilised either by repeated washing with 70% ethanol, followed by rinsing with distilled water and PBS. Static HDF cell controls were kept in sterile Petri dishes in standard culture medium and environmental conditions. Afterwards, cultured samples of CAMs were evaluated to study their mechanical properties and cellular activity using fluorescence microscopy.

7. SUMMARY OF RESULTS

All of the studies detailed in the practical section of this dissertation are the result of extensive, long-term experimental work. The very nature of these experiments demanded sustained attention to detail and a high degree of perseverance. Even the smallest mistake, or an unexpected contamination event, often meant that entire experimental series had to be repeated from the very beginning. Such setbacks were not only discouraging but also resulted in the loss of considerable amounts of time, energy, and resources. The process required constant vigilance, adaptability, and a willingness to learn from each challenge, no matter how minor it may have seemed at the outset.

When this research project was initiated, the world was still grappling with the far-reaching consequences of the COVID-19 pandemic. This global crisis had a profound impact on scientific work, particularly in terms of the availability of laboratory reagents and materials. Many essential reagents were difficult to obtain, with supply chains disrupted and delivery times uncertain. In particular, the lack of access to certain specialized reagents—such as crosslinkable collagen, which is indispensable for the preparation of the seeding layer—posed significant obstacles. These shortages necessitated a great deal of flexibility and creativity in the laboratory. Instead of following established protocols, it became necessary to adapt and optimize experimental procedures using whatever reagents were available at the time. This process of adaptation was often time-consuming and required repeated rounds of troubleshooting and optimization to achieve reliable and reproducible results.

Once the appropriate methods and experimental models had been successfully validated, these newly established approaches could be gradually implemented for the systematic measurement of the properties of various substances. This, in turn, enabled the progressive publication of the resulting data, contributing valuable new insights to the scientific community. However, it is important to note that many of the experimental series initiated during this research are still ongoing. Some lines of investigation have yet to reach completion, and much of the data generated has not yet been published. This reflects both the ambitious scope of the project and the inherent complexity of experimental science, where progress is often incremental and shaped by unforeseen challenges. Nevertheless, the work accomplished thus far lays a strong foundation for future research and underscores the resilience and adaptability required to conduct meaningful scientific inquiry in the face of adversity.

7.1 Establishment of an *in vitro* 3D Skin Culture Model

The first necessary step of the study was to identify a suitable protocol for developing a 3D skin model of human dermal fibroblast and keratinocyte. One approach regarding the supporting collagen matrix and the cell lines was used to produce a viable *in vitro* skin equivalent according to the modification to the protocols of Carlson *et al.* 2008 and Gantatirkar *et al.* 2007. This model aimed to enhance the interaction between keratinocytes and fibroblasts, thereby mimicking the natural architecture of human skin more closely. By utilizing a combination of cell lines, we sought to improve the overall functionality and stability of the skin equivalent.

The stages of *in vitro* 3D skin model development are shown in Figure 15, alongside a representative scheme.

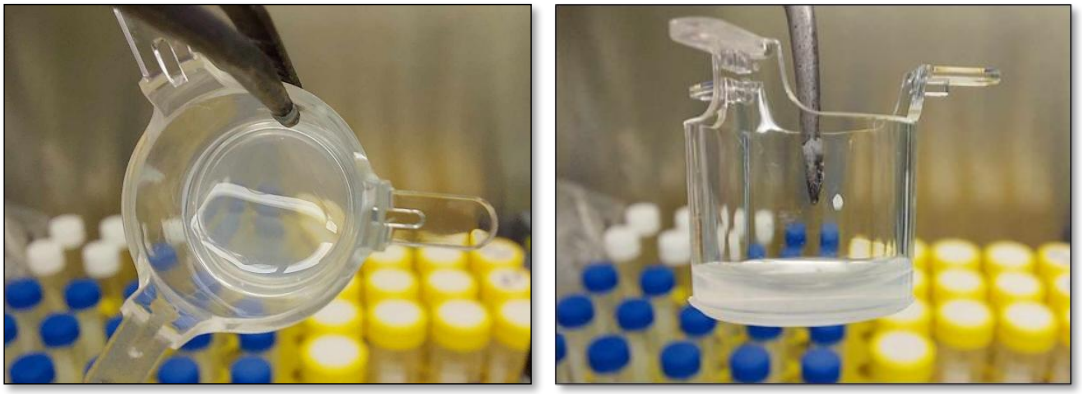

15A: Acellular collagen layer after 1h incubating at 37 °C

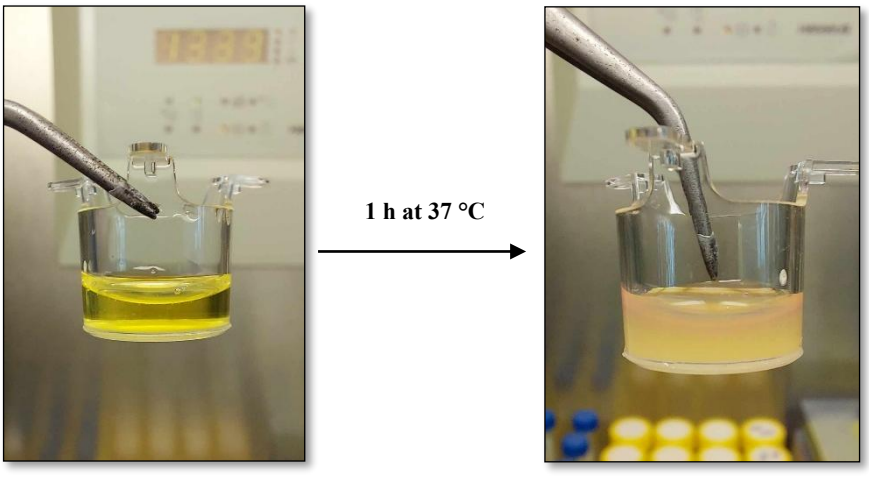

15B: Cellularized collagen (HDF cell line)

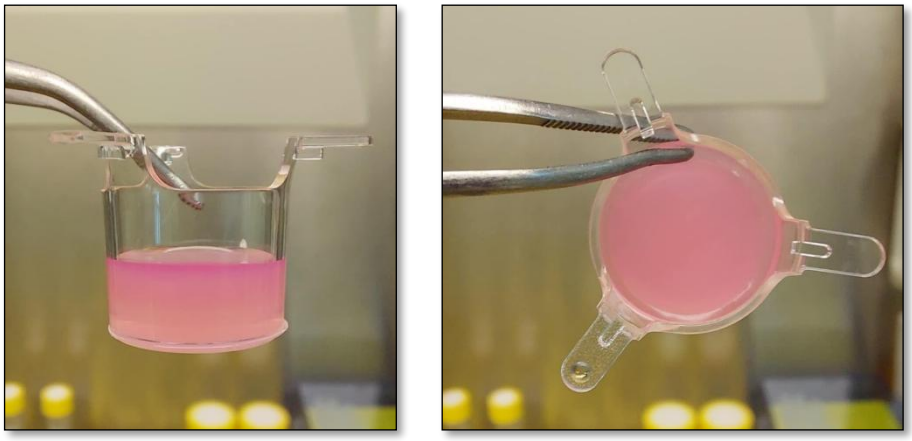

15C: Cellularized collagen after 7 days cultivation

15D: 3D Skin model - ALI system cultivation

Figure 15: Preparation of collagen-based 3D skin model
A: The preparation of acellullar collagen-based layer for the cell line seeding. B: Collagen-fibroblast layer od 3D skin model development.
C: Collagen- fibroblast layer after 7 days of culture. D: Fully mature in vitro 3D skin model (ALI system).

In this Figure 15, it is shown that the collagen gel was used as a substrate for cell cultivation. According to the manufacturer Corning®, this collagen can form a three-dimensional gel on the 3 μm porous polycarbonate membranes as collagen support. Solutions of collagen was solidified into a stable gel by neutralizing with NB puffer and warming to 37 °C (incubation time: 45 min). After this polymerization, the collagen can form a stable acellular layer as a support of the skin model (Figure 15A). Simultaneously, the 3D skin cultures of preparation of

the cellularized collagen with HDFs were assembled (Figures 15B). The cellular part consisting of the collagen matrix embedded with HDFs actively contracts over one week of culture in cultivation medium (Figure 15C). Subsequently, on the cellularized collagen, HaCaT were seeded. Finally, HSEs consist of a stratified epithelium grown at an air-liquid interface on a collagen matrix populated with HDFs (Figure 15D). Additionally, HaCaT used to seed the surface are also observed to form a fully confluent monolayer on the surface of the collagen, as the surface becomes opaque and white in colouration (in sharp contrast to the reddish-pink collagen-HDFs part, Figure 15C).

The established *in vitro* 3D skin model, which employs a collagen gel incorporated with HDF, and overlaid with HaCaT at the air-liquid interface (ALI), exhibits structural and functional attributes that are analogous to recognised *in vitro* skin equivalents. The documented contraction of the collagen matrix over a week of cultivation is consistent with the findings of Bell *et al.* 1981, who indicated that fibroblast-mediated contraction is a prevalent occurrence in collagen-based dermal equivalents, facilitating tissue maturation and enhancing mechanical stability. Furthermore, the development of a stratified epithelium by HaCaT cells on the cellular layer imitates dermal part mirrors the epidermal differentiation documented in other investigations utilising comparable co-culture systems (Souren *et al.* 1989; Joshi *et al.* 2023). The transition to ALI culture is imperative for fostering keratinocyte differentiation and stratification that highlight improved epidermal maturation under such conditions. In addition, the application of HaCaT cells, an immortalised keratinocyte line, has been corroborated in numerous studies for their ability to generate a functional epidermal layer within 3D *in vitro* skin models (Tsao *et al.* 2014). In aggregate, these correspondences substantiate the physiological significance of the fabricated skin model and its utility for subsequent TERM research and evaluations.

The *in vitro* 3D skin model was developed to mimic the fundamental architecture of human skin, comprising a dermal equivalent composed of a collagen matrix populated with HDFs, and an epidermal layer formed by HaCaT seeded onto this dermal equivalent. This bilayered structure is evident in the histological image presented in Figure 16, which showcases a cross-section of the model stained with hematoxylin and eosin (H&E).

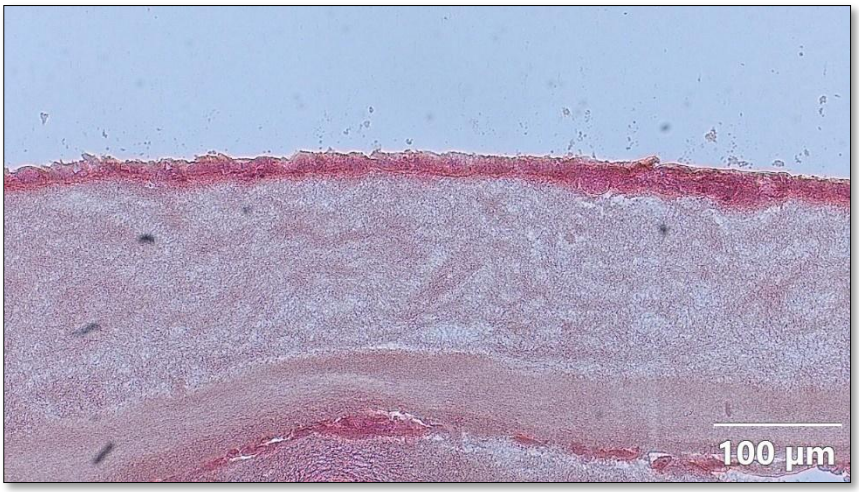

Figure 16: H&E stained cross-section of a in vitro 3D skin equivalent

Upon examination of the H&E-stained section (Figure 16), a distinct layered organization is observable. The lower region, characterized by lower cellular density and a lighter pink staining pattern, likely represents the collagen matrix containing the HDFs, thus forming the dermal compartment. The collagen appears as a lighter pink with the fibrillar network. The cellular density of this dermal equivalent can vary depending on the initial seeding conditions and the duration of the culture period. Superimposed on the dermal equivalent is a more cellular layer, which constitutes the epidermis formed by the HaCaT keratinocytes. This epidermal layer exhibits a more intense pinkish-purple staining due to the higher concentration of cell nuclei. Within this epidermal component, the initial stages of stratification can be potentially discerned, reflecting the proliferative and differentiating behavior of the keratinocytes. The interface between the dermal equivalent and the epidermal layer, the basement membrane zone (BMZ), is a critical structure in native skin responsible for cell adhesion and intercellular signaling. In this H&E-stained section, the BMZ may appear as a subtle, slightly more intensely stained line, although definitive identification of this structure would necessitate specific staining techniques targeting BMZ components such as laminin and collagen IV.

The utilization of *in vitro* 3D skin models as valuable tools for investigating skin biology, drug testing, and tissue engineering is well-established in the scientific literature. Previous studies have demonstrated the potential of these models to form a stratified epidermis with specific characteristics, when HaCaT are cultured on a fibroblast-containing dermal equivalent (Stark *et al.* 2004; Wong *et al.* 2019; Imran *et al.* 2024). The presence of fibroblasts within the dermal equivalent is crucial as they secrete growth factors and extracellular matrix components that promote keratinocyte differentiation and stratification (Bell *et al.* 1981).

To further standardize the *in vitro* skin equivalent model and mitigate variability, the spontaneously transformed human keratinocyte cell line HaCaT was employed instead of primary keratinocytes. HaCaT cells exhibit sustained genetic alterations indicative of transformed but non-tumorigenic cells (Boukamp *et al.* 1997). When cultured on cultivation flasks, HaCaT cells demonstrate continuous proliferation, independence from feeder cells, and a typical epithelial morphology with the expression of a broad range of keratins. However, the formation of multilayered epithelia by HaCaT cells in organotypic co-cultures can be delayed and may require a higher number of seeding fibroblast cells in the dermal part This delay has been attributed to certain deficiencies in HaCaT cells, such as reduced interleukin (IL-1) production and low expression of receptors for keratinocyte growth factor (KGF) and granulocyte-macrophage colony-stimulating factor (GM-CSF), which can be compensated by the application of transforming growth factor-alpha (TGF-α) (Breitkreutz *et al.* 1998; Mai *et al.* 2024). In 3D skin model of HaCaT cells with HDF, well-structured and differentiated stratified epithelia have been observed to develop, although the epdiermal part often remains parakeratotic, indicating incomplete keratinization.

In conclusion, the reproducible production and quality of HDF-HaCaT 3D co-cultures render them an excellent tool for large-scale investigations into the mechanisms regulating skin re-epithelialization and homeostasis within a tissue-like context. However, it is important to acknowledge that these *in vitro* models, including the one presented here, have limitations compared to native human skin. Aspects such as full epidermal barrier function, the presence of skin appendages (hair follicles, sweat glands), and complex immune cell interactions are typically not fully recapitulated in these simplified systems (Niehues *et al.* 2018). Therefore, the degree of stratification and differentiation observed in this image should be interpreted considering the specific culture conditions, the passage number of the cell lines used, and the duration of the experiment, all of which can significantly influence the final morphology of the reconstructed skin (Pampaloni *et al.* 2009).

Following the histological analysis of the 3D skin model, which showed light on its structural integrity and cellular arrangement, an additional tissue viability was evaluated using the MTT viability assay. This quantitative approach enables the assessment of metabolic activity in the cells of the reconstructed *in vitro* skin model. The outcomes of this viability and cytotoxicity assay are illustrated in Figure 17.

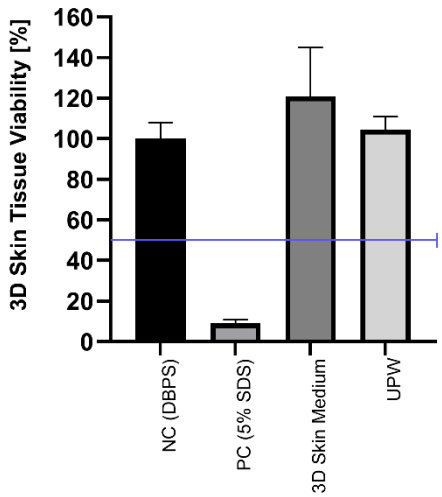

Figure 17: Viability of the 3D reconstructed skin model

Evaluating cell viability is a vital step in confirming the functionality and appropriateness of a reconstructed skin model for *in vitro* studies. The bar graph represents the mean viability of the 3D skin tissue for a treatment, and the error bars indicate the standard deviation. A blue line is drawn at the 50% viability threshold. A high baseline viability in the untreated control group is crucial to ensure the model retains its physiological traits and reactivity. A high viability in the negative control is crucial. It confirms that the vehicle or the basal conditions of the experiment do not negatively impact the skin tissue's health. (*In Vitro* EpiDerm™ Skin Irritation Test (EPI-200-SIT), MatTek [online]; OECD Test Guideline 439 *In Vitro* Skin Irritation: Reconstructed Human Epidermis Test Method [online]). Moreover, the model's capacity to show a substantial decrease in viability when exposed to a known cytotoxic agent, such as 5% SDS, acts as a positive control, validating the assay's sensitivity and the model's ability to respond to irritant agents. SDS is widely used as a strong irritant in such tests, and its cytotoxic effect, leading to a significant reduction in viability, is well-documented. A substantial difference between the negative and positive controls is essential for the assay's reliability (Rasmussen *et. al* 2010; OECD Test Guideline 439 *In Vitro* Skin Irritation: Reconstructed Human Epidermis Test Method [online]).

On the other hand, treatments with non-irritating substances, such as the cell culture medium itself or ultrapure water under specific exposure conditions, should ideally reflect high tissue viability, signifying the model's compatibility with standard laboratory practices and the lack of inherent cytotoxic effects from these substances. The high viability observed in the 3D skin tissue treated with medium alone is expected, as it provides the necessary nutrients and environment for cell survival. The high viability with UPW suggests that short-term exposure to ultrapure water under these experimental conditions does not significantly compromise the viability of the 3D skin model. This could indicate that UPW is not a significant irritant in this context. Finally, the results presented in the graph are generally consistent with expectations for a skin irritation test using a 3D skin model. These viability findings, when taken alongside histological results, provide a thorough assessment of the reconstructed skin model's reliability and its applicability for future experimental studies.

Moreover, I have fully validated the above-mentioned 3D skin models for laboratory practice at Tomas Bata University in Zlín. The validity of these models is demonstrated by the results presented desribed earlier, which provide strong evidence of their reliability and applicability in practical laboratory settings. The practical use of these validated models is currently exemplified in the SurfToGreen project (HORIZON-JU-IA-101157688), where we are investigating the effects of various types of surfactants. Specifically, our research focuses on comparing the properties and behaviors of different surfactant classes, such as ionic and cationic surfactants, in order to better understand their impact and potential applications. This ongoing work highlights the relevance and usefulness of the validated models in addressing real-world scientific questions and advancing our knowledge in the field of surfactant chemistry. However, due to the ongoing nature of the project and the intended use of the results within the framework of SurfToGreen, it is not possible to publish these findings at this time. We are committed to ensuring that the results are utilized effectively within the project before making them publicly available, in order to maximize their impact and maintain the integrity of our research process.

7.2 Bacterial behavior on HaCaT monolayers as a foundation for 3D skin model experiments

Before transitioning to complex bacteria-enriched *in vitro* 3D skin models, it is essential to understand the basic interactions between skin keratinocytes and representative bacterial strains under simplified conditions. To this end, a series of preliminary experiments were conducted using HaCaT monolayers exposed to both commensal and pathogenic bacterial species. These included the skin commensals *Staphylococcus epidermidis* and *Micrococcus luteus*, as well as the opportunistic pathogens *Staphylococcus aureus* and *Pseudomonas aeruginosa*, which are commonly implicated in skin infections and chronic wounds (Grice and Segre 2011; Sachdeva *et al.* 2022).

Keratinocytes are key components of the skin barrier and the chronic wound microenvironment. They not only play an essential role in re-epithelialization and wound healing but also contribute to immune defense by producing cytokines, chemokines, and AMPs. The interaction between keratinocytes and skin-residing microbes, particularly commensals, is increasingly recognized as critical for maintaining skin homeostasis. For example, *S. epidermidis* has been shown to induce AMP expression in keratinocytes and to modulate local immune responses beneficially (Lai *et al.* 2010; Kadam *et al.* 2019). Conversely, *P. aeruginosa*, although part of the skin microbiota, is an opportunistic pathogen associated with nosocomial infections, chronic wounds, and polymicrobial biofilm-associated conditions (Oliveira *et al.* 2023).

This part of study aimed to elucidate bacterial behavior and its impact on keratinocyte viability and proliferation, thereby providing a reference framework for subsequent integration of bacterial representatives into *in vitro* 3D skin constructs. Understanding whether commensals like *S. epidermidis* or *M. luteus* exert protective effects against pathogens such as *S. aureus* or *P. aeruginosa* may offer insights into microbiota-driven modulation of infection and tissue repair processes. Indeed, some probiotic and commensal bacteria have been shown to inhibit the adhesion and internalisation of *S. aureus* into keratinocytes, thereby reducing its pathogenic potential (Prince *et al.* 2012; Kiousi *et al.* 2024)

Three assays were performed, i. e. trypan blue viability assays, where the viability of HaCaT was evaluated following exposure to both whole bacterial cultures and their cell-free supernatants (lysates). To investigate whether bacterial lysates affect HaCaT regenerative potential, cell proliferation assay was monitored. And finally, since colonisation of epithelial surfaces often begins with adhesion, the capacity of bacterial strains to adhere to HaCaT monolayers was measured using adhesion test.

7.2.1 HaCaT viability and proliferation in the presence of microbiome

Understanding the interplay between skin cells, particularly keratinocytes, which constitute the majority of the epidermis, and these microorganisms is crucial for elucidating the mechanisms underlying skin health and potential disease. This study investigates the impact of soluble factors produced by selected commensal and pathogenic bacteria on the viability of human keratinocytes (HaCaT cell line). The rationale behind this investigation lies in the need to characterise the differential responses of skin cells to various bacterial signals, which can contribute to maintaining skin homeostasis or triggering pathological processes.

To assess the potential cytotoxic or protective effects of bacterial supernatants on HaCaT cells, the Trypan Blue exclusion assay was employed. This widely used method is based on the principle that viable cells possess intact cell membranes that exclude the membrane-impermeable dye Trypan Blue, while non-viable cells with compromised membranes allow the dye to enter, resulting in blue staining of the cytoplasm. In this assay, HaCaT cells were exposed to supernatants derived from cultures of *S. epidermidis, M. luteus, S. aureus* and *P. aeruginosa* + their lysates for specific time intervals (0, 2, 8, 24, and 48 hours), seen in Figure 18 and 19. Following incubation, the cells were harvested and incubated with Trypan Blue solution and quantified under a light microscope.

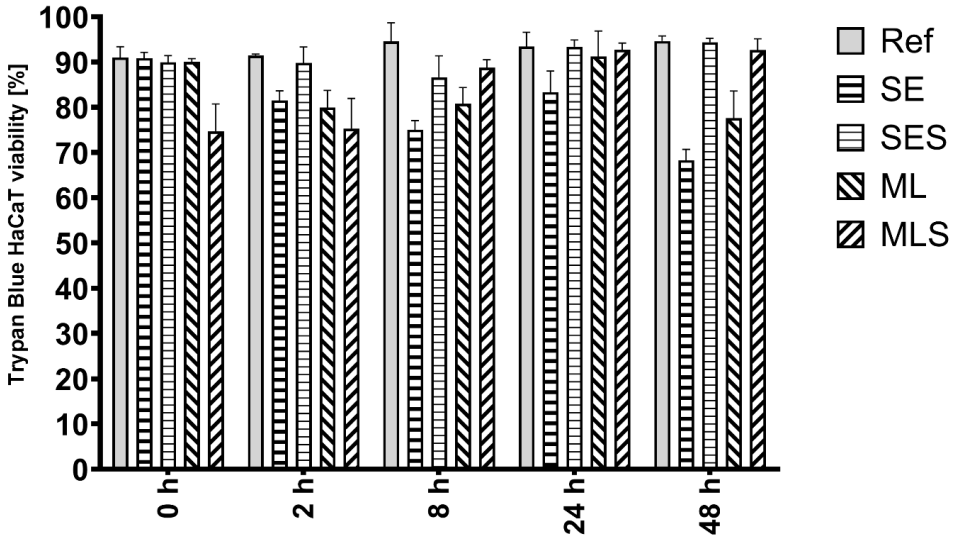

Figure 18: Effects of commensal bacteria/supernatants on HaCaT cell viability.

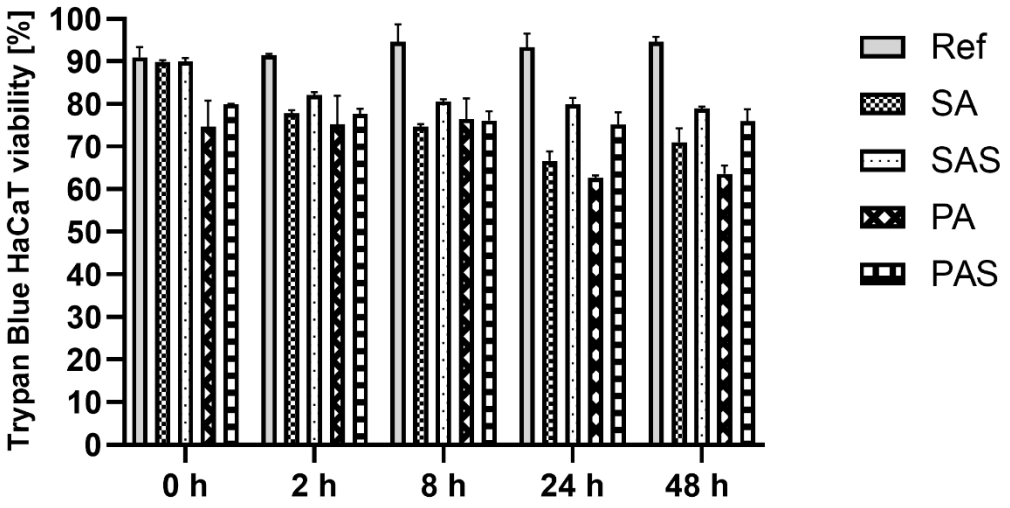

Figure 19: Effects of pathogenic bacteria/supernatants on HaCaT cell viability.

The bar graphs illustrate the Trypan blue HaCaT cell viability (%) at the specified time intervals. At the outset of the experiment (0 h), the viability of HaCaT cells is notably high, approximately 90-95 %, across all conditions, which is expected for healthy cells. The reference condition consistently shows high viability, remaining above 90 % throughout the 48h duration. The presence of both live (SE) and killed (SES) *S. epidermidis* supernatants seems to have a minimal effect on HaCaT cell viability over the 48 hours (Figure 18). The viability stays relatively high, generally above 85 %, with minor fluctuations. This indicates that soluble factors released by *S. epidermidis*, even when the bacteria are inactivated, do not significantly damage HaCaT cells in this experimental context. In the case of *M. luteus*, similarly to SA, both ML and MLS do not markedly reduce HaCaT cell viability over the 48h timeframe. The viability typically remains above 80 %, with some variation noted across time points.

Comparable testing was conducted with the pathogenic bacteria (Figure 19). The SE and SAS appear to adversely affect HaCaT cell viability over time. At 2 hours, the viability in both SA and SAS conditions is significantly lower than the reference. This decline becomes more pronounced at subsequent time points (24 h and 48 h), with viability decreasing to about 65–75 %. Notably, the SAS displays a similar trend to the live bacteria, indicating that the secreted factors or cellular components of *S. aureus* play a role in the decreased cell viability. PA and PAS also show a decline in HaCaT cell viability throughout this testing period, with viability dropping to roughly 60-70 %. Similar to *S. aureus*, the PAS shows a comparable effect to the PA, suggesting that the stable components of PA contribute to the observed cytotoxicity.

To evaluate the impact of bacterial components on keratinocyte proliferation, a metabolic MTT assay was conducted on HaCaT cells exposed to 10% sterile-filtered bacterial lysates of both commensal and pathogenic species.

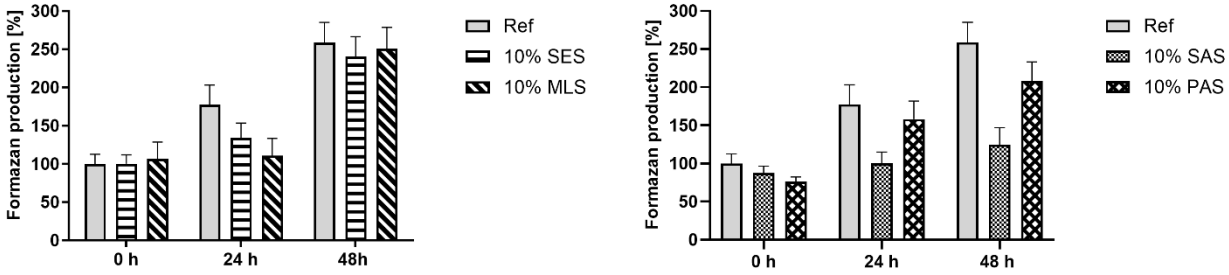

Figure 20: MTT proliferation assay in HaCaT monolayers exposed to bacterial supernatants over 0, 24, and 48 hours (expressed as % of time 0 reference). Left: Commensal bacteria (S. epidermidis – SES, M. luteus – MLS). Right: Pathogenic bacteria (S. aureus – SAS, P. aeruginosa – PAS).

Formazan production was measured at 0, 24, and 48 hours and normalized to the 0hour reference to assess relative changes over time (Figure 20). In the reference group (HaCaT monoculture without bacterial lysate influence), a consistent increase in formazan production was observed over time, indicating normal proliferation and metabolic activity under standard conditions. This trend served as a baseline to compare the impact of bacterial factors.

Exposure of HaCaT keratinocytes to bacteria and their lysates revealed distinct effects on cell viability and proliferation, reflecting the differential impact of commensal versus pathogenic microorganisms. Supernatants from *Staphylococcus epidermidis*, and *Micrococcus luteus* did not induce any significant deviations from the reference proliferation pattern, as indicated by comparable increases in formazan production at both 24 and 48 hours. This suggests that these commensal strains do not negatively affect HaCaT cell metabolic activity or viability (Cogen *et al*. 2010; Lai *et al*. 2009). *S. epidermidis* is known to support cutaneous homeostasis by promoting the production of AMPs and modulating host immune responses without harming keratinocytes. Although less is known about *M. luteus* in this context, its non-cytotoxic profile in the assay supports the hypothesis of its neutral or even beneficial interaction with host cells. Nevertheless, it is known to possess plant growth-promoting properties, indicating it may not be inherently toxic to mammalian cells (Ahmad *et al*. 2008). In contrast, supernatants from pathogenic bacteria, namely *Staphylococcus aureus* and *Pseudomonas aeruginosa*, significantly reduced HaCaT cell proliferation. SAS exposure led to a marked decrease in formazan production at both time points, consistent with the cytotoxic properties of *S. aureus*, which secretes

numerous virulence factors such as alpha-toxin and phenol-soluble modulins that compromise epithelial barrier integrity and trigger inflammatory damage (Otto 2014; Mohammedsaeed *et al.* 2014). Similarly, PAS exposure resulted in reduced metabolic activity, albeit to a lesser extent. *P. aeruginosa* is recognised for its cytotoxic effects on keratinocytes, driven by a variety of virulence factors, including exotoxins, proteases, and components of biofilms. However, this variation may be attributed to strain-specific virulence or the timing of supernatant collection, which influences the concentration of cytotoxic compounds like pyocyanin and elastase (Ichikawa *et al.* 2000; Gellanty and Hancock 2013).

Collectively, these observations highlight the differential influence of bacterial species on keratinocyte function, with commensal strains supporting or maintaining normal proliferation and pathogenic strains inducing variable degrees of cytotoxicity. These data contribute to the pre-validation of microbial effects using a 2D HaCaT monolayer system and provide a robust foundation for follow-up studies employing 3D *in vitro* skin models that better recapitulate *in vivo* microbe-host interactions.

7.2.2 The influence of bacteria adhesion on HaCaT cell line

An adhesion test was conducted to evaluate the adherence capacity of selected bacterial strains to HaCaT keratinocytes. The procedure involved incubating confluent monolayers of HaCaT cells with bacterial suspensions, both individual bacteria and in co-culture with HaCaT keratinocytes. Briefly, HaCaT cells were seeded in 12well microtiter plates and allowed to proliferate. Bacterial suspensions were then added to the cells and incubated under appropriate conditions (24 h). Following incubation, non-adherent bacteria were removed by washing, and the adherent bacteria were quantified by plate counting method, and expressed as log CFU/ml. This methodology enables the assessment of bacterial adhesion properties and the potential protective effects of commensal bacteria against pathogenic colonisation.

As depicted in Figure 21, the results demonstrated that SE exhibited a high level of adhesion to HaCaT. The presence of ML in co-culture with SE (SE + ML) did not significantly alter SE adhesion. Moreover, cultivation of ML alone did not result in detectable adhesion of this bacterium to keratinocytes, suggesting a limited role in epithelial colonisation. The high adhesion of SE to HaCaT aligns with its role as a commensal bacterium frequently colonising the skin surface (Scharschmidt and Fischbach 2013). The lack of significant impact of ML on SE adhesion suggests a neutral interaction in this context, indicating non-competitive or even synergistic relationships between skin commensals (Yang *et al.* 2022; Glatthardt *et al.* 2024).

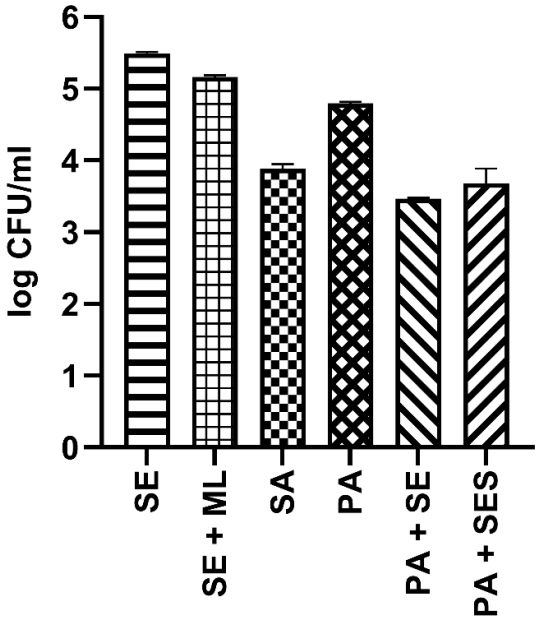

Figure 21: Adhesion profiles of skin-associated bacteria

In contrast, pathogen SA showed considerably lower adhesion. The lower adhesion of SA compared to SE in this assay is interesting, given its potential as a skin pathogen. This could reflect differences in specific adhesins and host cell receptors utilised by these two staphylococcal species (Mempel *et al.* 1998; Geoghegan and Dufrene 2018). PA displayed a moderate level of adhesion. Notably, the presence of SA, either live bacteria or in the form of lysate, reduced the adhesion of PA to keratinocytes, indicating a potential protective effect. This observation demonstrates that commensal bacteria can inhibit pathogen adherence through competitive exclusion mechanisms or the production of inhibitory substances. The fact that even the SE lysate exhibited this inhibitory effect suggests the involvement of secreted factors or cell wall components in this interaction. Further investigation into the specific molecules responsible for this anti-adhesive activity could lead to novel strategies for preventing *P. aeruginosa* infections (Prince *et al.* 2012; Alves *et al.* 2018).

7.3 Fabrication of CAM sheets as cell-made scaffolds

7.3.1 CAM sheets generation

During my dissertation research, I focused on the development and comprehensive characterization of cell-assembled matrix (CAM) scaffolds that closely mimic the structure and function of the native ECM. To produce structurally like ECM-based scaffolds, human dermal fibroblasts (HDFs) were cultured for extended periods, leading to the formation of homogeneous CAM sheets composed entirely of cell-secreted matrix components (Figure 22). These sheets were then carefully detached from the culture substrate, resulting in robust and uniform scaffolds suitable for further processing and application.

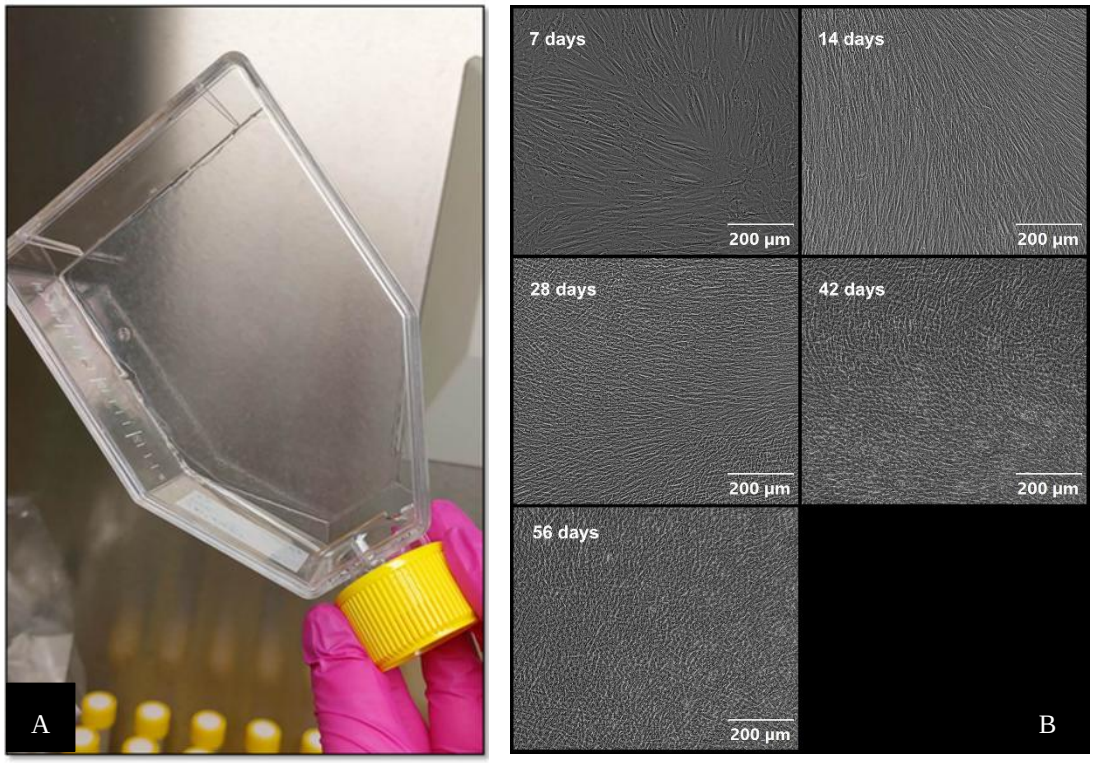

Figure 22. Generation and morphology of CAM sheet scaffold
A. Fully developed, CAM scaffold. B. In vitro formation of CAM sheet captured through photodocumentation.

To enhance their suitability as scaffolds, the CAM sheets underwent devitalization and decellularization, processes that effectively removed cellular material while preserving the extracellular matrix structure. Histological analyses confirmed that these procedures maintained tissue integrity and that essential matrix proteins, such as collagen, remained present. These results are in agreement with previous findings demonstrating that SDS-based decellularization protocols effectively eliminates immunogenic material while retaining the ECM framework necessary to support cell adhesion, migration, and tissue regeneration

(Gilbert *et al.* 2006; Smitt *et al.* 2017). Overall, the CAM decellularization protocol satisfies key histological benchmarks, resulting in cell-free yet structurally preserved scaffolds appropriate for both tissue engineering and in vitro model development.

The biological performance of the decellularized CAM scaffolds was evaluated by reseeding them with rat heart myoblasts, and fluorescence microscopy showed that these scaffolds promoted cell alignment and proliferation more effectively than standard culture surfaces (Figure 23). Therefore, the CAM sheet represents a completely cellular matrix produced by prolonged in vitro culture, offering a biologically native substrate. Similar to the other type of decellularized tissue, the CAM sheet, by its native cellular derivation, facilitate enhanced cell-mediated signalling. This, therefore, renders it more physiologically appropriate for tissue modeling and regenerative medicine (Badylak *et al.* 2009; Chen *et al.* 2024).

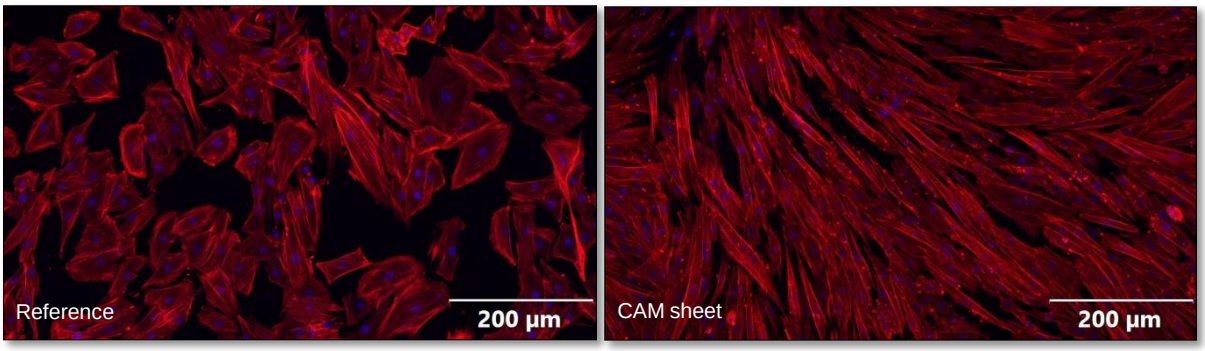

Figure 23: Fluorescence microscopy of H9c2 myoblast proliferation on standard culture flask and decellularized CAM scaffold. Fluorescent staining highlights actin filaments (red) and nuclei (blue), revealing improved cellular alignment and proliferation on the decellularized CAM scaffold compared to the standard culture surface

7.3.2 Impact of HDF-H9c2 co-culture on CAM scaffold generation and biochemical and molecular evaluation of CAM

The influence of different co-culture ratios on scaffold morphology and organization was systematically investigated. Thus, the composition and structural arrangement of cell-assembled matrix (CAM) scaffolds are significantly influenced by the types and ratios of cells used during their fabrication. In this part of study, we investigated how varying co-culture ratios of HDFs and H9c2 cardiomyoblasts influence ECM formation, cytoskeletal structure, and overall CAM scaffold architecture (Figure 24). CAM sheets were generated under each experimental condition described, and cytoskeletal (F-actin) and nuclear staining were performed to examine cellular activity and matrix formation over time (3rd and 7th day of cultivation).

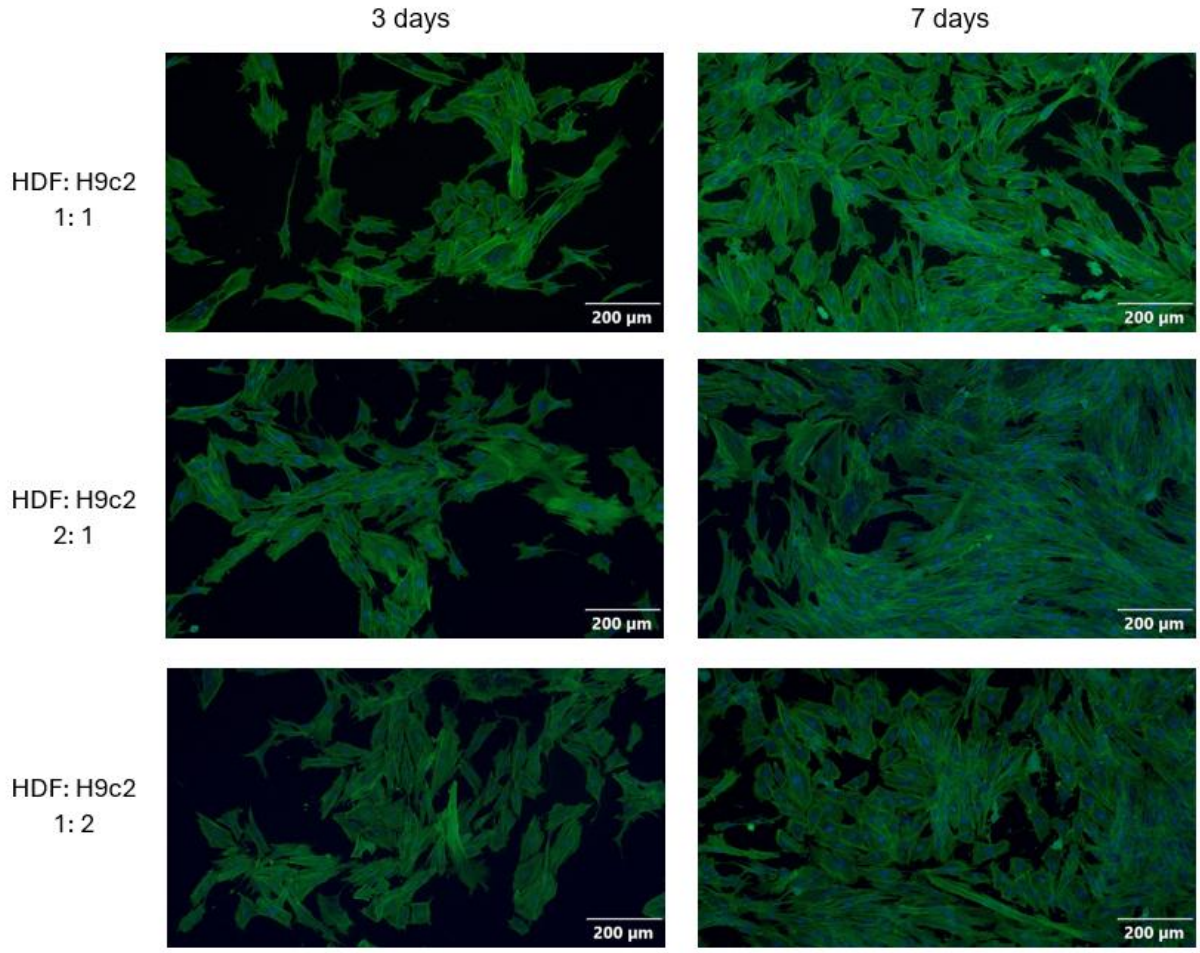

Figure 24: Fluorescence microscopy of CAM sheets formed from HDF:H9c2 co-cultures at varying ratios (3rd and 7th day proliferation). F-actin stained with ActinGreen 488 (green) and nuclei labeled with Hoechst 33258 (blue).

Balanced ratios of fibroblasts and cardiomyoblasts resulted in well-organized cellular networks and matrix structures, while other ratios led to less optimal scaffold architecture. These findings confirm that co-culture ratio plays a vital role in determining the structural and functional properties of engineered tissues, particularly regarding ECM dynamics and functional tissue replication. The balance between fibroblasts and cardiomyoblasts appears critical in promoting optimal ECM assembly, structural alignment, and finally biomimetic tissue development (Suhaeri *et al.* 2015; Brauer *et al.* 2023). Thus, properly optimized co-culture conditions are essential for generating physiologically relevant microenvironments, particularly in cardiac or vascular tissue models, where the dynamic interaction between stromal and parenchymal cells governs successful cell-made scaffold formation and integration (Zhang *et al.* 2012; Bartes *et al.* 2014).

The collagen content in the CAM sheets was assessed by quantifying hydroxyproline (Hyp), a major amino acid component of collagen, through a standard colourimetric assay. The measurement of hydroxyproline provides an indirect but reliable estimate of total collage. The conversion factor of 13 % is most commonly used to convert hydroxyproline to collagen (Edwards and O´Brien 1980; Reddy and Enwemeka 1996; Shoulders and Raines 2009). This assay revealed that co-cultures of fibroblasts and cardiomyoblasts—especially at balanced or fibroblast-enriched ratios—resulted in higher collagen deposition than monocultures. This finding underscores the importance of optimizing cell ratios to achieve robust matrix assembly, while also recognizing that excessive ECM production could hinder tissue remodeling if not properly controlled (Medugorac 1980; Susic and Frohlich 2011; Iwamiya *et al.* 2016; Jang *et al.* 2020; Mierke 2024). Despite all this, these types of CAM sheets could be promising candidates for tissue engineering applications requiring durable, bioactive matrices that can mimic or exceed the collagen content of native tissues.

To determine the biochemical stability and retention of key proteins in the CAM sheets following processing, SDS-PAGE electrophoresis and subsequent western blotting were performed. These procedures are standard in protein analysis, enabling the separation and immunodetection of target proteins based on molecular weight and antigenic determinants. SDS-PAGE provided a profile of the protein content of each CAM sample in this study, while western blotting facilitated the specific identification of laminin, β-actin, and GAPDH as a control – proteins relevant to ECM structure, cytoskeletal integrity, and cellular metabolism. In the next step of gene expression evaluation, the quantitative real-time PCR (qRT-PCR) using the RT PCR Mix SYBR® kit was chosen.

Evaluating protein preservation ang gene expression after devitalization and decellularisation is of essential importance, as these processes aim to remove cellular content while leaving ECM components that play a significant role in cell-made scaffold bioactivity and re-cellularisation intact. The analysis was performed on HDF, H9c2 cell line, and their co-culture of CAM sheets, giving insight into how matrix quality and scaffold suitability for tissue engineering applications are determined by cell composition and processing. The area of protein analysis and gene expression analysis was conducted during an international internship at the Biotechnology Centre of the Silesian University in Gliwice, where advanced molecular techniques were applied to further characterize the CAM scaffolds and their cellular interactions.

This experiments demonstrated that key extracellular matrix proteins like laminin were best preserved in scaffolds derived from fibroblast-dominated cultures (Gauvin *et al.* 2011; Mouw *et al.* 2014). It also confirmed the biochemical stability of the scaffolds after processing, supporting their suitability for reseeding

and tissue engineering applications (Jourdan-Lesaux *et al.* 2010; Yang *et al.* 2022; Golebiowska *et al.* 2023).

Due to the intention to publish these results in a scientific journal, it is not possible to include the detailed findings directly in the dissertation. However, for the purposes of the dissertation committee, the results are provided as a separate article attached to the thesis.

7.4 Characterization and biological evaluation of advanced polymeric materials

In addition to the primary focus of my doctoral thesis, various collaborative research initiatives were performer that have been published, particularly highlighting antimicrobial assessments of functional polymeric materials or their cytotoxicity. These investigations sought to evaluate the antibacterial characteristics of sophisticated nanocomposites and surface-modified substrates, employing standardized methods to guarantee reproducibility and comparability. Antimicrobial efficacy was measured by ISO 22196: Measurement of antibacterial activity on plastics and other non-porous surfaces, and ISO 20743: Textiles — Determination of antibacterial activity of textile products, which are internationally acknowledged standards for evaluating non-porous surfaces and textile materials (see List of publications). Following the ISO 22196 standard, conductive composite hydrogels featuring covalently bonded polypyrrole (PPy) nanoparticles (Káčerová *et al.* 2024), alongside crosslinked chitosan/PPy nanofibers with covalently anchored PPy (Muchová *et al.* 2025), were analyzed. The typical procedure includes inoculating the test surface with bacterial suspensions (e.g., *Staphylococcus aureus* and *Escherichia coli*), applying a film, incubating under regulated humidity and temperature, and quantifying viable bacteria after 24 hours to ascertain antibacterial effectiveness. For textile materials, the ISO 20743 standard was employed to evaluate cotton fabrics that had undergone plasma-assisted cationization with chitosan and quaternized poly[bis(2-chloroethyl) ether-alt-1,3-bis[3-(dimethylamino)propyl]urea], assessing bacterial reduction upon direct contact (Hamida *et al.* 2024). In addition to these antimicrobial evaluations, minimum inhibitory concentration (MIC) tests were conducted on colloidal systems, such as colloidal PPy (Káčerová *et al.* 2023) and composite colloids consisting of polyaniline (PANI) mixed with cellulose nanocrystals (CNC) or nanofibrils (CNF) (Korábková *et al.* 2024). The MIC assay identified the lowest concentration of the colloids necessary to prevent visible bacterial growth in broth culture, offering quantitative insights into the antimicrobial effectiveness of the dispersed nanomaterials. Furthermore, these contributions yielded valuable knowledge regarding the antimicrobial capabilities of innovative polymer-based substances and facilitated the advancement of multifunctional systems for biomedical and environmental purposes.

A series of cytotoxicity evaluations, conducted in line with ISO 10993-5, which delineates the procedure for *in vitro* cytotoxicity assessment of medical devices, were also carried out. This standard delineates protocols for evaluating the potential toxic effects of materials on cultured mammalian cells, typically utilizing assays such as MTT, which assess cell viability, metabolic activity, or membrane integrity following exposure to material extracts or direct contact with

test substances. In this context, several novel biomaterials, including a magneto-responsive hyaluronan-based hydrogel, developed for potential applications in mild hyperthermia and 3D bioprinting (Vítková *et al.* 2023), or alongside a collection of tritopic guest molecules (compounds 6a–6e) and cyclodextrin-modified hyaluronan polymers (CD-HA 12 and 14) (Jurtík *et al.* 2023), were evaluated. The findings provided crucial information on cell compatibility and material safety, which are vital parameters for subsequent in vivo testing or clinical application. They contributed to a broader understanding of how structural modifications of biopolymers and supramolecular assemblies affect cellular responses in tissue engineering and therapeutic environments.

8. CONTRIBUTION TO SCIENCE

Advancements *in vitro* skin tissue reconstitution techniques have resulted from diligent research, improved technological capabilities, and, in particular, deeper insights into focusing on 3D skin equivalents with more (patho)physiological functions to overcome the challenges of resembling the complex human skin. Various types of in vitro test skin models are being developed to assess the safety of drug testing or skin care products. Evaluating the toxicity of these substances applied directly to the skin depends not only on their chemical composition but also on their percutaneous absorption and xenobiotic metabolism (Choudhury and Das 2021; Hofmann *et al.* 2023). One such system, the full-thickness skin tissue model, consists of a human dermal fibroblast with epidermal-derived keratinocytes. These cells differentiate to form an epidermal-like structure, complete with basal, spinous, granular, and stratum corneum layers. In the preliminary studies of this doctoral thesis, the preparation of the given type of model, i.e. RHE, was accomplished. The preparation of RHE consisted of a dermal equivalent with human fibroblasts overlaying a stratified, well-differentiated epidermis derived from normal human keratinocytes cultured on an inert polycarbonate insert at an air-liquid interface. The *in vitro* skin irritation test and histological analysis of these 3D *in vitro* skin cultures demonstrated similarities in differentiation and metabolic cell viability properties to the skin. The established protocols significantly improve the potential of cell-biology laboratory at TBU in Zlín in providing of advanced experiments. Moreover, the initial experiments in bacteria/lysate enriched skin models were performed which is a state of art techniques opening a new horizon for wound healing experiments. Those models are the basis for highly *in vivo* mimicking experiments the laboratory will do in future.

Simultaneously with the previous study, the cell-assembled extracellular matrix (CAM) sheets, derived from human dermal fibroblast, were produced. Theoretically, CAM sheets refer to a method where cells are actively involved in the assembly of their extracellular matrix into sheet-like structures. It allowed the fibroblast cell line to produce and organize its own ECM components in a controlled manner (Fonseca *et al.* 2023). The CAM sheet production led to the creation of tissue-like structures with enhanced biomimicry and functionality thanks to the specific cultivating combination of an appropriate fibroblast density and culturing with the adding ascorbic acid as a collagen stimulant. Moreover, the decellularized process ensured the fabrication of acellular CAM scaffold for assessing cell line proliferation. Preliminary experiments have showcased the capacity of CAM sheets to facilitate the attachment and proliferation of various cell types, particularly demonstrating above-average growth and orientation of H9c2 myoblasts. Subsequently, the produced CAM sheets were scrutinized using

fluorescence microscopy and histological examination, affirming both their structural integrity and functional properties.

The foundation was established for inducing modifications in the internal architecture and composition of cell-made scaffolds by applying external stimuli (e.g., mechanical forces), which, through mechanotransduction, modulate cellular behavior and thereby drive scaffold remodeling. The knowledge and experience gained during these studies will facilitate further advancement in the field of tissue engineering by enabling the development of improved techniques, innovative models, and more effective therapeutic strategies. These insights will contribute to the ongoing progress and practical applications of tissue engineering in regenerative medicine and related disciplines.

REFERENCES

1. ABHISKEK, K. J.; DIVYA, S.; KAVITA, D.; RENUKA, M.; SANDEEP, M. and K. P. ALOK, 2018. Models and Methods for In Vitro Toxicity. In: DHAWAN, A., SEOK, K. In Vitro Toxicology. Academic Press, chapter 3, p. 45-65. Available from: https://doi.org/10.1016/B978-0-12-804667-8.00003-1. ISBN 9780128046678.
2. AHMAD, F., AHMAD, I. and M.S. Khan, 2008. Screening of free-living rhizospheric bacteria for their multiple plant growth promoting activities. *Microbiological Research* [online], vol. 163, iss. 2, p. 173-181. Available from: https://doi.org/10.1016/j.micres.2006.04.001.
3. AKIYAMA, M, 2017. Corneocyte lipid envelope (CLE), is the key structure for skin barrier function and ichthyosis pathogenesis. *Journal of Dermatological Science* [online], vol. 88, no. 1, p. 3–9. Available from: doi: 10.1016/j.jdermsci.2017.06.002
4. ALVES, P.M., AL-BADI, E., WITHYCOMBE, C., JONES, P.M., PURDY, K.J., MADDOCKS, S.E, 2018. Interaction between Staphylococcus aureus and Pseudomonas aeruginosa is beneficial for colonisation and pathogenicity in a mixed biofilm. *Pathogens and Disease* [online], vol. 76, no. 1. Available from: doi: 10.1093/femspd/fty003. PMID: 29342260.
5. ASSUNCAO, M., DEHGHAN-BANIANI D., YIU CH.K., SPÄTER T., BEYER S., BLOCKI A, 2020. Cell-Derived Extracellular Matrix for Tissue Engineering and Regenerative Medicine. *Frontiers in Bioengineering and Biotechnology* [online], vol. 3, no. 8: 602009. Available from: doi: 10.3389/fbioe.2020.602009.
6. AUXENFANS C., FRADETTE J., LEQUEUX C., GERMAIN L., KINIKOGLU B., BECHETOILLE N., BRAYE F., AUGER F.A., DAMOUR O, 2009. Evolution of three-dimensional skin equivalent models reconstructed in vitro by tissue engineering. *European Journal of Dermatology* [online], vol. 19 no.1, p. 107-13. doi: 10.1684/ejd.2008.0573.
7. AYDIN, O., PASSARO, A.P., RAMAN, R., SPELLICY, S.E., WEINBERG, R.P., KAMM, R.D., SAMPLE, M., TRUSKEY, G.A., ZARTMAN, J., DAR R.D., PALACIOS, S., WANG, J., TORDOFF, J., MONTSERRAT, N., BASHIR, R., SAIF, M.T.A., WEISS, R, 2022. Principles for the design of multicellular engineered living systems. *APL Bioengineering* [online], vol. 6. no. 1:010903. doi: 10.1063/5.0076635.
8. AVELAR-FREITAS, B.A.; ALMEIDA, V.G., PINTO, M.C.; MOURAO, F.A.; MASSENSINI, A.R.; MARTINS-FILHO, O.A.; ROCHA-VIEIRA, E.; BRITO-MELO G.E, 2014. Trypan blue exclusion assay by flow

cytometry. *Brazilian Journal of Medical and Biological Research* [online], vol. 47, no. 4, p. 307-15. Available form: doi: 10.1590/1414-431X20143437.

9. BADYLAK, S.F, 2002. The extracellular matrix as a scaffold for tissue reconstruction. Seminars in Cell and Developmental Biology [online], vol. 13, no. 5, p. 377-83. Available from: doi: 10.1016/s1084952102000940.
10. BADYLAK, S.F., FREYETES, D.O., GILBERT, T.W, 2009. Extracellular matrix as a biological scaffold material: Structure and function. *Acta Biomaterialia* [online], vol. 5, no. 1, p. 1-13. Available from: doi: 10.1016/j.actbio.2008.09.013.
11. BELL, E., EHRLICH, H. P., BUTTLE, D. J. & NAKATSUJI, T, 1981. Living tissue formed in vitro and accepted as skin-equivalent tissue of full thickness. Science, [online], vol. 211, p. 1052-1054. Available from: doi: 10.1126/science.7008197
12. BELLO Y.M., FALABELLA A.F., EAGLSTEIN W.H, 2001. Tissue-engineered skin. Current status in wound healing. *American Journal of Clinical Dermatology* [online], vol. 2, no. 5, p. 305-13. Available from: doi: 10.2165/00128071-200102050-00005.
13. BÉNYEI, É.B., NAZEER, R.R., ASKENASY, I., MANCINI, L., HO, P.M., GAC, S., SWAIN, J.E.V., WELCH, M, 2024. The past, present and future of polymicrobial infection research: Modelling, eavesdropping, terraforming and other stories *Advances in Microbial Physiology* [online], vol. 85, p. 259-323. Available from: doi:https://doi.org/10.1016/bs.ampbs.2024.04.002.
14. BISHOP, J.E., GREENBAUM, R., GIBSON, D.G., YACOUB, M., LAURENT, G.J, 1990. Enhanced deposition of predominantly type I collagen in myocardial disease. *Journal of Molecular and Cellular Cardiology* [online], vol. 22, no. 10, p. 1157-65. Available from: doi: 10.1016/0022-2828(90)90079-h.
15. BOJAR Richard A, 2015. Studying the Human Skin Microbiome Using 3D In Vitro Skin Models. *Applied In Vitro Toxicology* [online], vol. 1 no. 2, p. 165-171. Available from: http://doi.org/10.1089/aivt.2015.0002
16. BOSMAN, F.T. and I. STAMENKOVIC, 2003. Functional structure and composition of the extracellular matrix. *The Journal of Pathology* [online], vol. 200, no. 4, p. 423-428. Available from: https://doi.org/10.1002/path.1437
17. BOUKAMP, P., POPP, S., ALTMEYER, S., HULSEN, A., FASCHING C., CREMER, T., FUSENING N.E, 1997. Sustained nontumorigenic phenotype correlates with a largely stable chromosome content during long-term culture of the human keratinocyte line HaCaT. *Genes*

Chromosomes Cancer [online], vol. 19, no. 4, p 201-214. Available from: 10.1002/(sici)1098-2264(199708)19:4<201::aid-gcc1>3.0.co;2-0

18. BREITKREUTZ, D., SCHOOP, V.M., MIRANCEA, N., BAUR, M., STARK, H.J., FUSENING N.E, 1998. Epidermal differentiation and basement membrane formation by HaCaT cells in surface transplants. European Journal of Cell Biology [online], vol 75, no. 3, p. 273-286. Available from: 10.1016/S0171-9335(98)80123-4
19. BRAUER, J., LANGE, T., KELLER, D., GÖRLITZ, S., CHO, S., KEYE, J., GOSSEN, M., PETERSEN, A., KORNAK, U, 2023. Dissecting the influence of cellular senescence on cell mechanics and extracellular matrix formation in vitro. *Aging Cell* [online], vol. 22, no. 3:13744. Available from: doi: 10.1111/acel.13744.
20. BARTHES, J., ÖZCELIK, H., HINDIE, M., NDREU-HALILI, A., HASAN, A., VRANA, N.E, 2014. Cell microenvironment engineering and monitoring for tissue engineering and regenerative medicine: the recent advances. *BioMed Research International* [online]; 921905. Available from: doi: 10.1155/2014/921905.
21. BRAGULLA H.H. and D.G. HOMBERGER, 2009. Structure and functions of keratin proteins in simple, stratified, keratinized, and cornified epithelia. *Journal of Anatomy* [online], vol. 214, no. 4, p. 516-59. Available from: doi: 10.1111/j.1469-7580.2009.01066.x.
22. BÖTTCHER R.T. and C. NIEHRS, 2005. Fibroblast growth factor signaling during early vertebrate development. *Endocrine Reviews* [online], vol. 26, no.1, p. 63-77. Available from: doi: 10.1210/er.2003-0040. PMID: 15689573.
23. BYRD A.L., BELKAID Y., SEGRE J.A, 2018. The human skin microbiome. *Nature Reviews Microbiology* [online], vol. 16, no. 3, p. 143-155. Available from: doi: 10.1038/nrmicro.2017.157.
24. BORCHIELLINI, P., RAMES, A., ROUBERTIE, F., L´HEREUX, N. and F. KAWECKI, 2023. Development and characterization of biological sutures made of cell-assembled extracellular matrix. *Biofabrication* [online], vol. 15, no. 4. Available from: doi: 10.1088/1758-5090/acf1cf.
25. BOXBERGER, M., CENIZOV., CASSIR N. *et al*, 2021. Challenges in exploring and manipulating the human skin microbiome. *Microbiome* [online], vol. 9, no. 125. Available from: https://doi.org/10.1186/s40168-021-01062-5
26. CABALLERO-FLORES, G., PICKARD, J.M., NÚNEZ, G, 2023. Microbiota-mediated colonization resistance: mechanisms and regulation. *Nature Reviews Microbiology* [online], vol. 21, no. 6, p. 347-360. Available from: doi: 10.1038/s41579-022-008

27. CAI, R., GIMENEZ-CAMINO, N., XIAO, M., BI S. and K. A. DIVITO, 2023. Technological advances in three-dimensional skin tissue engineering. *Reviews of Advanced Material Science* [online], vol. 62, no. 1, pp. 20220289. Available from: https://doi.org/10.1515/rams-2022-0289
28. CHEN, Y.E., FISCHBACH, M.A., BELKAID, Y, 2018. Skin microbiota-host interactions. *Nature.* [online], vol. 24, no. 553(7689), p. 427-436. Available from: doi: 10.1038/nature25177.
29. CHEN, Z., DU, CH., LIU, S., LIU, J., YANG, Y., DONG, L., ZHAO, W., HUANG, W., LEI, Y, 2024. Progress in biomaterials inspired by the extracellular matrix. *Giant* [online], vol. 19:100323. Available from: https://doi.org/10.1016/j.giant.2024.100323
30. CHEN, H., ZHAO, Q., ZHONG, Q. *et al*, 2022. Skin Microbiome, Metabolome and Skin Phenome, from the Perspectives of Skin as an Ecosystem. *Phenomics* [online], vol. 2, p. 363–382. Available from: doi:https://doi.org/10.1007/s43657-022-00073-y
31. CHOI, M. and CH. LEE, 2015. Immortalization of Primary Keratinocytes and Its Application to Skin Research. *Biomolecules and Therapeutics* [online], vol. 23, no. 5, p. 391–399. Available from: doi: 10.4062/biomolther.2015.038
32. CHOUDHURY, S. and A. DAS, 2021. Advances in the generation of three-dimensional skin equivalents: pre-clinical studies to clinical therapies. *Cytotherapy.* [online], vol. 23 no. 1, p. 1-9. Available from: doi: 10.1016/j.jcyt.2020.10.001.
33. COGEN, A.L., YAMASAKI, K., MUTO, J., SANCHEZ, K.M., CROTTY, A. L., TANIOS J., LAI, Y., KIM, J.E., NIZET, V., GALLO, R.L, 2010. Staphylococcus epidermidis antimicrobial delta-toxin (phenol-soluble modulin-gamma) cooperates with host antimicrobial peptides to kill group A Streptococcus. *PLoS One* [online] vol. 5. no.1. Available from: doi: 10.1371/journal.pone.0008557.
34. DÍAZ-GARCÍA, D., FILIPOVÁ, A., GARZA-VELOZ, I., MARTINEZ-FIERRO, M.L., 2021 A Beginner's Introduction to Skin Stem Cells and Wound Healing. *International Journal of Molecular Sciences* [online], vol. 13, no. 22(20) pp. 11030. Available from: doi: 10.3390/ijms222011030.
35. DRISKELL, R.R. and F.M. WATT, 2015. Understanding fibroblast heterogeneity in the skin. *Trends in Cell Biology* [online], vol. 25, no. 2, p. 92-9. Available from: doi: 10.1016/j.tcb.2014.10.001.
36. DZOBO, K.; DANDARA, C., 2023. The ExtracellularMatrix: Its Composition, Function, Remodeling, and Role in Tumorigenesis.

Biomimetics [online], vol. 8, no. 146. Available from: https://doi.org/10.3390/biomimetics8020146
37. EBERLIN, S., da SILVA, M.S., FACCHINI, G., da SILVAi, G.H.; PINHERO, A.L., 2020 The ex vivo Skin Model as an Alternative Tool for the Efficacy and Safety Evaluation of Topical Products. *Alternatives to Laboratory Animals* [online], vol. 48, no. 1, p. 10-22. Available from: doi: 10.1177/0261192920914193
38. EDWARDS, C.A. and W. D. O'BRIEN, Jr., 1980. Modified assay for determination of hydroxyproline in a tissue hydrolyzate. *Clinica Chimica Acta* [online], vol.104, no. 2 p. 161-7. Available from: doi: 10.1016/0009-8981(80)90192-8.
39. EL GHALBZOURI, A., HENSBERGEN, P., GIBBS, S., KEMBENAAR, J., van der SCHORS R., PONEC, M., 2004 Fibroblasts facilitate re-epithelialization in wounded human skin equivalents. *Laboratory Investigation* [online], vol. 84, no. 1, p. 102-12. Available from: doi: 10.1038/labinvest.3700014. PMID: 14631386.
40. EL GHALBZOURI, A., COMMANDEUR, S., RIETVELD, M.H., MULDER, A.A., WILLEMZE, R., 2009. Replacement of animal-derived collagen matrix by human fibroblast-derived dermal matrix for human skin equivalent products. *Biomaterials*. [online], vol. 30, no. 1, p. 71–8. Available from: doi: 10.1016/j.biomaterials.2008.09.002
41. EMMERT, H., RADEMACHER, F., GLÄSER, R., HARDER, J., 2020. Skin microbiota analysis in human 3D skin models-"Free your mice". *Experimental Dermatology* [online], vol. 29, no. 11, p. 1133-1139. Available from: doi: 10.1111/exd.14164.
42. FELL, B., 2016. Organotypic Human Skin Disease Models for the Assessment of Novel Therapeutic Approaches. Doctoral Thesis. Centre for Cutaneous and Cell Biology, The Blizard Institute. Barts and the London School of Medicine and Dentistry. Queen Mary University London.
43. FLOWERS, L., GRICE, E.A., 2020 The Skin Microbiota: Balancing Risk and Reward. *Cell Host Microbe.* [online], vol. 28, no.2, p. 190-200. Available from: doi: 10.1016/j.chom.2020.06.017.
44. FONSECA, V. C. and V.V.C BLANCHE., 2023. Primary Human Cell-Derived Extracellular Matrix from Decellularized Fibroblast Microtissues with Tissue-Dependent Composition and Microstructure. *bioRxiv*, [online], preprint August 17. Available from: doi: https://doi.org/10.1101/2023.08.15.553420.
45. FRANTZ, C., STEWART, K.M., WEAVER, V.M., 2010. The extracellular matrix at a glance. *Journal of Cell Science* [online], vol. 15, no. 123, p. 4195-200. Available from: doi: 10.1242/jcs.023820.

46. FUCHS, E. Scratching the surface of skin development. *Nature* 2007, vol. 445, no. 7130, p. 834-42. Available from: doi: 10.1038/nature05659.
47. GALVAN, A., PELLICCIARI, C. and L. CALDERAN, 2024. Recreating Human Skin In Vitro: Should the Microbiota Be Taken into Account? *International Journal of Molecular Sciences* [online], vol 25, no. 2, p. 1165. Available from: https://doi.org/10.3390/ijms25021165
48. GANGATIKAR, P., PAGUET-FIFIELD, S., LI, A., ROSSI, R., KAUR, P., 2007. Establishment of 3D organotypic cultures using human neonatal epidermal cells. *Nature Protocols*. [online], vol. 2, p. 178-186. Available from: doi: 10.1038/nprot.2006.448.
49. GAUVIN, R., PARENTEAU-BAREIL, R., LAROUCHE, D., MARCOUX, H., BISSON, F., BONNET, A., AUGER, F.A., BOLDUC, S., GERMAIN, L, 2011. Dynamic mechanical stimulations induce anisotropy and improve the tensile properties of engineered tissues produced without exogenous scaffolding. *Acta Biomaterialia* [online], vol. 7, no. 9, p. 3294-301. Available from: doi: 10.1016/j.actbio.2011.05.034.
50. GARLICK, J. A., 2006. Engineering Skin to Study Human Disease – Tissue Models for Cancer Biology and Wound Repair. In: LEE, K., KAPLAN, D. Tissue Engineering II. Advances in Biochemical Engineering/Biotechnology. [online], Springer, Berlin, Heidelberg, p. 207-239. Available from: doi: https://doi.org/10.1007/b137206. eISBN: 978-3-540-36186-2
51. GELLANTLY, S.L. and R.E. HANCOCK, 2013. Pseudomonas aeruginosa: new insights into pathogenesis and host defenses. *Pathogens and Disease* [online], vol. 3, p. 159-73. Available from: doi: 10.1111/2049-632X.12033.
52. GEOGHEGAN, J.A., DUFRENE Y.F, 2018. Mechanomicrobiology: How Mechanical Forces Activate Staphylococcus aureus Adhesion. *Trends in Microbiology* [online] vol. 26, no. 8, p. 645-648. Available from: doi: 10.1016/j.tim.2018.05.004.
53. GILBERT, T.W., SELLARO, T.L., BADYLAK, S.F, 2016. Decellularization of tissues and organs. *Biomaterials* [online], vol. 27, no. 19, p. 3675-83. Available from: doi: 10.1016/j.biomaterials.2006.02.014.
54. GLATTHARDT, T., LIMA, R.D., de MATTOS, R.M., FERREIRA, R.B.R., 2024 Microbe Interactions within the Skin Microbiome. *Antibiotics (Basel).* [online], vol. 13, iss.1:49. Available from: doi: 10.3390/antibiotics13010049.
55. GOERS, L., FREEMONT, P., POLIZZI, K.M., 2014. Co-culture systems and technologies: taking synthetic biology to the next level. *The Journal of the Royal Society Interface* [online], vol. 11, no. 96:20140065. Available from: doi: 10.1098/rsif.2014.0065.

56. GOLEBIOWSKA, A.A., INTRAVAIA, J.T., SATHE, V.M., KUMBAR, S.G., NUKAVARAPU, S. P., 2023. Decellularized extracellular matrix biomaterials for regenerative therapies: Advances, challenges and clinical prospects. Bioact Mater. [online], vol. 4, no. 32, p. 98-123. Avaialable from: doi: 10.1016/j.bioactmat.2023.09.017.
57. GRICE, E. A., SEGRE, J. A., 2011. The skin microbiome. *Nature Reviews Microbiology* [online], vol. 9, no. 4, p. 244–253. Available from: doi:10.1038/nrmicro2537
58. GRICE, E. A., KONG, H.H., RENAUD, G., YOUNG, A.C., BOFFARD, G.G., *et al.*, 2008. A diversity profile of the human skin microbiota. *Genome Research*. [online], vol. 18, no. 7, p. 1043–50. Available from: doi: 10.1101/gr.075549.107.
59. CARLSON, M.W., ALT-HOLLAND, A., EEGLES, C., GARLICK, J.A., 2008. Three-dimensional tissue models of normal and diseased skin. *Current Protocols in Cell Biology* [online], ch. 19, u. 19.9. Available from: doi: 10.1002/0471143030.cb1909s41.
60. GRINNELL, F., 2008. Fibroblast mechanics in three-dimensional collagen matrices. *The Journal of Bodywork and Movement Therapies* [online], vol. 12, no. 3, p. 191-3. Available from: doi: 10.1016/j.jbmt.2008.03.005.
61. GRINNELL, F., 2003. Fibroblast biology in three-dimensional collagen matrices. *Trends in Cell Biology* [online], vol. 13, no. 5, p. 264-9. Available from: doi: 10.1016/s0962-8924(03)00057-6.
62. HABEEBUDDIN, M., KARNATI, R.K., SHIROORKAR, P.N., NAGARAJA, S., ASDAQ, S.M.B., KHALID, A.M., FATTEPUR, S., 2022. Topical Probiotics: More Than a Skin Deep. *Pharmaceutics* [online], vol. 14, no. 3, p. 557. Available from: doi: 10.3390/pharmaceutics14030557.
63. HANNIGAN, G.D., MEISEL, J.S., TYLDSLEY, A.S., ZHENG, Q., HODKINSON, B.P., SAN MIGUEL, A.J., MINOT, S., BUSHMAN, F.D., GRICE, E.A., 2015. The human skin double-stranded DNA virome: topographical and temporal diversity, genetic enrichment, and dynamic associations with the host microbiome. *mBio* [online], vol. 20, no. 6, p. 1578-15. Available from: doi: 10.1128/mBio.01578-15.
64. HAYDEN, P.J., HARBELL, J.W., 2021. Special review series on 3D organotypic culture models: Introduction and historical perspective. *In Vitro Cellular & Developmental Biology - Animal* [online], vol. 57, p. 95–103. Available from: https://doi.org/10.1007/s11626-020-00500-2
65. HEO, J.H., KANG, D., SEO, S.J., JIN, Y., 2022. Engineering the extracellular matrix for organoid culture. Int J Stem Cells. [online], vol. 15, no. 1, p. 60–9. Available from: doi: 10.15283/ijsc21190.

66. HO, B.X., PEK, N.M.Q., SOH, B.S., 2018. Disease modeling using 3D organoids derived from human induced pluripotent stem cells. *International Journal of Molecular Sciences* [online], vol. 19, no. 4, p. 936. Available from: doi: 10.3390/ijms19040936.
67. HOATH, S. B., MAURO, T. Fetal skin development. In: Eichenfeld, L, Frieden, I., Mathes, E. *et al*.. Neonatal and Infant Dermatology. 3rdeEdition, London, WB Saunders, 2014. [online]. eISBN: 9781455726394
68. HOFMANN, E., SCHWARZ, A., FINK, J., KAMOLZ, L-P., KOTZBECK, P., 2023. Modelling the Complexity of Human Skin In Vitro. *Biomedicines*. [online], vol. 11, no. 2, p. 794. Available from: https://doi.org/10.3390/biomedicines11030794
69. HONG, Z.X., ZHU, S.T., LI, H. *et al.*, 2023. Bioengineered skin organoids: from development to applications. *Military Medical Research* [online], vol. 10, no. 40. Available from: https://doi.org/10.1186/s40779-023-00475-7
70. HU, M. S., BORELLI, M. R., HONG, W. X., MALHORTA, S., CHEUNG, A. T. M., RANSOM, R. C., RENNERT, R.C., MORRISON, S. D., LORENZ, H. P. and M. T. LONGAKERA., 2018. Embryonic skin development and repair. *Organogenesis*, [online], vol. 14, no. 1, p. 46–63. Available from: doi: 10.1080/15476278.2017.1421882
71. HUSSEY, G.S., DZIKI, J. L. and S.F. BADYLAK., 2018 Extracellular matrix-based materials for regenerative medicine. *Nature Reviews Materials* [online], vol. 3, p. 159–173. Available from: https://doi.org/10.1038/s41578-018-0023-x
72. HWANG, B.K., LEE, S., MYOUNG, J., HWANG, S.J., LIM, J.M., JEONG, E.T., PARK, S.G., YOUN, S.H., 2021. Effect of the skincare product on facial skin microbial structure and biophysical parameters: A pilot study. *Microbiology open* [online], vol. 10, no. 5, p. 1236. Available from: doi: 10.1002/mbo3.1236.
73. ICHIKAWA, J.K., NORRIS, A., BANGERA, M.G., GEISS, G.K., van 't WOUT, A.B., BUMGARNER, R.E., LORY, S., 2000. Interaction of pseudomonas aeruginosa with epithelial cells: identification of differentially regulated genes by expression microarray analysis of human cDNAs. *Proceedings of the National Academy of Sciences* [online], vol. 97, no. 17, p. 9659-64. Available from: doi: 10.1073/pnas.160140297.
74. IDREES, A., SCHMITZ, I., ZOSO, A., GRUHN, D., PACHARRA, S., SHAH, S., CIARDELLI, G., VIEBAHN, R., CHIONO, V., SALBER, J., 2021. Fundamental in vitro 3D skin equivalnet tool development for assessing biological safety and biokompatibility – towards alternativ efor animal experiments. *4open* [online], vol. 4, no. 1, p. 21 Available from: https://doi.org/10.1051/fopen/2021001

75. IMRAN, M., MOYLE, P. M., KAMATO, D. and Y. MOHAMMED., 2024. Advances in, and prospects of, 3D preclinical models for skin drug Discovery. *Drug Discovery Today* [online], vol. 29, iss. 12. p. 104208. Available from: https://doi.org/10.1016/j.drudis.2024.104208
76. In Vitro EpiDerm™ Skin Irritation Test (EPI-200-SIT). For use with MatTek Corporation's Reconstructed Human Epidermal Model EpiDerm™ (EPI-200-SIT). MatTek [online] [cit. 2024-03-13]. Available from: https://www.mattek.com/wp-content/uploads/EPI-200-SIT-Skin-Irritation-MK-24-007-0023.pdf
77. IPPONJIMA, S., UMINO, Y., NAGAYAMA, M., and M. DENDA 2020. Live imaging of alterations in cellular morphology and organelles during cornification using an epidermal equivalent model. *Scientific Reports* [online], vol. 10, a.n. 5515. Available from: doi: 10.1038/s41598-020-62240-3¨
78. IWAMIYA, T., MATSUURA, K., MASUDA, S., SHIMIZUh, T., OKANO, T., 2016. Cardiac fibroblast-derived VCAM-1 enhances cardiomyocyte proliferation for fabrication of bioengineered cardiac tissue. *Regenerative Therapy* [online], vol. 1, no. 4, p. 92-102. Available from: doi: 10.1016/j.reth.2016.01.005.
79. JANG, Y., CHOI, S. C., LIM, D. S., KIM, J. H., KIM, J., PARK, Y., 2020. Modulating cardiomyocyte and fibroblast interaction using layer-by-layer deposition facilitates synchronisation of cardiac macro tissues. *Soft Matter* [online], vol. 16, p. 428-434. Available from: doi: https://doi.org/10.1039/C9SM01531K
80. JAMES, W. D., BERGER, T. G., ELSTON, D. M., 2006. Andrews' Diseases of the Skin. *Clinical Dermatology* [online], 10th ed. Saunders/Elsevier Inc., Philadelphia, p. 231-250.
81. JANG, H.J., LEE, J.B. and J. K. YOON., 2023. Advanced In Vitro Three-Dimensional Skin Models of Atopic Dermatitis. *Tissue Engineering and Regenerative Medicine* [online], vol. 20, no. 4, p. 539–552. Available from: https://doi.org/10.1007/s13770-023-00532-1
82. JÄRVELÄINEN, H., SAINIO, A., KOULU, M., WIGHT, T.N., PENTTINEN, R., 2009. Extracellular matrix molecules: potential targets in pharmacotherapy. *Pharmacological Reviews* [online], vol. 61, no. 2, p. 198-223. Available from: doi: 10.1124/pr.109.001289.
83. JOE, P., WOODLEY, D. W., LAMBERT, and I. O. ASENCIO, 2022. Understanding Fibroblast Behavior in 3D Biomaterials. *Tissue Engineering Part B: Reviews* [online], vol. 28, no. 3, p. 569-578. Available from: http://doi.org/10.1089/ten.teb.2021.0010

84. JOURDAN-LESAUX, C., ZHANG, J., LINDSEY, M.L., 2010. Extracellular matrix roles during cardiac repair. *Life Science* [online], vol. 87, no. 13-14, p. 391-400. Available from: doi: 10.1016/j.lfs.2010.07.010.
85. JOSHI, A.A., VOCANSON, M., NICOLAS, J-F., WOLF, P. and V. PATRA, 2023. Microbial derived antimicrobial peptides as potential therapeutics in atopic dermatitis. *Frontiers in Immunology* [online], vol. 14:1125635. Available from: doi: 10.3389/fimmu.2023.112563533-7.
86. JORDANA-LUCH, E., GARCIA, V., KINGDON, A.D.H., SINGH, N., ALEXANDER, C., WILLIAMS, P. and K. R. HARDIE, 2020.A Simple Polymicrobial Biofilm Keratinocyte Colonization Model for Exploring Interactions Between Commensals, Pathogens and Antimicrobials. *Frontiers in Microbiology* [online], vol. 11, p: 291. Available from: doi: 10.3389/fmicb.2020.00291
87. KADAM, S., SHAI, S., SHAHANE, A., KAUSHIK, K.S., 2019. Recent Advances in Non-Conventional Antimicrobial Approaches for Chronic Wound Biofilms: Have We Found the 'Chink in the Armor'? *Biomedicines* [online], vol. 7, no. 2. Available from: doi: 10.3390/biomedicines7020035.
88. KARAMANOS, N.K., THEOCHARIS, A.D., PIPERIGKOU, Z., MANOU, D., PASSI, A., SKANDALIS, S.S., VYNIOS, D.H., ORIAN-ROUSSEAU, V., Ricard-BLUM, S., SCHMELZER, C.E.H., DUCA, L., DURBEEJ, M., AFRATIS, N.A., TROEBERG, L., FRANCHI, M., MASOLA, V. and M. ONISTO 2021. A guide to the composition and functions of the extracellular matrix. *FEBS J*, [online], vol. 288, no. 24, p. 6850-6912. Available from: https://doi.org/10.1111/febs.15776
89. KAWECKI, F., GLUAIS, M., CLAVEROL, S., DUSSERRE, N, McALLISTER, T., L'HEUREUX, N., 2022. Inter-donor variability of extracellular matrix production in long-term cultures of human fibroblasts. *Biomaterial Science* [online], vol. 10, no. 14, p. 3935-3950. Available from: doi: 10.1039/d1bm01933c.
90. KIM, R., 2023. Advanced Organotypic In Vitro Model Systems for Host–Microbial Coculture. *BioChip Journal* [online], vol. 17, p. 147–173. Available from: https://doi.org/10.1007/s13206-023-00103-5
91. KIM, S., WONG, P. and P COULOMBE, 2006. A keratin cytoskeletal protein regulates protein synthesis and epithelial cell growth. *Nature* [online], vol. 441, no. 7091, p. 362–365. Available from: https://doi.org/10.1038/nature04659
92. KIOUSI, D.E., PANOPOULOU, M., PAPPA, A. and A. GALANIS, 2024. Lactobacilli-host interactions inhibit Staphylococcus aureus and Escherichia coli-induced cell death and invasion in a cellular model of infection. Fronties Microbiology [online]. Available from: doi: 10.3389/fmicb.2024.1501119.

93. KOLARSICK, P., KOLARSICK, A. and C. GOODWIN, 2011. Anatomy and Physiology of the Skin. Journal of the Dermatology Nurses' Association, [online], vol. 3, no. 4, p. 203–213. Available from: doi:10.1097/JDN.0b013e3182274a98.
94. KOSTER, M.I. and D. R. ROOP, 2007. Mechanisms regulating epithelial stratification. *Annual Review of Cell and Developmental Biology* [online], vol. 23, p. 93-113. Available from: doi: 10.1146/annurev.cellbio.23.090506.123357.
95. KUMAR, P., SATYAM, A., FAN, X., COLLIN, E., ROCHEV, Y., RODRIGUEZ, B.J., GORELOV, A., DILLON, S., JOSHI, L., RAGHUNATH, M., PANDIT, A., ZEUGOLIS, D.I., 2015. Macromolecularly crowded in vitro microenvironments accelerate the production of extracellular matrix-rich supramolecular assemblies. *Scientific Reports* [online], vol. 4, no. 5, p. 8729. Available form: doi: 10.1038/srep08729.
96. LAI, Y., COGEN, A.L., RADEK, K.A., PARK, H.J., MACLEOD, D.T., LEICHTLE, A., RYAN, A.F., Di NARDO, A., GALLO, R.L., 2010. Activation of TLR2 by a small molecule produced by Staphylococcus epidermidis increases antimicrobial defense against bacterial skin infections. *Journal of Investigative Dermatology* [online], vol. 130, no. 9, p. 2211-21. Available from: doi: 10.1038/jid.2010.123.
97. LAI, Y., Di NARDO, A., NAKATSUJI, T. *et al.*, 2009. Commensal bacteria regulate Toll-like receptor 3–dependent inflammation after skin injury. *Nature Medicine* [online], vol. 15, p. 1377–1382. Available from: ttps://doi.org/10.1038/nm.2062
98. LAI-CHEONG, J. E., and J. A. MCGRATH, 2017. Structure and function of skin, hair, and nails. *Medicine* [online], vol. 45, p. 347-351. Available from: doi: 10.1016/j.mpmed.2017.03.004
99. LALY, A.C., SLIOGERYTE, K., PUNDEL, O.J., ROSS, R., KEELING, M.C., AVISETTI D., WASEEM, A., GAVARA, N., CONNELLY, J.T., 2021. The keratin network of intermediate filaments regulates keratinocyte rigidity sensing and nuclear mechanotransduction. *Science Advances* [online], vol. 27, no. 7, p. 6187. Available from: doi: 10.1126/sciadv.abd6187.
100. LANZA, R., LANGER, R. and J. VACANTI. Principles of Tissue Engineering. Academic Press. Copyright© 2007, Elsevier Inc. ISBN: 978-0-12-370615-7
101. LAURENT, S., DENESVRE, C., 2021. 3D skin models in domestic animals. Veterinary Research. *BioMed Central* [online], vol. 52, no.1, p. 15. Available from: doi:10.1186/s13567-020-00888-5.

102. LAWLOR, K.T. and P. KAUR, 2015. Dermal Contributions to Human Interfollicular Epidermal Architecture and Self-Renewal. *International Journal of Molecular Sciences* [online], vol. 16, no. 12, p. 28098-107. Available from: doi: 10.3390/ijms161226078.
103. LEE, J., KOEHLER, K.R., 2021: Skin organoids: a new human model for developmental and translational research. *Experimental Dermatology* [online], vol.30, vol. 4, p. 613–20. Available from: doi: 10.1111/exd.14292.
104. LEE, D.Y., YANG, J.M., Park, K.H., 2007. A dermal equivalent developed from fibroblast culture alone: effect of EGF and insulin. *Wound Repair and Regeneration* [online], vol. 15, no.6, p. 936-9. Available from: doi: 10.1111/j.1524-475X.2007.00310.x.
105. LEIGHT, J.L., DRAIN, A.P. and V.M. WEAVER, 2017. Extracellular Matrix Remodeling and Stiffening Modulate Tumor Phenotype and Treatment Response. *Annual Review of Cancer Biology* [online], vol. 1, p. 313–334. Available from: doi: https://doi.org/10.1146/annurev-cancerbio-050216-034431
106. LIM, K.M., 2021. Skin Epidermis and Barrier Function. *International Journal of Molecular Sciences* [online], vol. 22, no.6, p. 3035. Available from: doi: 10.3390/ijms22063035.
107. LINEHAN, J.L., HARRISON, O.J., HAN, S.-J., BYRD, A.L., VUJKOVIC-CVIJIN, I., VILLARINO, A.V., *et al*., 2018. Non-classical immunity controls microbiota impact on skin immunity and tissue repair. *Cell* [online], vol. 172, no. 4, p. 784–96 e18. Available from: doi: 10.1016/j.cell.2017.12.033.
108. LIU, C., PEI, M., LI, Q., ZHANG, Y., 2022. Decellularized extracellular matrix mediates tissue construction and regeneration. *Front Med.* [online], vol. 16, no. 1, p. 56-82. Availabl from: doi: 10.1007/s11684-021-0900-3.
109. LIU, R., MENG, X., YU, X., WANG, G., DONG, Z., ZHOU, Z., QI, M., YU, X., JI, T., WANG F., 2022. From 2D to 3D Co-Culture Systems: A Review of Co-Culture Models to Study the Neural Cells Interaction. *International Journal of Molecular Sciences* [online], vol. 23, no. 21:13116. doi: 10.3390/ijms232113116.
110. LIU, S., ZHANG, H. D. E., 2013. Epidermal development in mammals: key regulators, signals from beneath, and stem cells. *International Journal of Molecular Sciences* [online], vol. 14, no. 6, p. 10869-95. Available from: doi: 10.3390/ijms140610869.
111. LIZARDO, M., MAGALHAES, R.M., TAVARIA, F.K., 2022. Probiotic Adhesion to Skin Keratinocytes and Underlying Mechanisms. *Biology* [online], vol.11, no. 9, p. 1372. Available from: doi: 10.3390/biology11091372.

112. LOH, Q.L., CHOONG, C., 2013. Three-dimensional scaffolds for tissue engineering applications: role of porosity and pore size. *Tissue Engineering Part B: Reviews* [online], vol. 19, no. 6, p. 485-502. Available from: doi: 10.1089/ten.TEB.2012.0437.
113. MAI, Y., KOBAYASHI, Y., KITAHATA, H., SEO, T., NOHARA, T., ITAMOTO, S., MAI, S., KUMAMOTO, J., NAGAYAMA, M., NISHIE, W., UJIIE, H., NATSUGA, K., 2024. Patterning in stratified epithelia depends on cell-cell adhesion. *Life Sci Alliance* [online], vol. 18, no. 7. Available from: doi: 10.26508/lsa.202402893.
114. MANGAN, L., LABRUNIE, G., MARAIS, S., REY, S., DUSSERRE, N., BONNEU, M., LACOMME, S., GONTIER, E., L'HEUREUX, N., 2018. Characterization of a Cell-Assembled extracellular Matrix and the effect of the devitalization process. *Acta Biomaterialia* [online], vol. 82, p. 56-67. Available from: doi: 10.1016/j.actbio.2018.10.006.
115. MANGAN, L., LABRUINE, G., FÉNELONé, M., DUSSERRE, N., FOULC, M.P., LAFOURCADE, M., SVAHN, I., GONTIER, E., VÉLEZ, V.J.H., McALLISTER, T.N, L' HEUREUX, N., 2020. Human textiles: A cell-synthesized yarn as a truly "bio" material for tissue engineering applications. *Acta Biomaterialia* [online], vol. 5, no. 105, p. 111-120. Available from: doi: 10.1016/j.actbio.2020.01.037.
116. MARANGIO, A., BICCARI, A., D'ANGELO, E., SENSI, F., SPOLVERATO, G., PUCCIARELLI, S., AGOSTINI, M., 2022. The Study of the Extracellular Matrix in Chronic Inflammation: A Way to Prevent Cancer Initiation? *Cancers* [online], vol. 14, no. 23, p. 5903. Available from: doi: 10.3390/cancers14235903.
117. MEDUGORAC, I., 1980. Collagen content in different areas of normal and hypertrophied rat myocardium, *Cardiovascular Research* [online], vol. 14, i. 9, p. 551–554. Available from: https://doi.org/10.1093/cvr/14.9.551
118. MEMPEL, M., SCHMIDT, T., WEIDINGER, S., SCHNOPP C., FOSTER, T., RING J., ABECK D., 1998. Role of Staphylococcus aureus surface-associated proteins in the attachment to cultured HaCaT keratinocytes in a new adhesion assay. *Journal of Investigative Dermatology* [online], vol. 111, iss. 3, p. 452-6. Available from: doi: 10.1046/j.1523-1747.1998.00293.x.
119. MIERKE, C.T., 2024. Extracellular Matrix Cues Regulate Mechanosensing and Mechanotransduction of Cancer Cells. *Cells* [online], vol. 13, no. 1:96. Available from: doi: 10.3390/cells13010096.
120. MIKKOLA, M.L., 2007. Genetic basis of skin appendage development. *Seminars in Cell & Developmental Biology* [online], vol. 18, no. 2, p. 225-36. Available from: doi 10.1016/j.semcdb.2007.01.007. PMID: 17317239.

121. MOHAMMEDSAEED, W., McBAIN, A.J., CRUICKSHANK, S.M., O'NEIIL C.A., 2014. Lactobacillus rhamnosus GG inhibits the toxic effects of Staphylococcus aureus on epidermal keratinocytes. *Applied and Environmental Microbiology* [online], vol. 18, p. 5773-81. Available from: doi: 10.1128/AEM.00861-14.
122. MONTAGNA W., 1974. The Structure and Function of Skin. 3rd Edition. ©Academic Press, pages: 448. ISBN: 9780323138697.
123. MOSMANN T., 1983. Rapid colorimetric assay for cellular growth and survival: Application to proliferation and cytotoxicity assays. *Journal of Immunological Methods* [online], vol. 65, iss. 1–2, p. 55-63. Available from: https://doi.org/10.1016/0022-1759(83)90303-4.
124. MOUW, J.K., OU, G., WEAVER, V.M., 2014. Extracellular matrix assembly: a multiscale deconstruction. *Nature Reviews Molecular Cell Biology* [online], vol. 15, no. 12, p. 771-85. Available from: doi: 10.1038/nrm3902.
125. MURPHY, G., 1997. Histology of the Skin. In: ELDER D. E., *et al*. Lever's Histopathology of the Skin. Lippincott-Raven, Philadelphia. Chapter 3, pages: 5-50. ISBN: 0-397-51500-6.
126. MUKHERJEE, P., ROY, S., GHOSH, D. *et al.*, 2022. Role of animal models in biomedical research: a review. *Laboratory Animal Research* [online], vol.38, no. 1, p. 18. Available form: https://doi.org/10.1186/s42826-022-00128-1
127. MUNCIE, J.M., WEAVER, V.M., 2018. The Physical and Biochemical Properties of the Extracellular Matrix Regulate Cell Fate. *Current Topics in Developmental Biology* [online], vol. 130, p. 1-37. Available from: doi: 10.1016/bs.ctdb.2018.02.002.
128. NAKAZAWA, K., KALASSY, M., SAHUC, F., COLLOMBEL, C., DAMOUR, O., 1998. Pigmented human skin equivalent--as a model of the mechanisms of control of cell-cell and cell-matrix interactions. *Medical and Biological Engineering and Computing* [online], vol. 36, no. 6, p. 813-20. Available from: doi: 10.1007/BF02518888.
129. NEIL, J. E., BROWN, M. B. and A. C. WILLIAMS 2020. Human skin explant model for the investigation of topical therapeutics. *Scientific Reports* [online], vol. 10, no. 1, p. 21192. Available from: DOI: 10.1038/s41598-020-78292-4
130. NEISHABOURI, A., SOLTANI, K.A., DAGHIGH, F., KAJBAFZADEH, A-M. and M. MAJIDI ZOLBIN, 2022. Decellularization in Tissue Engineering and Regenerative Medicine: Evaluation, Modification, and Application Methods. *Frontiers in Bioengineering and Biotechnology* [online], vol. 10, p. 805299. Avaialble from: doi: 10.3389/fbioe.2022.805299

131. NESS, M.J., DAVIS, D.M., CAREY W.A., 2013. Neonatal skin care: a concise review. *International Journal of Dermatology* [online], vol. 52, no. 1, p. 14-22. Available from: doi: 10.1111/j.1365-4632.2012.05687.x.
132. NETZLAFF, F., LEHR, C.M., WERTZ, P.W., SCHAEFER. U.F., 2005. The human epidermis models EpiSkin, SkinEthic, and EpiDerm: an evaluation of morphology and their suitability for testing phototoxicity, irritancy, corrosivity, and substance transport. *The European Journal of Pharmaceutics and Biopharmaceutics* [online], vol. 60, no. 2, p. 167-78. Available from: doi: 10.1016/j.ejpb.2005.03.004. PMID: 15913972.
133. NG dART RT Kit [online] [cit. 2024-05-26]. Available from: https://eurx.com.pl/docs/specs/en/e0801.pdf
134. NIEHUES, H., BOUWSTRA, J.A., GHALBZOURI, A.E., BRANDER, J.M., ZEEUWEN, P.J.L., van den BOGAARD, E.H., 2018: 3D skin models for 3R research: The potential of 3D reconstructed skin models to study skin barrier function. *Experimental Dermatology* [online], vol. 27, no. 5, p. 501-511. Available from: doi: 10.1111/xd.13531
135. NICOLAS, J., MAGLI, S., RABBACHIN, L., SAMPAOLESI, S., NICOTRA, F., RUSSO, L., 2020. 3D Extracellular Matrix Mimics: Fundamental Concepts and Role of Materials Chemistry to Influence Stem Cell Fate. *Biomacromolecules* [online], vol. 21, no. 6, p. 1968-1994. Available from: doi: 10.1021/acs.biomac.0c00045.
136. NEWSTEAD, L.L., VARJONEN, K., NUTTALL, T., PATERSON, G.K., 2020. Staphylococcal-Produced Bacteriocins and Antimicrobial Peptides: Their Potential as Alternative Treatments for Staphylococcus aureus Infections. *Antibiotics* [online], vol. 9, no. 2, p. 40. Available from: doi: 10.3390/antibiotics9020040.
137. OECD Test Guideline 439 In Vitro Skin Irritation: Reconstructed Human Epidermis Test Method [online] [cited 2025-04-29]. Available from: https://www.oecd.org/content/dam/oecd/en/publications/reports/2021/06/test-no-439-in-vitro-skin-irritation-reconstructed-human-epidermis-test-method_g1g59b2f/9789264242845-en.pdf
138. OLIVEIRA, M., CUNHA, E., TAVARES, L., SERRANO, I., 2023. P. aeruginosa interactions with other microbes in biofilms during co-infection. *AIMS Microbiology* [online]. vol. 9, no. 4, p. 612-646. Available from: doi: 10.3934/microbiol.2023032.
139. OLIVEIRA, H., MÉDINA, C., LABRUINEa G., DUSSERRE N., CATROS, S., MANGAN, L., HANDSCHIN, C., STACHOWICZ, M.L., FRICAIN, J.C., L'HEUREUX, N., 2021. Cell-assembled extracellular matrix (CAM): a human biopaper for the biofabrication of pre-vascularized tissues able to connect to the host circulationin vivo.

Biofabrication [online], vol. 14, no. 1 Available from: doi: 10.1088/1758-5090/ac2f81.

140. OTTO M., 2014. Staphylococcus aureus toxins. *Current Opinion in Microbiology* [online], vol. 17, p. 32-7. Available from: doi: 10.1016/j.mib.2013.11.004.
141. PAMPALONI, F., STELZER E. H., and A. MASOTTI, 2009. Three-dimensional tissue models for drug discovery and toxicology. *Recent Patents on Biotechnology* [online], vo. 3, no. 2, p. 103-17. Available from: doi: 10.2174/187220809788700201. PMID: 19519566.
142. PAPPINEN, S., PRYAZHNIKOV, E., KHIROUG, L., ERICSON, M.B., YLIPERTTULA, M., URTTI, A., 2012. Organotypic cell cultures and two-photon imaging: tools for in vitro and in vivo assessment of percutaneous drug delivery and skin toxicity. *The Journal of Controlled Release* [online], vol. 161, no. 2, p. 656-67. Available from: doi: 10.1016/j.jconrel.2012.03.005.
143. PAPPINEN, S., HERMANSSON, M., KUNTSCHE, J., SOMRHARJU, P., WERTZ, P., URTTI, A., and SUHONEN, M., 2008. Comparison of rat epidermal keratinocyte organotypic culture (ROC) with intact human skin: Lipid composition and thermal phase behavior of the stratum corneum. *Biochimica et Biophysica Acta* [online], vol. 1778, no. 4, p. 824-34. Available from: doi: 10.1016/j.bbamem.2007.12.019.
144. PATRA, V., GALLAIS SÉRÉZAL, I., WOLF, P., 2020. Potential of Skin Microbiome, Pro- and/or Pre-Biotics to Affect Local Cutaneous Responses to UV Exposure. *Nutrients* [online], vol. 12, no. 6, p. 1795. Available from: doi: 10.3390/nu12061795.
145. PISPA, J., THESLEFF, I., 2003. Mechanisms of ectodermal organogenesis. *Developmental Biology* [online], vol. 262, no. 2, p. 195-205. Available from: doi: 10.1016/s0012-1606(03)00325-7.
146. PLIKUS, M.V., WANG, X., SINHA, S., FORTE, E., THOMPSON, S.M., HERZOG, E.L., DRISKELL, R.R., ROSENTHAL, N., BIERNASKIE, J., HORSLEY, V., 2021. Fibroblasts: Origins, definitions, and functions in health and disease. *Cell Press* [online], vol. 184, no. 15, p. 3852-3872. Available from: doi: 10.1016/j.cell.2021.06.024.
147. PONMOZHI, J., DHINAKARAN, S., VARGA-MEDVECZKY, Z., FÓNAGY, K., BORS, L.A., IVÁN, K., ERDÖ, F., 2021. Development of Skin-On-A-Chip Platforms for Different Utilizations: Factors to Be Considered. *Micromachines* [online], vol. 12, no. 3, p. 294. Available from: https://doi.org/10.3390/mi12030294
148. POPOV, L., KOVALSKI, J., GRANDI, G., BAGNOLI, F., AMIEVA, M.R., 2014. Three-Dimensional Human Skin Models to Understand Staphylococcus aureus Skin Colonization and Infection. *Frontiers in*

Immunology [online], vol. 6, no. 5, p. 41. Available from: doi: 10.3389/fimmu.2014.00041.
149. Protocol Guide: MTT Assay for Cell Viability and Proliferation. [online] [cit. 2024-03-11]. Available from: https://www.sigmaaldrich.com/technical-documents/protocols/biology/roche/cell-proliferation-kit-i-mtt.html
150. POUMAY, Y., FAWAY, E., 2023. Human Epidermal Keratinocytes in Culture: A Story of Multiple Recipes for a Single Cell Type. *Skin Pharmacology and Physiology* [online], vol. 36, no. 5, p. 215-224. Available from: doi: 10.1159/000534137.
151. PEDROSA, T.D.N., CATARINO, C.M., PENNACCHI, P.C., ASSIS, S.R., GIMENES, F., CONSILARO, M.E.L., BARROS, S.B.M., MARIA-ENGLER, S.S., 2017. A new reconstructed human epidermis for in vitro skin irritation testing. *Toxicology in Vitro* [online], vol. 42, p. 31-37. Available from: doi: 10.1016/j.tiv.2017.03.010.
152. POTART, D., GLUAIS, M., GAUBERT, A., DA SILVA, N., HOURQUES, M., SARRAZIN, M., IZOTTE, J., CHARROT, L. M., L´HEREUX, N., 2023. The cell-assembled extracellular matrix: A focus on the storage stability and terminal sterilization of this human "bio" materiál. *Acta Biomaterialia* [online], vol. 66, p. 133-146. Available from: https://doi.org/10.1016/j.actbio.2023.05.002.
153. PRINCE, T., McBAIN, A.J., O'NEILL, C.A., 2012. Lactobacillus reuteri Protects Epidermal Keratinocytes from Staphylococcus aureus-Induced Cell Death by Competitive Exclusion. *Applied and Environmental Microbiology* [online], vol. 78, no. 15. Available from: https://doi.org/10.1128/AEM.00595-12
154. RADEMACHER, F., SIMANSKI, M., GLÄSER, R., HARDER, J., 2018. Skin microbiota and human 3D skin models. *Experimental Dermatology* [online], vol. 27, no. 5, p. 489-494. Available from: doi: 10.1111/exd.13517.
155. RISUENO, I., VALENCIA, L, JORCANO, J.L., VELASCO, D., 2021. Skin-on-a-chip models: General overview and future perspectives. *APL Bioengineering* [online], vol. 5, no. 3, p. 030901. Available form: doi: 10.1063/5.0046376.
156. RANDALL, M. J., ASTRID, J., and M. RIMANN., 2018. Advances in the Biofabrication of 3D Skin in Vitro: Healthy and Pathological Models. *Frontiers in Bioengineering and Biotechnology* [online], vol. 6, p. 412822. Available from: https://doi.org/10.3389/fbioe.2018.00154.
157. RASMUSSEN, C., GRATZ, K., LIEBEL, F., SOUTHALL, M., GARAY, M., BHATTACHARYYA, S. SIMON, N., ZANDEN, M. V., WINKLE Van K., PIRNSTILL, J., PIRNSTILL, S., COMER, A., ALLLEN-

HOFFMANN B., 2010. The StrataTest® human skin model, a consistent in vitro alternative for toxicological testing. *Toxicology in Vitro* [online], vol. 24, no. 7, p. 2021-2029. Available from: https://doi.org/10.1016/j.tiv.2010.07.027.

158. REDDY, G.K., ENWEMEKA, C.S., 1996. A simplified method for the analysis of hydroxyproline in biological tissues. *Clinical Biochemistry* [online], vol. 29, no. 3, p. 225-9. Available from: doi: 10.1016/0009-9120(96)00003-6. PMID: 8740508.
159. ROGER, M., FULLARD, N., COSTELLO, L., BRADBURY, S., MARKIEWICZ, E., O'REILLY, S., DARLING, N., RITCHIE, P., MÄÄTTÄ, A. KARAKESISOGLOU, I., 2019. Bioengineering the microanatomy of human skin. *Journal of Anatomy* [online] vol. 234, no. 4, p. 438-455. Available from: doi: 10.1111/joa.12942.
160. ROTHER, J., RICHTER, C., TURCO, L., KNOCH, F., MEY, I., LUTHER, S., JANSHOFF, A., BODENSCHATZ, E., TARANTOLA, M., 2015. Crosstalk of cardiomyocytes and fibroblasts in co-cultures. *Open Biology Journal* [online], vol. 5, no. 6:150038. doi: 10.1098/rsob.150038.
161. ROSSI, A., APPELT-MENZEL, A., KURDYN, S., WALLES, H., GROEBER, F., 2015. Generation of a three-dimensional full thickness skin equivalent and automated wounding. *JoVE* [online], vol. 26, no. 96, p. 52576. Available from: doi: 10.3791/52576.
162. ROZARIO, T., DeSIMONE, D.W., 2010. The extracellular matrix in development and morphogenesis: a dynamic view. *Developmental Biology* [online], vol. 341, no. 1, p 126-40. Available from: doi: 10.1016/j.ydbio.2009.10.026.
163. SACHDEVA, C., SATYAMOORTHY, K., MURALI, T.S., 2022. Microbial Interplay in Skin and Chronic Wounds. *Current Clinical Microbiology Reports* [online], vol. 9, p. 21–31. Available from: https://doi.org/10.1007/s40588-022-00180-4
164. SAJI, J. J., TEBOGO, M. S., and M. NTWASA., 2019. Two-Dimensional (2D) and Three-Dimensional (3D) Cell Culturing in Drug Discovery. *Cell Culture* [online], Available from: doi:10.5772/intechopen.81552
165. SAVOJI, H., GODAU, B., HASSANI, M.S. and M. AKBARI., 2018. Skin Tissue Substitutes and Biomaterial Risk Assessment and Testing. *Frontiers in Bioengineering and Biotechnology* [online], vol. 6, p. 86. Available from: doi: 10.3389/fbioe.2018.00086
166. SFRISO, R., EGERT, M., GEMPELER, M., VOEGELI, R., CAMPECHE, R., 2020. Revealing the secret life of skin - with the microbiome you never walk alone. *International Journal of Cosmetic Science* [online], vol 42, no. 2, p.116–26. Available from: doi: 10.1111/ics.12594.

167. SCHARSCHMIDT, T.C., and M.A. FISHCBACHF, 2013. What Lives On Our Skin: Ecology, Genomics and Therapeutic Opportunities Of the Skin Microbiome. *Drug Discovery Today: Disease Mechanisms* [online], vol. 10, iss. 3-4, p.83-89. Available from: doi: 10.1016/j.ddmec.2012.12.003.
168. SCHMIDT, F.F., NOWAKOWSKI, S. and P.J. KLUGER, 2020. Improvement of a Three-Layered in vitro Skin Model for Topical Application of Irritating Substances. *Frontiers in Bioengineering and Biotechnology* [online], vol. 8, p. 388. Available from: doi: 10.3389/fbioe.2020.00388
169. SCHMITT, A., CSIKI, R., TRON, A., SALDAMLI, B., TÜBEL, J., SIEBENLIST F.K., BALMAYOR, E., and R. BURGKART 2017. Optimized protocol for whole organ decellularization. *European Journal of Medical Research* [online], vol. 22, no. 31. Available from: https://doi.org/10.1186/s40001-017-0272-y.
170. SCHARSCHMIDT, T.C., FISCHBACH, M.A., 2013. What lives on our skin: Ecology, genomics and therapeutic opportunities of the skin microbiome. *Drug Discovery Today: Disease Mechanisms* [online], vol. 10, no. 3-4, p. e83-e89. Available from: doi: 10.1016/j.ddmec.2012.12.003.
171. SHOULDERS, M.D., RAINES, R.T., 2009. Collagen structure and stability. *Annual Review of Biochemistry* [online], vol. 78, p. 929-58. Available from: doi: 10.1146/annurev.biochem.77.032207.120833.
172. SORRELL, J.M., CAPLAN, A.I., 2009. Fibroblasts-a diverse population at the center of it all. *International Review of Cell and Molecular Biology* [online], vol. 276, p. 161-214. Available from: doi: 10.1016/S1937-6448(09)76004-6.
173. SOUREN, J.M., PONEC, M., van WIJK, R., 1989. Contraction of collagen by human fibroblasts and keratinocytes. *In Vitro Cellular & Developmental Biology – Animal* [online], vol. 25, no. 11, p. 1039-45. Available from: doi: 10.1007/BF02624138.
174. STARK, H.J., SZABOWSKI, A., FUSENIG, N.E.; MASS-SZABOWSKI, N., 2004. Organotypic co-cultures as skin equivalents: A complex and sophisticated in vitro system. *Biological Procedures Online*. [online], vol. 6, p. 55-60. Available from: doi: 10.1251/bpo72.
175. STERN, C.D., 2005. Neural induction: old problem, new findings, yet more questions. *Development.* [online], vol. 132, no. 9, p. 2007-21. Available from: doi: 10.1242/dev.01794.
176. STROBER, W., 2015. Trypan Blue Exclusion Test of Cell Viability. *Current Protocols in Immunology* [online]. Available from: doi: 10.1002/0471142735.ima03bs111.

177. SUHAERI, M., SUBBIAH, R., KIM, S.H., KIM, C,H,, OH, S.J., KIM, S.H., PARK, K., 2017. Novel Platform of Cardiomyocyte Culture and Coculture via Fibroblast-Derived Matrix-Coupled Aligned Electrospun Nanofiber. *ACS Applied Materials & Interfaces* [online], vol. 9, no. 1, p. 224-235. doi: 10.1021/acsami.6b14020.
178. SUHAERI, M., SUBBIAH, R., VAN, S.Y., DU, P., KIM, I.G., LEE, K., PARK, K., 2015. Cardiomyoblast (H9c2) differentiation on tunable extracellular matrix microenvironment. *Tissue Engineering Part A* [online], vol. 21, p. 11-12:1940-51. Available from: doi: 10.1089/ten.TEA.2014.0591.
179. SUHONEN, T.M., PASONENS-SEPPANEN, S., KIRJAVAINEN, M., TAMMI, M., TAMMI, R., and A. URTTI, 2003. Epidermal cell culture model derived from rat keratinocytes with permeability characteristics comparable to human cadaver skin. *Eur J Pharm Sci* [online], vol. 20, no. 1, p. 107-113. Available from: doi: 10.1016/s0928-0987(03)00176-3.
180. SUSIC, D., FROHLICH, E.D., 2011: Increased collagen, per se, may not affect left ventricular function in spontaneously hypertensive rats. *Ochsner Journal* [online], vol. 11, no. 3, p. 241-5. PMID: 21960757; PMCID: PMC3179202.
181. SYLVESTER P.W., 2011. Optimization of the tetrazolium dye (MTT) colorimetric assay for cellular growth and viability. *Methods in Molecular Biology* [online], vol. 716, p. 157-168. Available from: doi: 10.1007/978-1-61779-012-6_9.
182. Total RNA Mini Manual. [online] [cit. 2024-05-26]. Available from: https://www.aabiot.com/en/download?code=f4db219a4dcb85f5df40ed091532f7956cde12d3
183. TORRES, Y., GLUAIS, M., Da SILVA, N., REY, S., GRÉMARE, A., MANGAN, L., KAWECKI F., L'HEUREUX N., 2021. Cell-assembled extracellular matrix (CAM) sheet production: Translation from using human to large animal cells. *Journal of Tissue Engineering and Regenerative Medicine* [online], vol. 12: 2041731420978327. Available from: doi: 10.1177/2041731420978327.
184. TSAO, C.T., LEUNG, M., ChANG, J.Y., ZHANG, M., 2014. A simple material model to generate epidermal and dermal layers in vitro for skin regeneration. *Journal of Materials Chemistry B* [online], vol. 2, no. 32, p. 5256-5264. Available from: doi: 10.1039/C4TB00614C.
185. van BELKUM, A., LISOTTO, P., PIROVANO, W., MONGIAT, S., ZORGANI, A., GEMPELER, M., BONGONI, R. and E. KLAASSENS 2023. Being friendly to the skin microbiome: Experimental assessment. *Frontiers in Microbiomes* [online], vol. 1, p. 1077151. Available from: doi: 10.3389/frmbi.2022.1077151

186. VIS, M.A.M., ITO, K., HOFMANN, S., 2020. Impact of Culture Medium on Cellular Interactions in in vitro Co-culture Systems. *Frontiers in Bioengineering and Biotechnology* [online], vol. 4, no. 8:911. Available from: doi: 10.3389/fbioe.2020.00911.
187. WALTERS, K. W., and M. S. ROBERTS. Skin Morphology, Development and Physiology. In: BENSON, H.A.E., BENSON, H., ROBERTS, M. S., LEITE-SILVA V. R. and K. WALTERS, 2019. Cosmetic Formulation. Principles and Practice. [online] 1st Edition. 514 pages Boca Raton. Available from: doi: https://doi.org/10.1201/9780429190674. eISBN:9780429190674.
188. WASAKATSUKI, T., KOLODNEY, M.S. ZAHALAK, G.I. and E.L. ELSON, 2000. Cell Mechanics Studied by a Reconstituted Model Tissue. *Biophysical Journal* [online], vol. 79, no. 5, p. 2353–2368. Available from: doi: 10.1016/S0006-3495(00)76481-2
189. WATT, F.M., FUJIWARA, H., 2011. Cell-extracellular matrix interactions in normal and diseased skin. *Cold Spring Harbor Perspectives in Biology* [online], vol. 3, no. 4, p. a005124. Available from: doi: 10.1101/cshperspect.a005124.
190. WONG, T., McGRATH, J. A., and H. NAVSARIA, 2017. The role of fibroblasts in tissue engineering and regeneration. *British Journal of Dermatology* [online], vol. 156, no. 6, p. 1149–1155. Available from: doi:10.1111/j.1365-2133.2007.07914.x
191. WONG, C.W., LeGRAND, C.F., KINNEAR, B.F., 2019. *In Vitro* Expansion of Keratinocytes on Human Dermal Fibroblast-Derived Matrix Retains Their Stem-Like Characteristics. *Scientific Reports* [online], vol. 9, no. 18561 Available from: https://doi.org/10.1038/s41598-019-54793-9
192. WU, M-Y. and X. YAO, 2023. Skin Microbiota and the Skin Barrier. *International Journal of Dermatology and Venereology* [online], vol. 7, no. 1, p. 18-26. Available from: doi: 10.1097/JD9.0000000000000334
193. XING, H., LEE, H., LUO, L., KYRIAKIDES, T.R., 2020. Extracellular matrix-derived biomaterials in engineering cell function. *Biotechnology Advances* [online], vol. 42, p. 107421. Available from: doi: 10.1016/j.biotechadv.2019.107421.
194. YADAY, N., PARVEEN, S., CHAKRAVATY, S. and M. BANERJEE. Skin Anatomy and Morphology. In: YADAY, N., PARVEEN, S., CHAKRAVATY, S. and M. BANERJEE, 2019. Skin Aging & Cancer. Ambient UV-R Exposure. Springer Singapore. [online]. ISBN: 978-981-13-2541-0. Available from: doi: https://doi.org/10.1007/978-981-13-2541-0

195. YANG, J., DANG, H., XU, Y, 2022. Recent advancement of decellularization extracellular matrix for tissue engineering and biomedical application. *Artif Organs*. [online], vol. 46, no. 4, p. 549-567. Available from: doi: 10.1111/aor.14126.
196. YANG, S., HU, H., KUNG, H., ZOU, R., DAI, Y., HU, Y., WANG, T., LV, T., YU, J., LI F, 2023. Organoids: The current status and biomedical applications. *MedComm (2020)*, [online], vol. 4, no. 3, p. e274. Available from: doi: 10.1002/mco2.274.
197. YANG, Y., QU, L., MIJAKOVICi, I. *et al.*, 2022. Advances in the human skin microbiota and its roles in cutaneous diseases. *Microbial Cell Factories* [online], vol. 21, no. 176. Available from: https://doi.org/10.1186/s12934-022-01901-6
198. YAO, Q., ZHENG, Y.W., LAN, Q.H., KOU, L., XU, H.L., ZHAO Y.Z., 2019. Recent development and biomedical applications of decellularized extracellular matrix biomaterials. *Materials Science & Engineering C-Materials for Biological Applications* [online], vol. 104 p. 109942. Available from: doi: 10.1016/j.msec.2019.109942.
199. ZHANG, Z., MICHNIAK-KOHN, B.B., 2012. Tissue-engineered human skin equivalents. *Pharmaceutics.* [online], vol. 4, no. 1, p. 26-41. Available from: doi: 10.3390/pharmaceutics4010026.
200. ZHANG, P., SU, J., MENDE, U., 2012. Cross talk between cardiac myocytes and fibroblasts: from multiscale investigative approaches to mechanisms and functional consequences. *American Journal of Physiology-Heart and Circulatory Physiology* [online], vol. 303, no. 12, p. H1385-96. Available from: doi: 10.1152/ajpheart.01167.2011.
201. ZHENG, D., LIWINSKI, T., ELINAV, E., 2020. Interaction between microbiota and immunity in health and disease. *Cell Research* [online], vol. 30, no. 6, p. 492-506. Available from: doi: 10.1038/s41422-020-0332-7.
202. ZHONG, S.P., ZHANG, Y.Z. and C.T. LIM, 2010. Tissue scaffolds for skin wound healing and dermal reconstruction. *WIREs Nanomedicine and Nanobiotechnology* [online], vol. 5, no. 2, p. 510-525. Available from: https://doi.org/10.1002/wnan.100

LIST OF FIGURES

Figure 1: Structure of the skin (Kolarsick P., Kolarsick A. and Goodwin 2011)... 14

Figure 2: Signalling steps in the specification of embryonic skin (Fuchs 2007).15

Figure 3: Embryonic skin maturing (adapted from Hu et al. 2018),.....17

Figure 4: Schematic diagram of normal keratinocytes in different layers of the epidermal tissue. An arrow indicates the direction and levels of epithelial differentiation (Choi and Lee 2015)…….....18

Figure 5: Skin-specific fibroblast organization and lineage relationships (Plikus et. al. 2021)…....…….22

Figure 6: Keratinocytes differentiation process (adapted from Eckert and Rocke 1989; Gutowska-Owsiak et al.2020).....25

Figure 7: An overview of 3D skin models (Jang et al. 2023) 28

Figure 8: Bacteria distribution on the skin sites (Grice and Segre 2011) 34

Figure 9: Extracellular matrix composition (Dzobo et al. 2023) 411

Figure 10: Overview of co-culture systems (Goers et al. 2014). (1) Natural interactions between cell lines. (2) Improving cultivation success for certain cell lines. (3) Establishing synthetic interactions between cell lines…….....44

Figure 11: 3D skin model condition.....52

Figure 12: Diagram of *in vitro* 3D skin irritation test 58

Figure 13: CAM sheet production overview – from HDF cell line to biomaterial scaffold ……...64

Figure 14: Technical drawing of mechanical stimulation device housing……..74

Figure 15: Preparation of collagen-based 3D skin model. A: The preparation of acellullar collagen-based layer for the cell line seeding. B: Collagen-fibroblast layer od 3D skin model development. C: Collagen- fibroblast layer after 7 days of culture. D: Fully mature in vitro 3D skin model (ALI system)…….....77

Figure 16: H&E stained cross-section of a in vitro 3D skin equivalent……..79

Figure 17: Viability of the 3D reconstructed skin model……...81

Figure 18: Effects of commensal bacteria/supernatants on HaCaT cell viability.84

Figure 19: Effects of pathogenic bacteria/supernatants on HaCaT cell viability.85

Figure 20: MTT proliferation assay in HaCaT monolayers exposed to bacterial supernatants over 0, 24, and 48 hours (expressed as % of time 0 reference). Left: Commensal bacteria (S. epidermidis – SES, M. luteus – MLS). Right: Pathogenic bacteria (S. aureus – SAS, P. aeruginosa – PAS)…….86

Figure 21: Adhesion profiles of skin-associated bacteria…….88

Figure 22: Generation and morphology of CAM sheet scaffold A. Fully developed, CAM scaffold. B. In vitro formation of CAM sheet captured through photodocumentation ……...89

Figure 23: Fluorescence microscopy of H9c2 myoblast proliferation on standard culture flask and decellularized CAM scaffold. Fluorescent staining highlights actin filaments (red) and nuclei (blue), revealing improved cellular alignment and proliferation on the decellularized CAM scaffold compared to the standard culture surface …….90

Figure 24: Fluorescence microscopy of CAM sheets formed from HDF:H9c2 co-cultures at varying ratios (3rd and 7th day proliferation). F-actin stained with ActinGreen 488 (green) and nuclei labeled with Hoechst 33258 (blue)……91

LIST OF TABLES

Table 1: Preparation of the NB buffer.....53
Table 2: Construction of cellularized collagen matrix.....54
Table 3: In vitro skin equivalent culture media.....55
Table 4: H&E staining.....56
Table 5: Primer sequences used for real-time PCR analysis……...68
Table 6.1 Selected ECM-relevant genes for CAM scaffold analysis……..69
Table 6.2: Selected ECM-relevant genes for CAM scaffold analysis ……..….70
Table 7: Composition of resolving/stacking gels for SDS-PAGE electrophoresis……..…71

LIST OF ABBREVIATIONS AND SYMBOLS

ALI	Air-liquid interface
BMP	Bone morphogenetic protein
CAM	Cell-assembled extracellular matrix
DED	Decellularized de-epidermized dermis
DMSO	Dimethylsulfoxide
ECM	Extracellular matrix
EVs	Extracellular vesicles
FGF	Fibroblast growth factor
GAGs	Glycosaminoglycans
HSE	Full-thickness human skin equivalents
LDH	Lactate dehydrogenase
MMPs	Matrix metalloproteinases
MTT	(3-(4,5-dimethylthiazol-2-yl) -2,5-diphenyltetrazolium bromide)
NB	Neutralization buffer
PFA	Paraformaldehyde
PGs	Proteoglycans
RHE	Reconstructed human epidermis
SDS	Sodium dodecyl sulfate
SE	Skin equivalent
TERM	Tissue engineering and regenerative medicine

CURRICULUM VITAE

Personal information	Valášková Kristýna, Ing. Contact: k1_valaskova@utb.cz Sex: Female | Date of birth: 12/4/96 | Nationality: Czech
Education	**2021 – present** *Doctoral Degree* The Centre of Polymer Systems, Tomas Bata University in Zlín (Czech Republic) **Field of study: Biomaterials and Biocomposites** **Thesis: Preparation of reconstituted tissues** **2019 – 2021** *Master´s degree* Faculty of Technology, Tomas Bata University in Zlin (Czech Republic) **Field of study: Biomaterials and cosmetics** **Thesis: Scaffolds in tissue engineering** **2016 – 2019** *Bachelor´s degree* Faculty of Science, Palacký University Olomouc (Czech Republic) **Field of study: Molecular and cell biology** **Thesis: Development of CRISPR/Cas9-based reporter cell**
Education internships	**12 May – 10 June 2025** Biotechnology Centre, Silesian University of Technology; Gliwice, Poland **September 2024** 3D Cell Culture, practical course Institute of Biophysics, The Czech Academy of Sciences; Brno, Czech Republic **August 2023** Institute of Animal Physiology and Genetics CAS, The Czech Academy of Sciences; Brno, Czech Republic

November 2022 (1 week)
MatTek In Vitro Life Science Laboratories; Bratislava, Slovak Republic

October 2021 (1 week)
Institute of Biophysics, The Czech Academy of Sciences; Brno, Czech Republic

---

Conferences

5 – 6 June 2025
XIV Ogólnopolska Konferencja Studentów Slaskiej Wyzszej Szkoly Medycznej w Katowicach
Katowice, Poland
Presentation type: Oral

30 June – 3 July 2024
ESB 2024, 29th Congress of the European Society of Biomechanics, Edinburgh, Scotland
Poster presenter

Work on projects

2025 – present
SurfToGreen – 101157688, Horizone-JU-CBE-2023
Member of the team

2025 – present
GAČR 25-17718S, Ex vivo tissue models for small intestine tissue
Member of the project

2025 – present
GAČR 23-07425S, Anisotropic and Electro-Conducting Biomaterials
Member of the project team

2024
IGA/CPS/2024/007, Designing Smart Biomaterials for Tissue Engineering
Leader of the project team

2023 – 2024
GAČR 19-16861S, Interaction of biomaterials with stem cells under *in vivo* simulated conditions
Member of the project team

2023 - 2024
GAČR 22-33307S, Development of novel 3D hierarchically structured polysaccharides and proteins porous systems
Member of the project team

2023
IGA/CPS/2023/001, Development of Advanced Biomaterials and Their Future Applications
Member of the project team

September 2022 – January 2023
JUNG-2020-007, Development of biopolymer-based hydrogels for microextrusion
Member of the project team

2022
IGA/CPS/2022/001, Preparation of advanced biomaterials and their application
Member of the project team

2021 – 2022
GAČR 20-28732S, Colloidal systems for topical formulations. Pickering emulsions and polymer-based colloids.
Member of the project team

LIST OF PUBLICATIONS

Articles published in journals indexed on Web of Science:

1. Muchová, M.; Münster, L.; **Valášková, K.**; Lovecká, L.; Víchová, Z.; Osicka, J.; Kaspárková, V.; Humpolícek, P.; Vasícek, O.; Vícha, J. One-step fabrication of chitosan/dialdehyde cellulose/polypyrrole composite nanofibers with antibacterial, antioxidant, and immunomodulatory effects. *International Journal of Biological Macromolecules* 2025, vol. 308, part 1. Available from: doi: 10.1016/j.ijbiomac.2025.142105

2. Hamida, S.B.; Stepánová, V. ; Zahedi, L.; Kovácová, M.; Nasadil, P.; **Valášková, K**.; Humpolícek, P.; Kovácik, D. Enhancement of the dyeability and antibacterial properties of cotton fabric by plasma assisted cationization using chitosan and quaternized poly[bis(2-chloroethyl) ether-alt-1,3-bis[3-(dimethylamino)propyl]urea. *Cellulose* 2024, vol. 31, iss. 11, p. 7119-7136. Available from: doi: 10.1007/s10570-024-06027-z.

3. Kácerová, S.; Muchová, M.; Doudová, H.; Münster, L.; Hanulíková, B.; **Valášková, K.**; Kaspárková, V.; Kuritka, I.; Humpolícek, P.; Víchová, Z.; Vasícek, O.; Vícha, J. Chitosan/dialdehyde cellulose hydrogels with covalently anchored polypyrrole: Novel conductive, antibacterial, antioxidant, immunomodulatory, and anti-inflammatory materials. *Carbohydrate Polymers*, 2024, 327. Available from: doi:10.1016/j.carbpol.2023.121640.

4. Korábková, E.; Kaspárková, V.; Vasícek, O.; Víchová, Z.; Kácerová, S.; **Valášková, K.**; Urbánková, L.; Vícha, J.; Münster, L.; Skopalová, K.; Humpolícek, P. Pickering emulsions as an effective route for the preparation of bioactive composites: A study of nanocellulose/polyaniline particles with immunomodulatory effect. *Carbohydrate Polymers*, 2024, 323. Available from: doi:10.1016/j.carbpol.2023.121429.

5. Kácerová, S.; Víchová, Z.; **Valášková, K.**; Vícha, J.; Münster, L.; Kaspárková, V.; Vasícek, O.; Humpolícek, P. Biocompatibility of colloidal polypyrrole. *Colloids and Surfaces B-Biointerfaces*, 2023, 232. Available from: doi:10.1016/j.colsurfb.2023.113605.

6. Vítková, L.; Kazantseva, N.; Musilová, L.; Smolka, P.; **Valášková, K.**; Kocourková, K.; Humeník, M.; Minarík, A.; Humpolícek, P.; Mrácek, A.; Smolková, I. Magneto-responsive hyaluronan hydrogel for hyperthermia and bioprinting: Magnetic, rheological properties and biocompatibility. *APL Bioengineering*, 2023, 7(3). Available from: doi:10.1063/5.0147181.

7. Jurtík, M.; Gresková, B.; Prucková, Z.; Rouchal, M.; Dastychová, L.; Vítková, L.; **Valášková, K.**; Achbergerová, E.; Vícha, R. Assembling a supramolecular 3D network with tuneable mechanical properties using adamantylated cross-linking agents and β-cyclodextrin-modified hyaluronan. *Carbohydrate Polymers*, 2023, 313. Available from: doi: 10.1016/j.carbpol.2023.120872